FABRICATION AND CHARACTERIZATION OF SELF-SENSING NANOCOMPOSITE - "SMART SKIN"

Gurtej Singh Sidhu

A THESIS SUBMITTED TO THE FACULTY OF GRADUATE STUDIES
IN PARTIAL FULFILLMENT OF THE REQUIREMENTS FOR THE DEGREE OF
MASTER OF SCIENCE

Graduate Program in Mechanical Engineering
York University
Toronto, Ontario

November 2018

Abstract

This study characterizes the behaviour and properties of self-sensing polymer nanocomposite. Specifically, we studied the Electrical, Mechanical and Piezoresistive properties. Electrically the material is conductive with a linear response to change in applied strain. Mechanically the material behaves like apolymer, whose Young's Modulus increases with added MWCNT. From a piezoelectricalperspective this material is stable and can maintain its electrical and mechanical behaviour for 50 cycles of repeated loading at 2mm/min. When producing thin sheets of nanocomposite, the effects of material thickness on piezoresistivity are negligible.

The nanocomposite is fabricated by mechanically mixing multiwalled carbon nanotubes (MWCNT) with 2-part polydimethylsiloxane (PDMS). The randomly aligned MWCNT-PDMS is fabricated for two configurations, Type I and Type II. In these configurations, Type I is read longitudinal to force using 4-Probe method and Type II is read perpendicularly with 2-Probe method. The strain is applied to Type I in tension and Type II in compression. The Type I characterizes the bulk conductivity for varying wt% of MWCNT. The Type II looks at the sheet conductivity for varying thickness.

Acknowledgements

I acknowledge the past successes and failures of countless scientists and researchers whose incremental contributions allowed me to work with carbon nanotubes, a material of wonder.

I would like to thank Prof. Zheng Hong Zhu, whose dedication to research has been the source of my motivation more than once. Your commitment to students is reflected in your long hours and constant availability, be it early morning or late evening. I am very thankful that you gave me the room to grow; you listened to my ideas with patience and gave positive criticism, even when they were way out of the box. I have learned much under your guidance. Truly, thank you.

I would also like to extend my appreciation to Dr. G. Vukovichfor his support and guidance. Further, toDr. A. Czekanski for this technical expertise and resources. Finally, I would like to thank my grandfather who has supported me unconditionally in my educational endeavours.

Table of Contents

List of Tables

List of Figures

Notations

Correction factor	C
Electrical conductivity	σ
Electrical current	I
Electrical resistivity	ρ
Inter probe distance of Type I sample	s
Length of Type I sample	a
Length of Type II sample	L
Pi	π
Sheet conductivity	σ_s
Sheet resistivity	ρ_s
Thickness	w
Voltage potential	V
Width	d

Chapter 1 INTRODUCTION AND JUSTIFICATION

Summary: In this chapter, we define the problem, justify the undertaking of the research and outline the method of approach adopted in achieving the set objectives. Furthermore, we provide a summary of the layout of the thesis.

1.1 Multifunctional/PiezoresistiveNanocomposite

The world of engineering is as diverse as it is ever growing. New feats of engineering continue to build on our past successes and push on the boundary of our capabilities, forever merging the realm of imagination with technological achievements. These new challenges impose new constrains and requirements for the designers. Often, advanced materials either discovered or developed by material scientist and engineers facilitate these innovations. Material scientists have long coveted materials that fulfill the multifunctional role of providing structural support along with an ability to sense their environment. Attention has been paid to developing nanocomposites from polymers and added fillers for enhancing the material with the desired properties. Generally, changes in a nanocomposite's electrical conductivity is used as a method of sensing the surrounding

environment. This has led to the development of conductive polymer composites (CPCs). They are lightweight, flexible, tunable, and easy to manufacture. The CPCs have the aptitude to fulfill various applications in flexible tactile sensing, artificial electronic skin[1-3], skin-mountable devices[4-6]and in large area pressure sensing [7-9].

These composite sensors use various fillers including metal nanowires, nanoparticles, silicon nanoribbons, carbon nanotubes, graphene, nano clay and carbon black. Carbon nanotubes in particular have drawn attention due to their outstanding electrical and mechanical properties. They are utilised as fillers to enhance the electrical, thermal, and mechanical properties of the substrate. Various CNT embedded polymer composites have reached percolation threshold at a lower weight percentage than other commonly used nanofillers (metal particles/flakes, carbon black, etc.) [10]. The low percolation threshold is desirable when preserving the original polymer properties. The polymer matrix needs to maintain its low Young's modulus to remain flexible. Polydimethylsiloxane (PDMS), polyimide, polymethylmethacrylate andpolyvinylpyrrolidone are some of the polymers used in composites. The polymer matrix polydimethylsiloxane (PDMS)canundergo over 100% of tensile strain without any structural failure [11, 12]. Further, the polymer PDMS is chemically inert, biocompatible and is widely used in microfluidics and biomedical areas [13]. However, these nanocomposite sensors are reported to operate at low strains for few cycles of deformation and do not provide detailed measurements for the performed action and its

corresponding electrical signals.

Therefore, the objective of this thesis is to bridge the gap for designers by developing and testing a PDMS-MWCNT sensing composites at high strain for repeated cycles of deformation. In depth data collection during experimentation will further our understanding of the relation between the mechanical strain and its corresponding change in electrical conductivity.

1.2 Justification of the Research

Smart materials with the ability to sense their environment are highly prized in engineering for multiple reasons. However, ensuring their integrity and reliability is of paramount concern for the designers. Our current knowledge on nanocomposite's piezoresistivity, which relates physical deformation of composite to change in composite's conductivity, is limited. This makes the incorporation of smart materials as standard engineering practice challenging.

Moreover, our understanding of the effects of a large stain range on piezoresistivity for polymer nanocomposite is also limited. To the best of author's knowledge, no study has explored the bulk piezoresistive effect for CNT-PDMS composites at large strain, as well as their characterization under repeated loading. A detailed comprehensive study, which looks at the base properties of CNT piezoresistivity in polymers, by directly correlating the stress, strain and conductivity together is lacking. Most studies use the CNT piezoresistivity to explore applications for the nanocomposite-

based sensors. However, such application dependent explorations are not suitable for quantitative understanding the behaviour of these nanocomposite sensors.

Finally, the flexible thin film sensor has the potential to revolutionize the sensing market in the area of in situ sensing and machine health monitoring, but its development and fabrication technology are mainly limited in the lab scale. The main challenge is producing nanocomposites economically, which maintain their material integrity over time, while achieving high piezoresistive sensitivity. Having a robust flexible sensor has far reaching implications, from machine health monitoring to human-like robots with a sense of touch.

This study takes the first steps to bridging our knowledge gap and provides general guidelines to developing and testing a piezoresistive nanocomposite.

1.3 Objectives of the Research

This thesis is dedicated to the development and characterization of carbon nanotube based piezoresistive nanocomposites for potential use as a multifunctional sensor. Here, we develop a fabrication method, which does not require specialised manufacturing equipment and perform tests, which further our understanding of piezoresistive property of polymer nanocomposites at high deformation with repeated cycles of loading. Primarily, our current efforts are devoted to:

(i) Develop a fabrication procedure to produce piezoresistive nanocomposite economically, which ensuring carbon nanotube dispersion into the polymer

matrix.

(ii) Characterize the piezoresistive properties at high strain for repeated loading and obtain stable relationship among stress, strain, and electrical conductivity.

(iii) Obtain a range of MWCNT wt% loading suitable for developing the nanocomposite sensor.

(iv) Characterize the piezoresistivity for two scenarios, where force is applied parallel and perpendicular to the sensing direction.

(v) Characterize and ensure the nanocomposite sensitivity and stability overtime and under repeated loading for high strains.

1.4 Method of Approach

The outline of the method adopted to achieve the above stated objectives is shown in Figure1.1. In the development of a thin film piezoresistive sensor, the work starts with the design consideration of electrodes and the mold for making samples. Different materials are given careful consideration, with copper shim and 20 gauge copper wire being chosen for use as electrodes. The mold is made from an aluminium plate of 6.35 mm (¼") thick. Techniques for incorporating the electrode, pre-fabrication and post fabrication were explored. We found that a shim is best incorporated pre-fabrication, whereas the wire can be inserted after the manufacturing of nanocomposites. Two type of testing samples are made. Type I samples, where deformation is applied in parallel with the sensing direction,

are used to obtain the bulk conductivity of the nanocomposite for different weight percentage (wt%) of MWCNT dispersed into the polymer substrate. The different amount of added MWCNT within the nanocomposites provided us with the conductivity information as well as the percolation threshold for the PDMS-MWCNT nanocomposite. The conductivity of Type I samples was measured while subjected to cyclic tensile loadings. It gave us the piezoresistive behaviour over the spectrum of conductivity curve. From this spectrum, we picked suitable MWCNT loadings, where a good trade-off can be made between piezoresistive sensitivity and noise, to develop the Type II samples. Type II samples are thin film samples, where the load is applied perpendicular to the sensing (current) direction. The conductivity of Type II samples with different thickness of the thin film for a particular MWCNT loading was measured while underwent cyclic compressive loads.

Analysis of the Type I and Type II samples provides us with the piezoresistive property in the parallel and perpendicular direction to deformation, as well as it catalogs the effects of thickness for a thin film. These pieces of information are crucial to developing a reliable thin film sensor, which will not only provide load magnitude, but also its location.

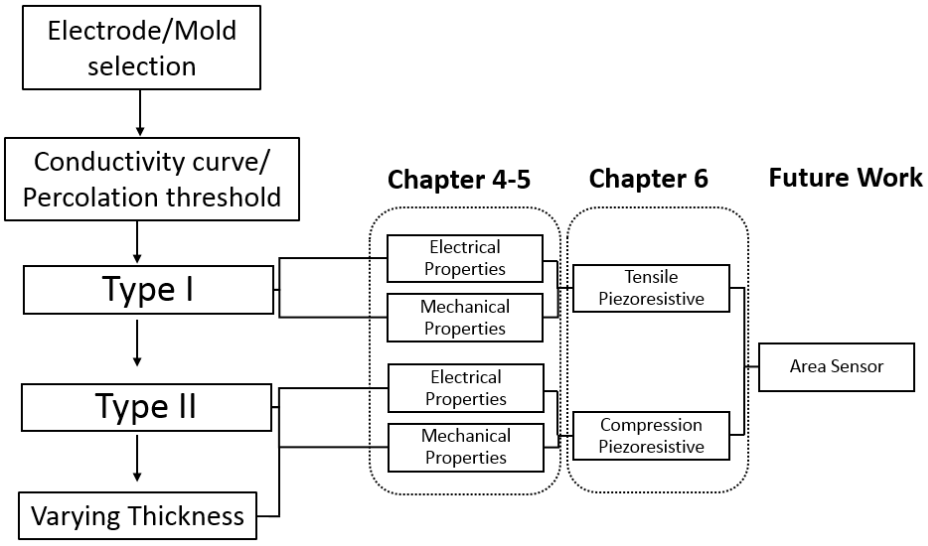

Figure 1.1 Method of Approach

1.5 Layout of Thesis

This thesis contains seven chapters. Following the introductory Chapter 1, Chapter 2 provides a critical review of existing conductive nanocomposites. It provides an overview of different fillers used to tailor the polymer properties, explores the applications of nanocomposite sensors, and covers the challenges involved in development of composite sensors. Chapter 3 outlines the experimental setup and the instruments used in experimentation and data collection. In Chapter 4, we provide a detailed account of the electrical properties and stability for PDMS-MWCNT nanocomposite. In Chapter 5, we address nanocomposite's mechanical properties, where we give a detailed look at the stress-strain curves as well as material degradation after repeated deformation. In Chapter

6, we present our findings on the piezoresistive properties of the nanocomposite. We pay attention to the relationship between deformation and changes in electrical signal. Moreover, we characterize the strain gauge factor and its stability overtime. In Chapter 7, we conclude the work and outline suggestions for related future work.

Chapter 2 LITERATURE REVIEW

Summary: This literature review is divided into three main sections. The first section provides an overview of polymers and different fillers used to tailor the composite properties. The second section is devoted to the research activities in the field of nanocomposite sensing. Work done by researchers and highlighting the potential of polymer sensors are presented. The third section covers the challenges involved in developing conductive polymer composites (CPC).

2.1 Tailoring the Composite Properties

Polymers have a unique property of undergoing large deformations without damage and are often used as a base for conductive polymer composites (CPC). This material flexibility is attributed to their long network of polymer chains. Fillers may be added to the polymers in order to alter the overall material behavior and properties. The last decades have seen an extensive use of nanoparticles, due to their small size and large surface areas. In particular, multiwall and single wall carbon nanotubes have been added as fillers in various polymers to tailor their electric conductivity

One of the most significant ways to utilize the potential of CPC is in the thin film pressure sensors, where the limited flexibility and sensitivity of traditional metal and semiconductor sensors is inadequate. Nanocomposites with properties of high piezoresistive sensitivity, low Young's modulus and high piezoresistivity is required for flexible sensor[5, 14, 15]. The stretchable nanocomposite sensors have used various nano-fillers including metal nanowires, nanoparticles, silicon nanoribbons, carbon nanotubes, graphene, nano clay and carbon black in conjunction with different polymer substrates, extending from silicone, rubber, PVDF, just to name a few.

The carbon nanotubes (CNT) in particular have drawn specific attention since their advent in 1991 by Ijima due to their outstanding electrical and mechanical properties. The multiwalled carbon nanotubes (MWCNTs) were first produced via arc-discharge method, in 1993 by Ijima et al. [16] and in 1996, using the more efficient laser-ablation technique by Thess et al. [17] to produce bundles of aligned single walled carbon nanotubes (SWCNTs).

The carbon nanotube based flexible devices have grown due to an astonishing array of CNT properties and reduced cost of manufacturing. Carbon nanotubes aredispersed within polymers as fillers to enhance the electrical, thermal, and mechanical properties of the substrate and have been extensively studied. The electrical properties of CNT-based polymer composites depend primarily on the size and the aspect ratio of the CNTs, their spatial distribution within the polymer matrix, interactions between the CNT

surface and the matrix, as well as the inter-nanotube contact resistances. Moreover, various CNT embedded polymer composites have reached percolation threshold at a lower weight percentage than other commonly used nanofillers (metal particles/flakes, carbon black, etc.) [10]. This low percolation threshold is important in order not to change the material properties of the polymer extensively. The high aspect ratio of tubular structures of CNTs allows for the formation of a more efficient electron conducting networks, which is probably the underlying mechanism for low percolation threshold in composites[8]. Furthermore, the CNTs when exposed to tensile and compressive strain, undergo change in their geometry and interconnections between nanotube. This physical response of CNTs leads to a change in their electrical resistance, which makes them ideal to be used within the polymer matrix for a piezoresistive strain sensor[12]. Furthermore, CNTs are one of the strongest materials, with tensile strength of up to 63 GPa[18]. Thus, multiwalled carbon nanotubes (MWCNTs), with their high aspect ratio (>1000), electrical conductivity (> 100 S/cm) and tensile strength are ideal to prepare the piezoresistive nanocomposites [5, 19]. As summarized by Obitayo et al. the MWCNT-based thin film sensors had better sensing capabilities over a larger working strain range than SWCNT-based thin film sensors. Thus, MWCNTSwere thus selected as the filler in this work[20].

The addition of well dispersed CNTs can significantly increases the electrical conductivity of polymers. A well dispersed composite generally has higher number of

conducting paths. The critical CNT concentration, which leads to a sharp decrease in electrical resistance, is known as the percolation threshold, illustrated in Figure 2.1.

The polymer selection for the MWCNTs embedded nanocomposite is equally important as the binding matrix should have a low Young's modulus for flexibility. Various materials such as polydimethylsiloxane(PDMS), polyimide, polymethylmethacrylate and polyvinylpyrrolidonehave been explored as the matrix for sensing applications. When compared with metals, semiconductors and other polymers, the polymer matrix polydimethylsiloxane(PDMS) has superior mechanical elasticity, as it easily holds over 100% of tensile strain without any structural failure [11-12]. The polymer PDMS is chemically inert, biocompatible and coupled with its flexibility, is widely used in microfluidics and biomedical areas [13]. Thus, Polydimethylsiloxane (PDMS) was chosen as the polymer matrix because of its low Young's modulus (<1 MPa), flexibility and bio compatibility.

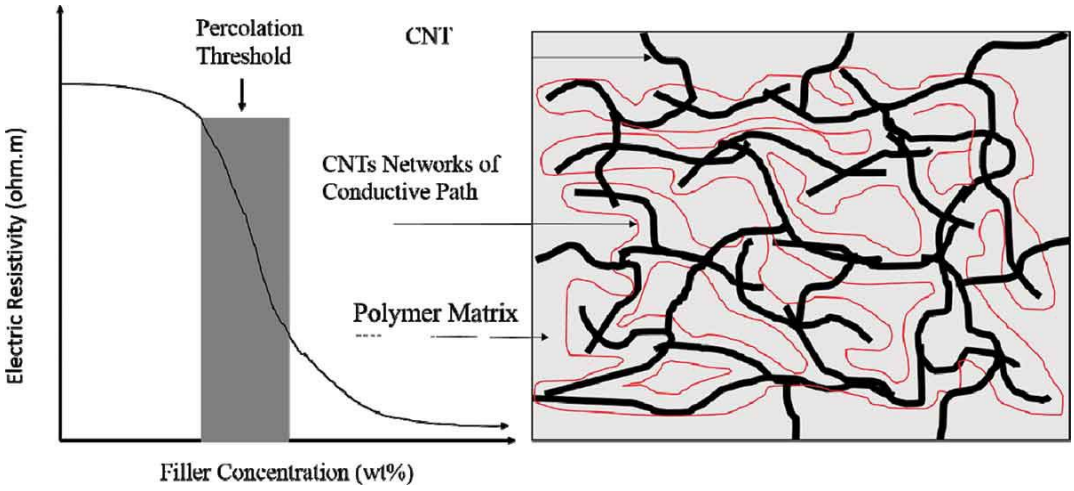

Figure 2.1 An illustration of the percolation threshold[21].

2.2 CNT-Based Polymer Nanocomposite

The carbon nanotube based polymer composites have gained significant interest as sensors due to their excellent piezoresistive properties. The properties of CNT based composites have been characterized for potential applications in the domain of wearable electronics[22, 23], skin mounted sensors[24], tactile sensing[25], structural monitoring, in-situ sensing and area pressure sensing[9].

Researchers have considered carbon nanotube based polymer composites for applications where in-situ and real time data is required. The sensing capabilities of CNT nanocomposites is due to measurable changes in the macroscale piezoresistive property. The electrical resistance changes with polymer deformation and this phenomenon is being investigated under both quasi static and cyclic loading. The CNT nanocomposite can be fabricated as patches [26], thin films [27, 28] and used in structural composites with embedded strain and damage sensing [29-31].

The literature on CNT based piezoresistive response has focused on nanocomposites fabricated by doping polymers with randomly oriented and well dispersed carbon nanotubes. The disruption and formation of conductive CNT percolation network within the material, has been associated with the change in the macroscale piezoresistivity. The piezoresistivity of the overall material is associated with the electron hopping/tunneling effect between neighboring CNTs, rather than the changes in

individual CNT piezoresistivity [7]. The piezoresistive sensitivity of randomly oriented and well dispersed CNT nanocomposites is assessed by the metric of gauge factor. A higher gauge factor signifies high piezoresistivesensitivity of the nanocomposite material. However, large variation can exist, which are due to differences in the processing, polymer properties, randomness in CNT orientation and microscale dispersion. The optimum concentration of CNTs to produce sufficient number of tube-tube contacts for high piezoresistive sensitivity is either near or just above the percolation threshold, as shown by Gong et al.[32, 33].

The alignment of CNT has been extensively studied for increasing the gauge factor. The documented techniques for alignment of CNTs in nanocomposites include application of acoustic wave[34, 35], magnetic field [36], electric field[37, 38] and mechanical stretching [39, 40]. Aviles et al. used AC electric fields to align MWCNT in polysulfone. Their results showed doubling of the gauge factor when comparing aligned CNT to the randomly oriented samples for the same concentration and strain [37]. Parmar et al. studied the anisotropic piezoresistivity of 5wt% MWCNT-polycarbonate composites with CNT aligned by the use of an injection molding process. They observed that the piezoresistive sensitivity in the inflow direction was increased to a gauge factor of 3.65 from 2.62, for samples with randomly oriented CNTs [41].

Lu et al studied the dispersion of MWCNTs into a PDMS matrix. They characterized the mechanical and electromechanical properties of the material under

different conditions and developed a micro pressure sensor [42]. Zhang et al. developed poly(phenylmethylsiloxane) functionalized MWCNTs for better dispersion into the PDMS matrix to obtain a high performance nanocomposite for flexible tactile sensing [5]. A flexible strain sensor was fabricated using microcontact printing and screen printing by Liu et al. They conducted high strain tensile cyclic loading for 9 wt% of MWCNT and noted hysteresis[12]. Zeng et al. tested a carbon black-PVDF based sensor for in situ detection of elastic disturbances caused by low and high frequency ultrasonic waves. They used a conventional strain gauge and piezoelectric transducer to evaluate the performance of the sensor, which showed excellent correlation but with a higher gauge factor and frequency independent piezoresistive behavior[43]. Yao et al. developed a micropatterned flexible microtube pressure sensor for in situ fluid pressure sensing. Their sensor has high sensitivity, 0.047 kPa^{-1} in gas sensing and 5.6 x 10^{-3} kPa^{-1} in liquid sensing with low power consumption <180 μW for use in implantable medical devices, industrial pipeline, and microfluidic chip where in situ sensing is required[44]. Liu et al. presented a graphene woven fabric (GWF) with polydimethylsiloxane composite as a flexible strain sensor capable of detecting human motions. The flexible wearable device has high piezoresistive gauge factor of 223 at a strain of 3%. They demonstrated a prototype made with the sensor by converting human motions to music of different instruments and sounds[6]. Hu et al. developed a CNT based flexible tactile sensor, which is integrated with a flexible print circuit connector and their preliminary tests, show the

detection of both normal and shear forces[45]. Dharap et al. developed a CNT film sensor by using randomly aligned SWCNTs in order to produce an isotropic film capable of detecting strain uniformly in all directions. Traditional sensors give discrete point and fixed directional measurements, which their sensor overcame and provided linear relation between strain and electrical voltage when subjected to tensile and compressive stresses[46]. Kim et al. conducted a preliminary hysteresis compensation study and by using the compensated output based on the Duhem hysteresis model, showed a linear relationship between loading and electrical resistance[47].

The field of nanocomposite sensors has grown immensely in the recent years, with new works being added regularly. However, most of this effort is based on individual laboratories, which has led to fragmentary development of the nanocomposite field. Lu et al [42]studied the dispersion but did not look at the effects of high strain at the nanocomposite. Liu et al[12] have used dispersed MWCNT to conducted high strain cyclic loading, but they did so for 12 cycles that shows the initial settling but not the long term settled behavior of the sensor. A holistic study is needed which looks at these different aspects and presents them together.

2.3 Challenges

There are many challenges associated with the development of CNT based nanocomposites. In general, an electrically conductive nanocomposite requires a filler and a polymer. The filler must be evenly distributed within the matrix for high gauge

factor and reliability of the output electrical signal. Further, the long-term mechanical stability of the composite is crucial when undergoing large deformations, while compensating for hysteresis.

The selection of a suitable base is crucial as the polymer chains must allow room for embedding the CNTs and provide a degree of freedom, depending on the application. This selection is further complicated when considering the environment of operation such as temperature extremes and rate of loading. The material requirements of electrical and thermal conductance, biocompatibility and the like further constrain the available polymer base. We selected Polydimethylsiloxane (PDMS), as this material is widely used by other researchers. The key benefit of PDMS is its uncured liquid state. The CNTscan be mixed into the fluid base more readily than a powder base. Moreover, PDMS is biocompatible. The processing of the material and dispersion of CNTs is the next obstacle and is largely based on the available equipment. A well-documented and viable processing technique is a must for developing CNT based sensors. The flexible thin film sensor has the potential to revolutionize the sensing market, but its development and fabrication have not been engineeringly successful. The main challenge is of maintaining material integrity over time, while achieving high piezoresistive sensitivity. Further, few studies have explored the bulk piezoresistive effect for CNT-PDMS composite at high strain, as well as their characterization under repeated loading. In addition, these studies did not pay attention to the long termsensitivity and stability of the nanocomposite.

In this study, the strain sensing properties of multiwalled carbon nanotubes are characterized for different weight percent of MWCNTs. We have expanded upon the work of Liu et al[12] and subjugated the developed nanocomposite sensor to fifty cycles of repeated loading and unloading.This characterization is done for two scenarios rather than just one; where the applied deformation is parallel to the sensing direction and where the deformation is perpendicular to the sensing direction. Most importantly, we look at the electrical and mechanical stability of the nanocomposite for a longer duration, where we find a linear relation between strain and change in conductivity.

Chapter 3 EXPERIMENTAL METHODOLOGY AND SETUP

Summary: In this chapter, we outline the setup procedure and the instruments used for experimentation and data collection. This chapter is a guide to making and testing polymers embedded with conductive nanoparticles. We laid out: (i) the essential steps to fabricating flexible piezoresistive polymer nanocomposite, (ii) the techniques used to measure electrical properties, (iii) the techniques used to measure mechanical properties, and (iv) the methodology for categorizing a piezoresistive polymer nanocomposite.

3.1 Sample Preparation

The polymer nanocomposite samples are made from polymer and nanoparticles. This section lays the essential steps to mixing powdered nanoparticles with a liquid state polymer matrix. The resulting viscous mixture is then cured at an elevated temperature to obtain a flexible piezoresistive nanocomposite. The nanocomposite samples are fabricated for two test conditions, tensile loading (Type I) and compressive loading (Type II).

Multi-walled carbon nanotubes (MWCNT) (Nanocyl grade NC7000) were used in this study as conductive nanofillermaterials. The Figure 3.1shows the MWCNT powders. The physical properties of NC7000 MWCNTs are given in Table 3.1. The Polydimethylsiloxane (PDMS) silicone (Sylgard 184 from Dow Corning) is used as the polymer matrix, see Figure 3.2and their physical properties aregiven in Table 3.2. The uncured PDMS is a two part liquid solution. The Part-A (Base) and Part-B (curing agent) is mixed in the 10:1 base to curing agent ratio.

Figure 3.1 Nanocyl grade NC7000 (MWCNT)

Figure 3.2 Dow Corning Slygard 184

Table 3.1 Physical Properties of Nanocyl grade NC7000 [48]

Properties	Value
Average Diameter	$9.5*10^{-9}$m
Average Length	1.5 **µ**m
Purity	90%
Surface Area	250-300 m^2/g
Volume Resistivity	10^{-4}**Ω**.cm

Table 3.2 Physical Properties of Slygard 184 [49]

Properties	Value
Viscosity (Mixed)	3500 cP
Thermal Conductivity	0.27 W/m ^{o}K
Specific Gravity (Cured)	1.03
Cure Time at 100^{o}C	35 minutes
Dielectric Strength	500 volts/mil
Volume Resistivity	2.9*10^{14}Ω.cm
Tensile Strength	6.7 MPa

Two types of samples were fabricated, Type I and Type II. The Type I, is a dog bone sample based on ASTM D 638-02a and are used in the tensile testing. Figure 3.3shows the shape and dimensions of the sample. The second type, Type II, is rectangular thin film sample and are used in the compression testing. Figure3.4 shows the shape and dimensions of the sample.

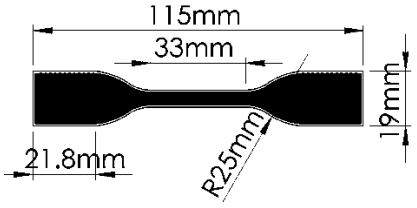

Figure 3.3 Size and dimensions of Type I samples

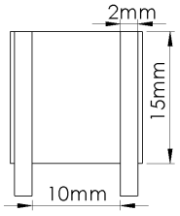

Figure 3.4 Size and dimensions of Type II samples

The process of making MWCNT-embedded nanocomposite starts with measuring a precise amount of powdered MWCNTs in a container; see Figure 3.5. The PDMS Part

A is poured into the container.The solution with MWCNTsis mechanically stirred at 2050 rpm for 15 minutes. The method of mechanical stirring is effective in mixing the carbon nanotubesinto the PDMS but introduces air to the solution, which needs to be de-gassed by additional processing.The solution is then placed in an ultra-sound bath for 3 hours per day, Type I is sonicated for 90 hours (30 days) and Type II for 54 hours (18 days). The ultra-sonication of the mix is crucial as it disperses the MWCNTs within the PDMS solution uniformly and prevents agglomeration.The PDMS Part B is then mixed into the mix solution of Part A and MWCNT.The mix solution is again mechanically stirred for 20 minutes. The solution of PDMS-MWCNT mix is poured into the mold and then placed in a vacuumto remove the air trapped. The mold is prepared separately, it is cleaned with organic solvent acetone and air dried. The mold is then waxed for easy release and the MWCNT-PDMS mixture is poured into the mold. The Type I samples are fabricated according to the ASTM D 638-02a[50], dog bone shape with length, width and thickness of 115mm, 10mm and 4mm respectively. The Type II samplesare poured into a rectangular mold, which is wrapped in a release film, and metal strips are used as spacers to control the thickness of thin film. Due to high percentage of nanotubes, the mixture for Type II is viscous and does not require fluid tight seal when moulding. The moulded film is preembedded with copper shims which are used as electrodes. The mixture with trapped air is vacuumed for four cycles, 20 minutes per cycle. Due to the introduction of MWCNT, the PDMS solution becomes viscous and vacuuming alone is not sufficient to

de-gas it. After each cycle, the surface tension was broken by leveling it off with a spatula. However, the samplesmay be vacuumed for more cycles if visual observations suggest trapped air.The solution is pressure molded at 130^{o}C, in a 12 tonne hydraulic press.The mold is heated using a hot plate and is not pre-heated. Pre-heating the mold may cause a rapid change of temperature within the mixture, inducing thermal shocking. Due to the potential of rapid temperature change, the mold is not directly in contact with the hot plate.Instead, a steel block is used to gradually bring the mold up to 130^{o}C.The mold is pressure heated for at least 3 hours and left to cure overnight.The cured MWCNT-PDMS composite is demolded and post treated by baking at 120^{o}C for 20 minutes to release any residual stresses formed during the fabrication process. The prepared samples have randomly aligned MWCNTs in order to produce a sensor which is isotropic in nature and uniformly measures stresses in all direction. The fabrication procedure of Type I samples is illustrated in Figure 3.5. The fabrication of Type II samples is similar with the exception of the mold design, which is shown in Figure3.6. The final Type II samples after demoulding is shown in Figure 3.9, it is cut to final film size before being tested. The fabrication fixture is shown in Figure 3.8.

Step 1. Add MWCNT to PDMS Part-A

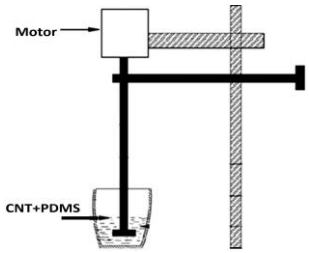

Step 2. Mix solution 15min, 2050rpm

Step 3. Ultrasonic bath to disperse CNT

Step 4. Mix Part-B and pour solution into mold

Step 5. Vacuum: 20 minutes, repeat if required

Step 6. Break the surface tension

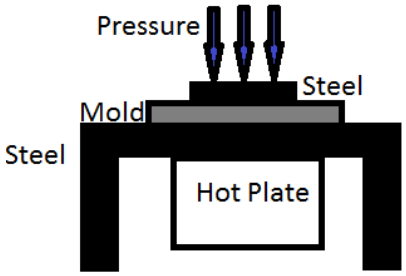

Step 7. Pressure mold: 130℃, 3 hours

Step 8. De-mold and post treated by baking at 120°C for 20 minutes. (Type I)

Figure 3.5 Fabrication process for nanocomposite samples

Figure 3.6 Mold for Type II sample

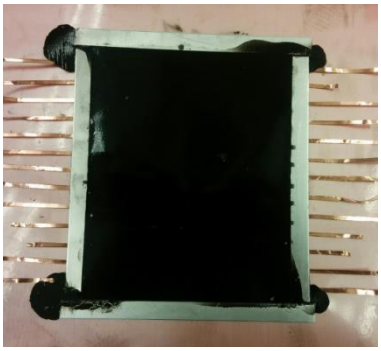

Figure 3.7 Cured Type II film

Figure 3.8 Nanocomposite Fabrication setup

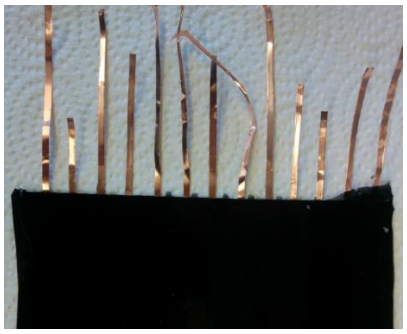

Figure 3.9 Cured Type II sample film

3.2 Measurement of Electrical Properties

The methodology and experimental setup for measuring electrical properties of Type I (tensile) and Type II (compression) samples, is covered in this section. Measurements taken: Time, Voltage potential, current and voltage supply. Properties determined from the measurements are: Percolation threshold, Conductivity, Gauge factor. The electrical properties were measured simultaneously with the mechanical properties.

The electrical properties of the nanocomposites are a direct result of adding MWCNTs into the PDMS matrix. Thus, the electrical properties are influenced by the amount of added MWCNTs. Two methods were used for measuring, the four probe method for Type I samples and two probe method for Type II samples. The conductivity of the nanocomposite with different weight percentage of MWCNTs is measured and the percolation threshold of the nanocomposite is identified. The percolation threshold is the point when the added MWCNTs are just enough to start conducting. This point normally has the highest sensitivity in terms of piezoresistivity.

3.2.1 Type I Samples

The four probe methodsupplies current and measures the voltage potential, its schematic is shown in Figure 3.10. This method infers the resistance of nanocomposite and is used to measure the bulk conductivity of the nanocomposite. Using four probe method, reduces measurement errors due to probe resistance and contact resistance between the probe and conducting nanocomposite. The challenge with this approach is the specialized equipment required to take measurements. A standard multimeteris replaced by voltage meter used in conjunction with a power source. A voltmeter with a high internal resistance is required near the percolation threshold, where the resistance of the measuring device must be higher than the resistance of the nanocomposite. The voltmeter and power supply used for this setup are Keighley 6517B Electrometer/High resistance meter and Keighley 6220 Precision current source, respectively. The instruments are

shown in Figure3.12 and Figure 3.13.

Measuring the conductivity of the nanocomposite requires four wires to be inserted into the finished samples by making holes 2 mm apart from each other, in the middle section of the sample. Type I sample with inserted wires can be seenin Figure 3.11. A spacing tool was used while inserting the wires and care must be taken not to bend the wires. A bent wire will not be parallel to the rest of probes which can change the distance between the probes and result in improper readings. Moreover, a bent wire will cause internal stresses which produces noise in the measured signal.

The electrical response of the composite was measured using the four-point probe method. The conductivity of different weight percent MWCNT in PDMS samples was measured to characterize the conductivity response with varying CNT weight percentage. This is done in order to find the percolation threshold of the MWCNT-PDMS nanocomposite sample. The electrical conductivity (σ) was computed using the equation[51]:

$$\sigma = \frac{1}{\rho} \tag{3.1}$$

whereσ is the electrical conductivity (S/m) and ρ is the electrical resistivity (Ω.m). The resistivity (ρ) according to Smits[51]for an infinite sheet is given by:

$$\rho = \rho_s = \frac{V}{I}\frac{\pi}{\ln 2} \tag{3.2}$$

where$V$ is the voltage drop between the inner probes, I is the electrical current supplied to

the probes and subscript *s* stands for sheet.

For a finite rectangular sheet, Eq. (3.2) must be corrected by applying a correction factor C, such that:

$$\rho_s = \frac{V}{I} C\left(\frac{a}{d};\frac{d}{s}\right) \tag{3.3}$$

wherea is the length of sheet, d is the width of sheet and s is the inter probe distance.

For small d/s, Eq. (3.3) can be applied to measuring sheet resistivities with four-point probe on narrow structures by using the correction factor C':

$$\rho_s = \frac{V}{I}\frac{d}{s} C'\left(\frac{a}{d}\right) \tag{3.4}$$

For an infinite slice of finite thickness w, the resistivity can be expressed with the correction factor F as:

$$\rho = \rho_s w = \frac{V}{I} w \frac{\pi}{\ln 2} F\left(\frac{w}{s}\right) \tag{3.5}$$

By applying equation (3.4) to (3.5), we can obtain the body resistivity of a thin sample:

$$\rho = \rho_s w = \frac{V}{I} w \frac{d}{s} C'\left(\frac{a}{d}\right) F\left(\frac{w}{s}\right) \tag{3.6}$$

This forms the basis for calculating the conductivity. Here, a is the length, d the width, s the distance between probes, V the voltage measure and I the current applied across the probes. The correction factors C' and F are dependent on a/d and w/s

respectively, which were obtained from table in Smits[51]. The value of the parameters for our calculations were as follows: S=2mm, d=5.75mm, w= 4.65mm, a=30-35mm, F= 0.6336, C'= 0.9002

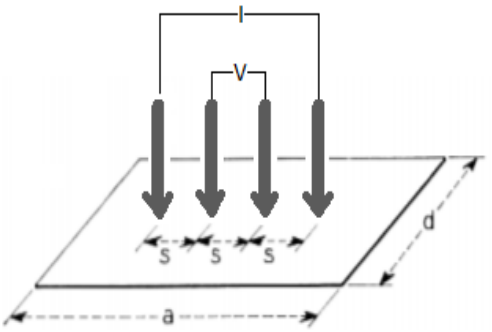

Figure 3.10 Schematic of four probe measurement method

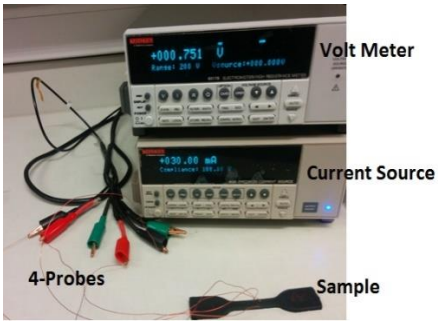

Figure 3.11 Setup for Type I

Figure 3.12 Keighley 6517B Electrometer/High resistance meter

Figure 3.13 Keighley 6220 Precision current source

3.2.2 Type II Samples

Two probemethod is used to measure thesurface conductivity of the nanocomposite. The two probe method is a passive measurement technique. Unlike the four probe method, which supplies current and measures the voltage; the two probe method allows for directmeasurements of resistance. Two probe however, is not suitable for measuring high

resistances.The percolation threshold region has the highest resistance was determined from Type I samples. The fabricated Type II samples are outside of this high resistance range, allowing for measurements via two probes to be viable. The Type II sampleis shown in Figure 3.14. The resistance meter used is Keighley 2450 SourceMeter, shown in Figure 3.15. The electrical conductivity of Type II is computed using the equation[52]:

$$\sigma_s = \frac{1}{\rho_s} \tag{3.7}$$

$$\rho_s = \frac{R * A}{L} \tag{3.8}$$

where σ_s is the electrical sheet conductivity (S/m), ρ_s is the electrical sheet resistivity (Ω.m), A is the area between probes and L is the horizontal distance between the probes.

Figure 3.14 Type II sample, cut to size

Figure 3.15 Resistance Meter

3.3 Measurement of Mechanical Properties

This section lays out the setup for measuring mechanical properties of Type I (tensile) and Type II (compression) samples. Measurements taken: Time, Force, Gripper displacement and Laser displacement. Properties determined: Stress, Strain, Young's Modulus.

The mechanical properties of the nanocomposite were measured using a universal testing machine (MTS Criterion Model 43). The samples used for tensile (Type I) and compression (Type II) testing underwent 50 cycles of loading and unloading at a rate of 2mm/min. The MTS Criterion is connected to the desktop computer and synchronized using a software package. The MTS Criterion provides measurements of time, force, and gripper displacement. A Laser Extensometer provides the Laser Displacement. The mechanical properties were measured simultaneously with the electrical properties.

3.3.1 Type I Samples

The Type I samples were firmly held by the grippers (MTS Criterion) at top and bottom, approximately 10-15mm in from both ends. A laser instrument (Laser extensometer LX500) is used to measure the displacement between two strips of reflective tape, placed on the surface at a central location of the nanocomposite. The instruments used are shown in Figure 3.17 and Figure 3.18. The test setupfor Type I can be seen in Figure 3.16.

A laser device is used to take the displacement measurement instead of the standard MTS Criterion gripper displacement. A laser unit provides better measurements by focusing on a local area of interest, instead of displacement over the whole sample

with elastic properties.

Figure 3.16 Test Setup for Type I

Figure 3.17 MTS Criterion Model 43

Figure 3.18 Laser extensometer LX500

3.3.2 Type II Samples

The thin film sampleis placed on a solid surface, within the testing area of MTS Criterion. An insulated aluminium bar is placed within the top gripper and is used to apply compressive pressure on an area, 6.8 mm in width and 17.9 mm in length. The test setup can be seen in Figure 3.19. The displacement measurements are taken from the standard gripper displacement on MTS Criterion. Samples with two different thicknesses are tested, 1.4 mm (Thick) and 1.0 mm (Thin). The thick samples are pre strained to 0.3 mm. In the successive cycles, the sample is always kept loaded by ranging the extension from 0.3 mm to 0.7 mm, with a total deformation of 0.4 mm. The thin samples are pre strained to 0.2 mm. In the successive cycles, the sample is always kept loaded by ranging the extension from 0.2 mm to 0.5 mm, with a total deformation of 0.3 mm.

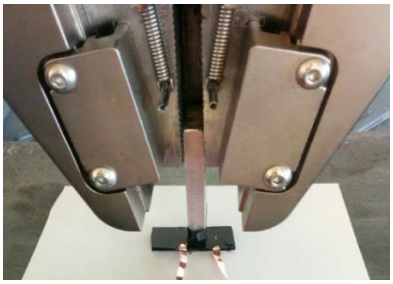

Figure 3.19 Test Setup for Type II

3.4 Measurement of Piezoresistive Properties

This section lays out the setup for measuring piezoresistive properties of Type I (tensile) and Type II (compression) samples. The piezoresistive response is measured by simultaneous reading the electrical and mechanical properties of the nanocomposite. This is done over 50 cycles of loading and unloading, at a rate of 2 mm/min. During the setup and testing, it is observed that any forces acting on the electrodes (wires or shim) cause noise in the measured electrical signal. Thus, care must be taken when connecting the electrodes to the measuring instruments and the possibility of pushing or pulling on the electrodes be reduced.

3.4.1 Type I Samples

The piezoresistive response of Type I is measured using MTS Criterion and four probe method. Four wires are inserted into the middle section of the samples at an equidistance of 2 mm. A spacing tool is used while inserting the wires and care must be taken not to bend the wires. The wired composite sample is then loaded into universal testing machine

(MTS Criterion Model 43), where it is subject to 50 cycles repeated tensile loading and unloading at a rate of 2mm/min.

The piezoresistive response is measured using volt meter (Keighley 6517B Electrometer/high resistance meter) and power supply (Keighley 6220 Precision current source). The MTS initially strains the sample to 7.5mm and unloads to 1mm in the first cycle. In the successive cycles, the sample is always kept loaded by ranging the extension from 1mm to 7.5mm, with a total deformation of 6.5mm. The applied tensile load is measured by the universal test machinewhile a laser (Laser extensometer LX500)is used to measure the deformation at the active central region around the embedded wires. The deformation of the whole sampleis provided by the MTS. The strain was measured at the narrow middle section of the sample via placing two pieces of reflective tape, roughly 23mm apart. The test setup is shown in Figure 3.20, where the four probes connected to current source and voltmeter are used in conjecture with MTS Criterion while loading.

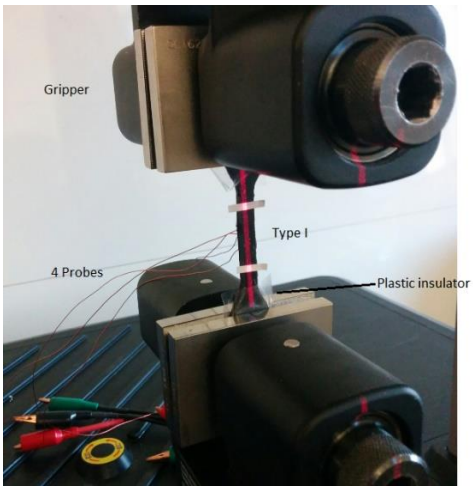

Figure 3.20 Setup for Type I Piezoresistive properties

3.4.2 Type II Samples

The piezoresistive response of Type II is measured using MTS Criterion and two probe method. The Type II samples have two wires embedded during the fabrication process. The wired composite sampleis placed within the testing area of MTS Criterion, where it is subject to 50 cycles of repeated tensile loading and unloading at a rate of 2mm/min.This setup can be seen in Figure 3.21. The stages of cyclic deformation are shown in Figure 3.22.

The resistance response is measured using Keighley 2450 SourceMeter, which is connected to the desktop computer. The displacement measurements are taken from the standard gripper displacement on MTS Criterion. Samples with two different thicknesses are tested, 1.4 mm (Thick) and 1.0 mm (Thin). The thick samples are pre strained to 0.3 mm. In the successive cycles, the sample is always kept loaded by ranging the extension from 0.3 mm to 0.7 mm, with a total deformation of 0.4 mm. The thin samples are pre strained to 0.2 mm. In the successive cycles, the sample is always kept loaded by ranging the extension from 0.2 mm to 0.5 mm, with a total deformation of 0.3 mm.

During the experiments, it is observed that the material tends to rebound slower over the successive cycles, illustrated in Figure 3.22.

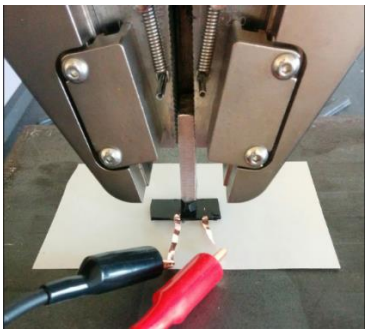

Figure 3.21 Type II Piezoresistive test setup

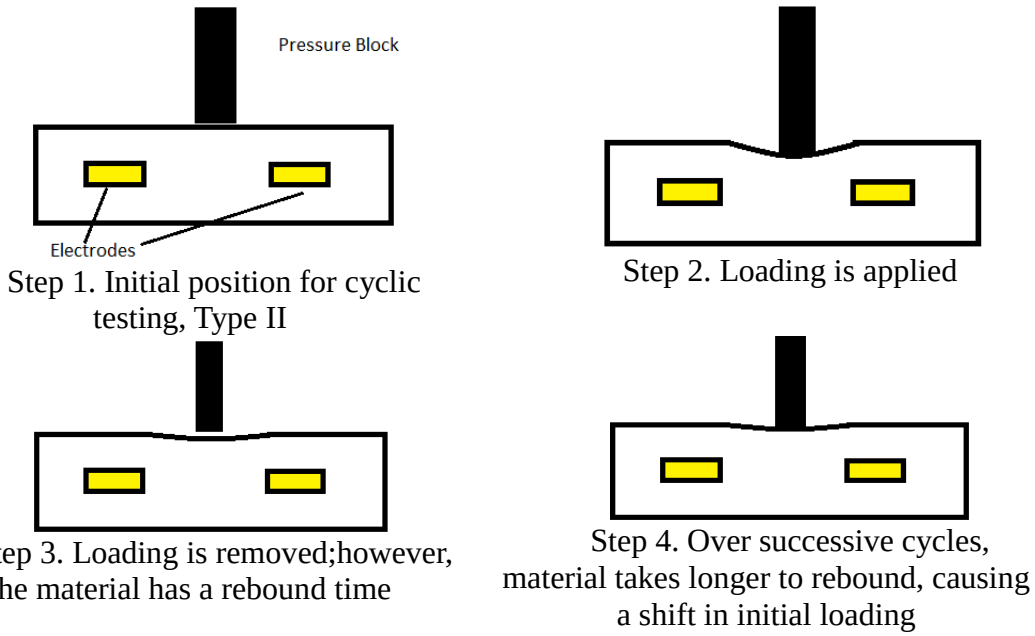

Step 1. Initial position for cyclic testing, Type II

Step 2. Loading is applied

Step 3. Loading is removed;however, the material has a rebound time

Step 4. Over successive cycles, material takes longer to rebound, causing a shift in initial loading

Figure 3.22 Stages ofcyclic piezoresistive deformation

Chapter 4 MEASUREMENT OF ELECTRICAL PROPERTIES

Summary: In this chapter, we present and discuss experimental results for the electrical properties of PDMS-MWCNT nanocomposites.

4.1 Introduction

The measurements of electrical properties of PDMS-MWCNT nanocomposites are taken in tandem with mechanical properties. The properties are measured over 50 cycles of repeated loading and unloading. We characterised (i) the change in electrical conductivity of the nanocomposite, with varying weight percentage of MWCNTs, and (ii) the stability of the electrical conductivity under repeated mechanical loading. An electrically stable nanocomposite is essential to producing a viable piezoresistive sensor. The stability is examined by recording the changes in electrical conductivity over time. Furthermore, we examined the electrical hysteresis by plotting voltage versus strain for selected key cycles, which provided us with a detailed settling behaviour of the nanocomposite. Finally, in this chapter, we show the peak-to-valley analysis of the voltage signal for each loading cycle. This analysis provides information on the sensor range and its stability.

The electrical properties of the nanocomposites are influenced by the amount of added MWCNTs. Two methods were used for measurement: the four probe method for Type I samples and two probe method for Type II samples. The conductivity of the nanocomposite with different weight percentage of MWCNTs was measured.The percolation threshold of the nanocomposite was identified because the piezoresistivity reaches its highest sensitivity at this point [53].

4.2 Electrical Conductivity

In this section, we show the measured electric conductivity of the nanocomposite as a function of added MWCNTs. The MWCNTs were embedded into the polymer matrix in the fabrication process. Two types of electrical conductivity were measured: the bulk conductivity for Type I samples and the sheet conductivity for Type II samples.

4.2.1 Type I Samples

The electrical conductivity of Type I samples was measured with the four-probe method. It is well-known that the electrically nonconductive PDMS polymer can become conductive by adding sufficient amount of CNTs, which form conductive percolation networks of CNTs.

An important characteristic in electrical conductivity of nanocomposites is the electrical percolation. The electrical percolation is an indicator of when the conductive networks have formed in the polymer matrix. Thus, characterization of the percolation

threshold was one of the initial quantifications we conducted. We determined the percolation threshold to be the first point where we were able to detect the electrical conductivity in our samples.

Figure 4.1 shows the variation of measured electrical conductivity versus different weight percentages of MWCNTs. It could be observed that the percolation threshold occursaround 0.5 wt% for the PDMS-MWCNT nanocomposites. The conductivity measurements were also made for samples with 0.1 wt% and 0.075 wt% MWCNT. However, we were unable to detect any electrical response.

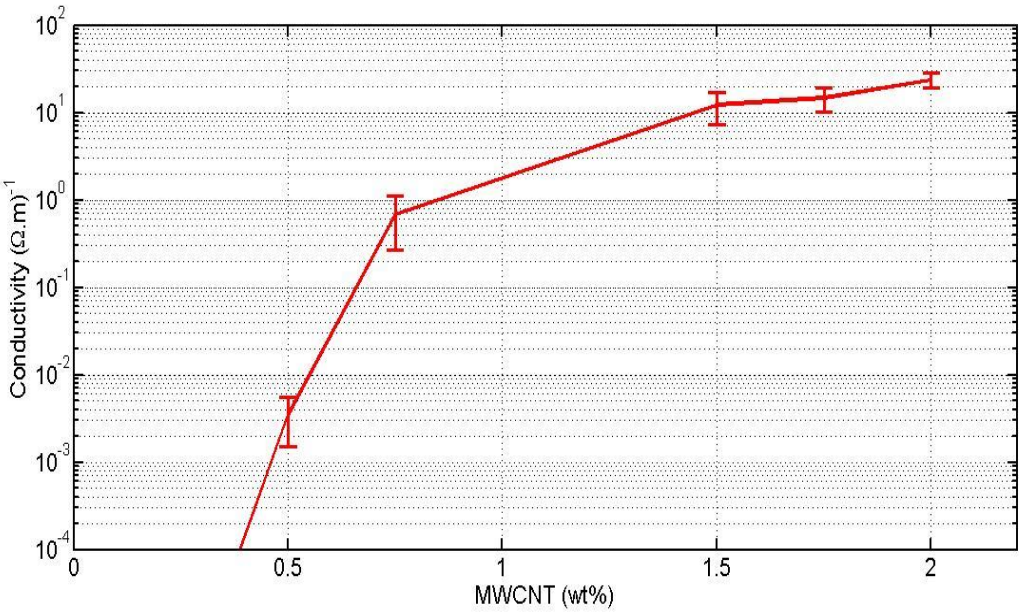

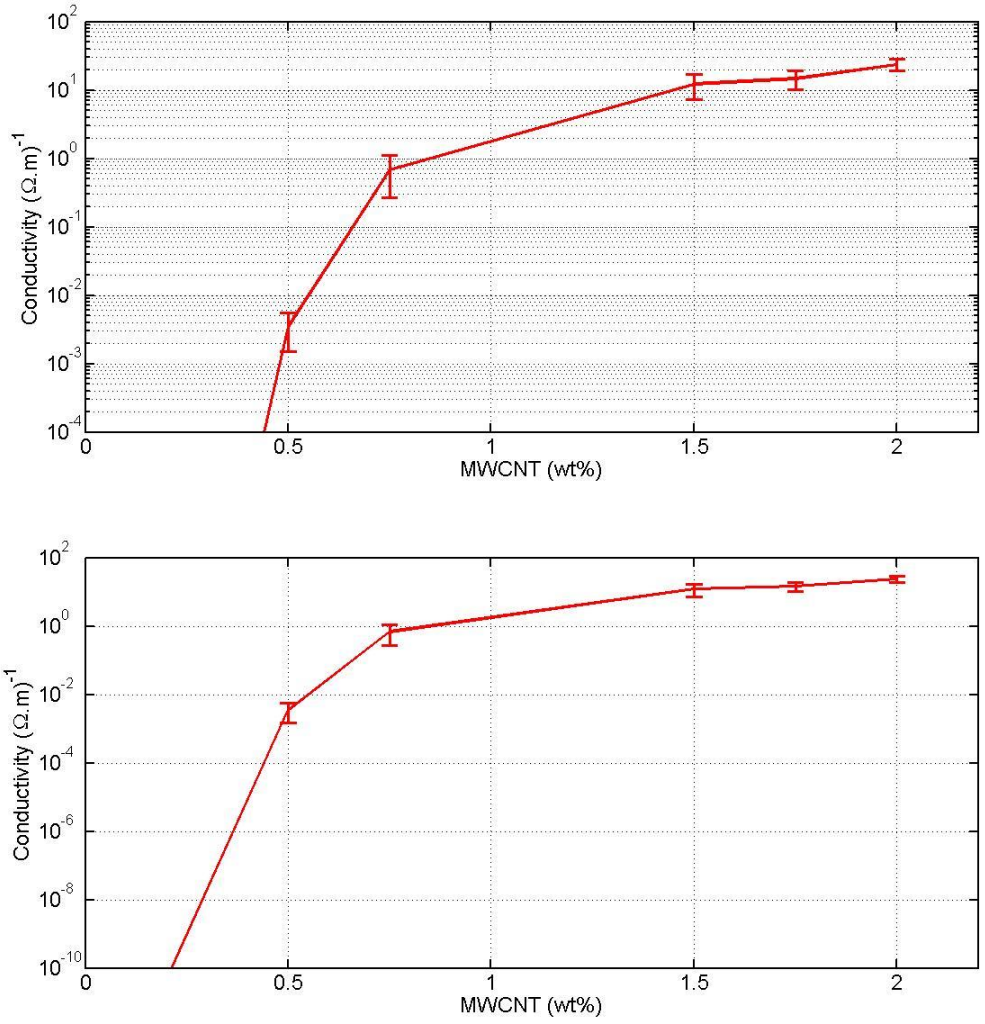

Figure 4.1 Electrical conductivity of nanocomposite vswt% MWCNTs.

The parameters used for the Type I experimental setup and the measured electrical conductivity for different wt% of MWCNTs were summarised in Table 4.1. The parameters were chosen based on nanocomposites' response.

Table 4.1 Type I experimental parameters and results

MWCNT (wt%)	Applied Current (mA)	Applied Voltage (V)	Electrical Conductivity $(\Omega.m)^{-1}$	
			Mean	Standard Deviation
0.075	-	-	0	0
0.1	-	-	0	0
0.50	0.05	100	0.0035	0.002
0.75	10.00	100	0.6916	0.427
1.50	80.00	100	12.3002	4.945
1.75	50.00	100	14.7211	4.574
2.00	80.00	100	23.6998	4.674

4.2.2 Type II Samples

The conductivity of Type II samples was measured by the two probe method and the results are shown in the Figure 4.2, where the variation of electrical conductivity is plotted versus different weight percentage of MWCNT. Furthermore, two samples with different thickness were made for each weight percentage of MWCNTs to examine the influence of thickness on the sheet conductivity.

As expected, the conductivity of 1.5 wt% samples is higher than 1 wt% nanocomposite samples. This occurs because the increased amount of MWCNTs provide more pathways for current to travel, making the overall nanocomposite to be more conductive.

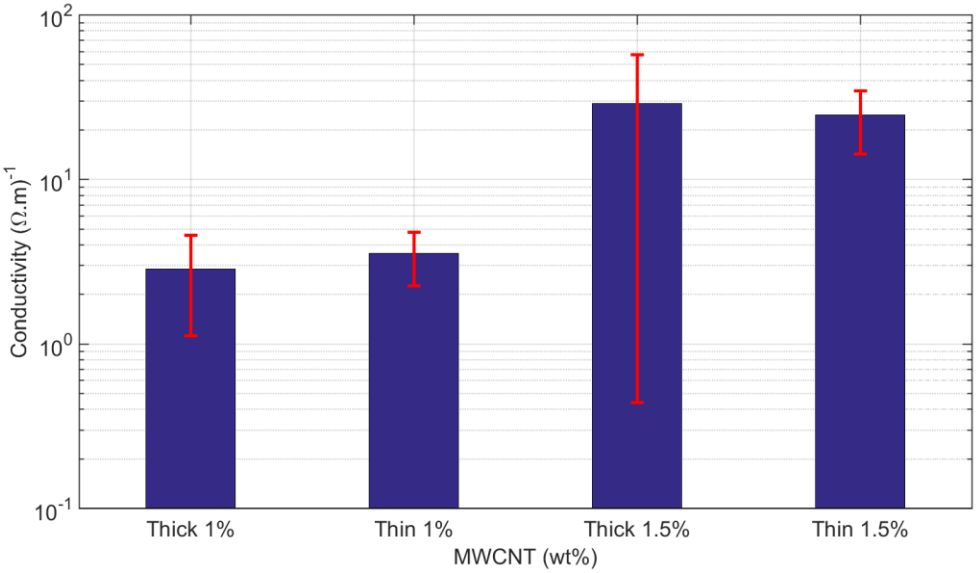

Figure 4.2 Conductivity for Type II for different samples.

The Table 4.2 outlines the parameters used for the Type II experimental setup and the measured conductivity for different wt% of MWCNT.

Table 4.2 Type II experimental parameters and results

Type II Samples		**Conductivity $(\Omega.m)^{-1}$**	
MWCNT wt%	**Thickness (mm)**	**Mean**	**Standard Deviation**
1.0	1.4	2.85	1.73
1.0	1.0	3.53	1.26
1.5	1.4	28.82	28.38
1.5	1.0	24.52	10.21

Conductivity of the Type II samples is comparable to the Type I samples for

similar wt% MWCNT. The difference may be due to the contact resistance in the two-probe method compared with the four-probe method. This indicates the necessity to characterize the electrical conductivity by the four-probe method. However, for sensing application, the two-probe method is acceptable because the effect of contact resistance can be properly accounted for by calibration of individual samples.

4.3 Electrical Stability

An electrically stable nanocomposite is necessary for developing a practical sensor. A nanocomposite, where the electrical signal drifts randomly with time, or a signal which changes erratically with applied loading would be unsuitable for practical applicationsbecause of its unpredictability. To determine the electrical stability of nanocomposites, we measured and analyzed various trends. It was foundthat the electrical properties of nanocompositescould be stabilizedbycycling loads over a certain period.

4.3.1 Type I Samples

The electrical stability of the material was determined by three different analyses. First, the conductivity response to cyclic strains for different wt%of MWCNT is shown in Figure 4.3.Second, thekey cycles in voltage response to applied strain are shownfrom Figure 4.4 to Figure 4.8. Lastly, we looked at the peak-to-valley trend for the voltage to time response for varying MWCNT in Figure 4.10 to Figure 4.14. In each test the Type I samples underwent cycling tensile loading for 50 cycles.

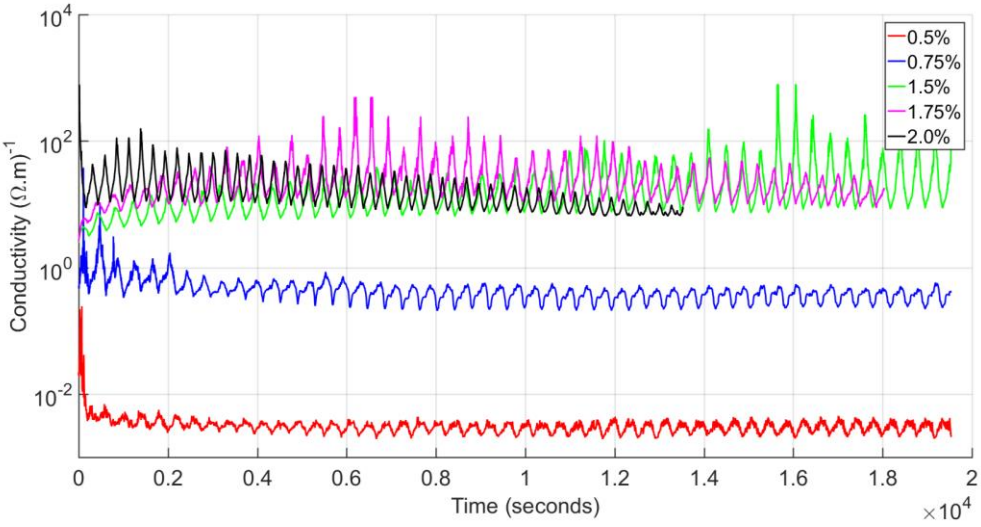

Figure 4.3 Type I conductivity for different wt% over time

The linear and horizontal trends of the conductivity curve over time for different wt% MWCNT (Figure 4.3) signifies that the material is electrically stable.There is also a significant increase in conductivity from 0.5 wt% to 1.5 wt%. This increase is due to saturation of polymer by MWCNT, which opens multiple conducting pathways. However, the increased conductivity comes at a cost of reduction in sensitivity and piezoresistivity.

The nanocomposite exhibited the presents of electrical hysteresis, which can be seen in the voltage to strain relation. This hysteresis exists due to the initial random orientation of MWCNTs and their gradual alignment due to mechanical stretching. It may also exist due to buildup of charge within the composite and nanotubes combined with polymer acting as nano-capacitors.

It was revealed that the hysteresis in the material causes the relation between

voltage and strain to drift over multiple cycles. However, the hysteresis between consecutive cycles decreases as the total number of cycles increases. Overall, the response in each cycle is a linear relation.In order to better understand the changes occurring within the nanocomposite, analysis of voltage and strain relation for select cycles was performed. These findings are shown in Figure 4.4 to Figure 4.8. The voltage data presentedhas been normalized, with minimum voltage being set to zero.

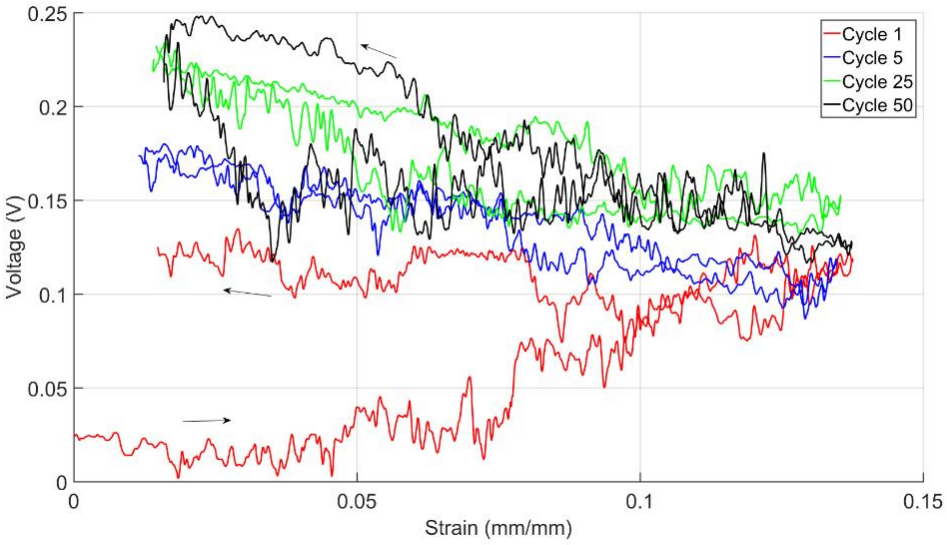

Figure 4.4 Voltage-Strain relation of 0.5 wt% for selective cycles

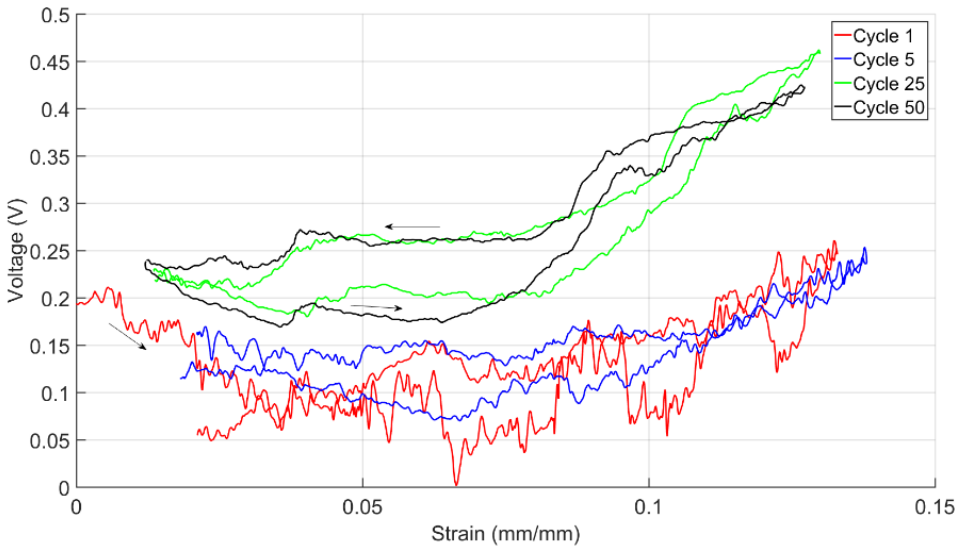

Figure 4.5 Voltage-Strain relation of 0.75 wt% for selective cycles

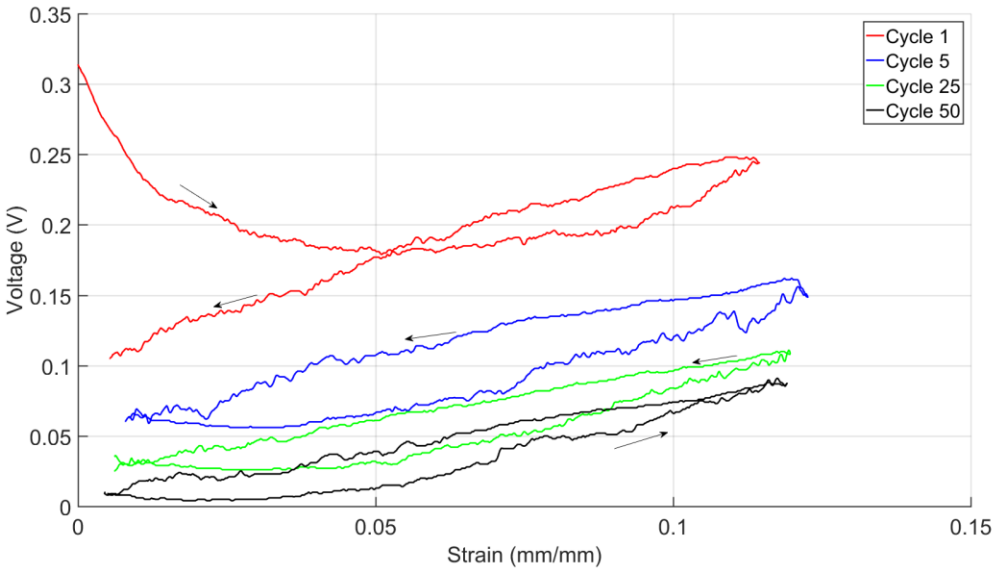

Figure 4.6 Voltage-Strain relation of 1.5 wt% for selective cycles

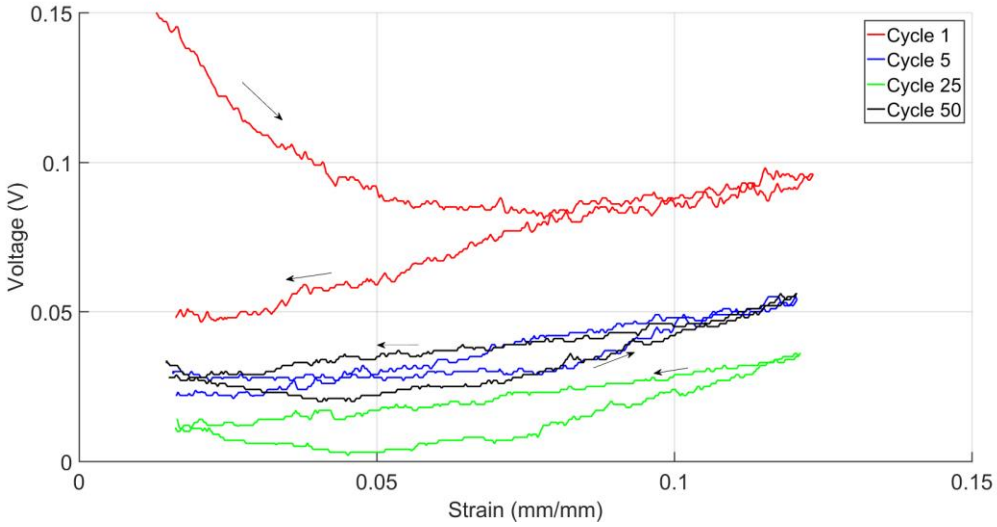

Figure 4.7 Voltage-Strain relation of 1.75 wt% for selective cycles

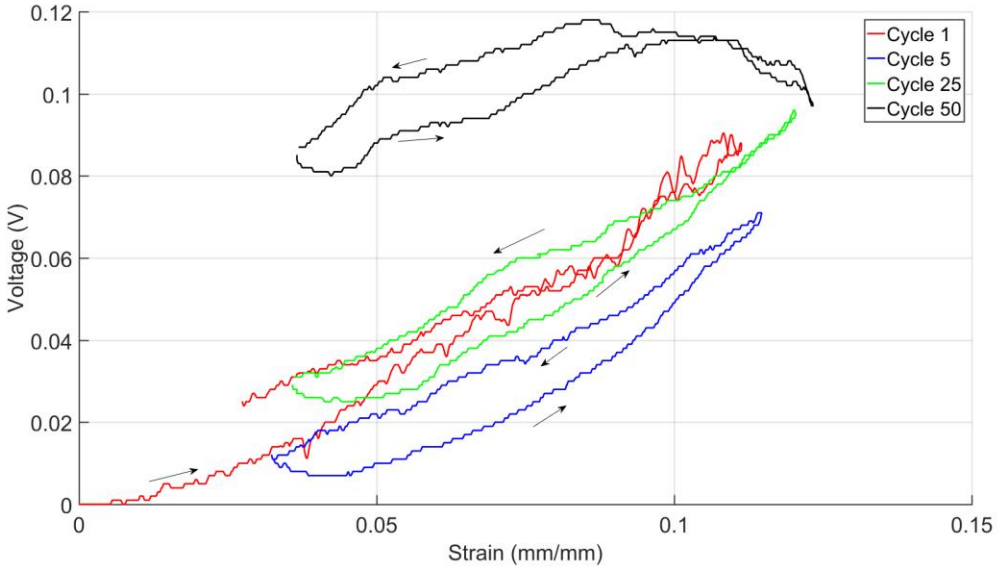

Figure 4.8 Voltage-Strain relation of 2.0 wt% for selective cycles

Figure 4.4 to Figure 4.8 show that the electrical hysteresis settles over subsequent cycles, with the voltage-strain relation overlapping in the later cycles. This settling is significant and can be seen beginning from the fifth cycle. Cycles 5, 25, 50 tend to be closer to each other while cycle 1 is the outlier. Moreover, different percentage of MWCNT will settle differently and at different rates. The nanocomposite in tension experiences a decrease in conductivity due to applied strain. This decrease is related to the structural change, as the length of nanocomposite increases the distance between nanotube increases, causing a reduction in conductivity (Figure **4.9**).

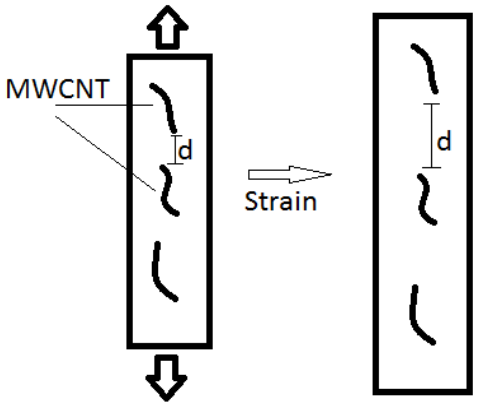

Figure 4.9 Structure change and conductivity (Type I)

There are two noteworthy properties when comparing the voltage-strain between two different MWCNT weight percentages. The first one is the noise of the signal as the material undergoes deformation. The second one is the linearity of the trend,when the sample is stressed and unstressed, the signal increase and decrease linearly with deformation. It is important for a piezoresistive sensor to have low noise in the signal and

have linear relation with deformation.

It was noticed that as the amount ofadded MWCNT increases, the signal becomes less noisy and the trend of the signal becomes more linear. This can be seen when comparing 0.75wt% to 1.5wt%, where the higher percentage of MWCNT is significantly more linear. However, the increase in linearity causes a reduction in sensing sensitivity.

The 2 wt% response is an example of signal withmaterial degradation, Figure 4.8. The curve for cycle 50 is non-linear which is due to the material deteriorating overtime. Overall, the responses tend to overlap after undergoing higher iterations of cyclic loading and unloading. The voltage to strain responses become linear after the first few cycles, this is a good indicator for the electrical stability. However, the 0.5 wt% and 0.75 wt% are nonlinear, making them less suitable for use as a sensor.

Furthermore, the peak-to-valley trend was plotted and presented from Figure 4.10 to Figure 4.14. The linearity of the trend overtime shows electrical stability of the nanocomposite and is paramount in 1.5 wt% and 1.75wt%. The peaks are chosen as the highest points of deformation, with valleys being the relaxed states within the cycle.

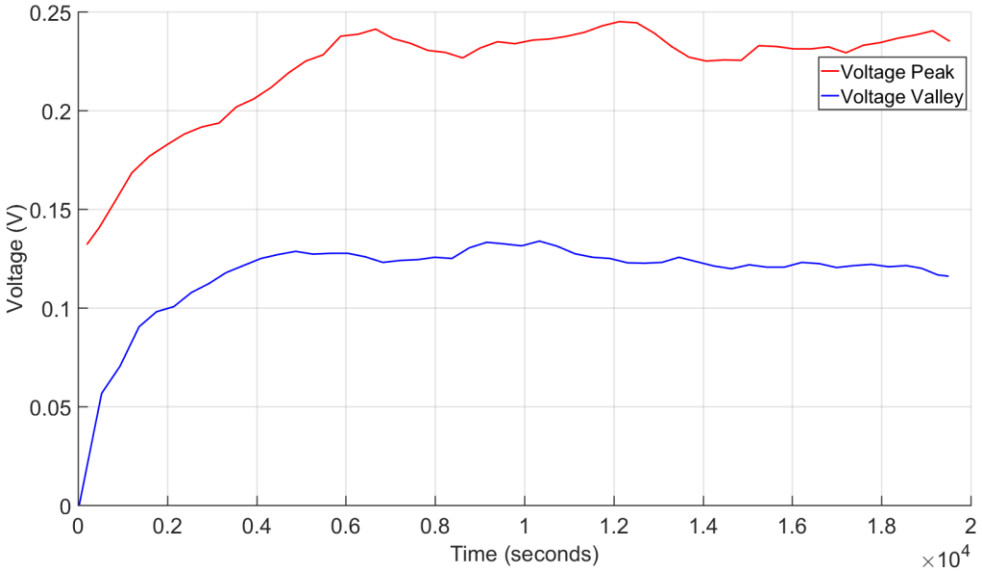

Figure 4.10 Peak and valley trend for 0.5 wt%

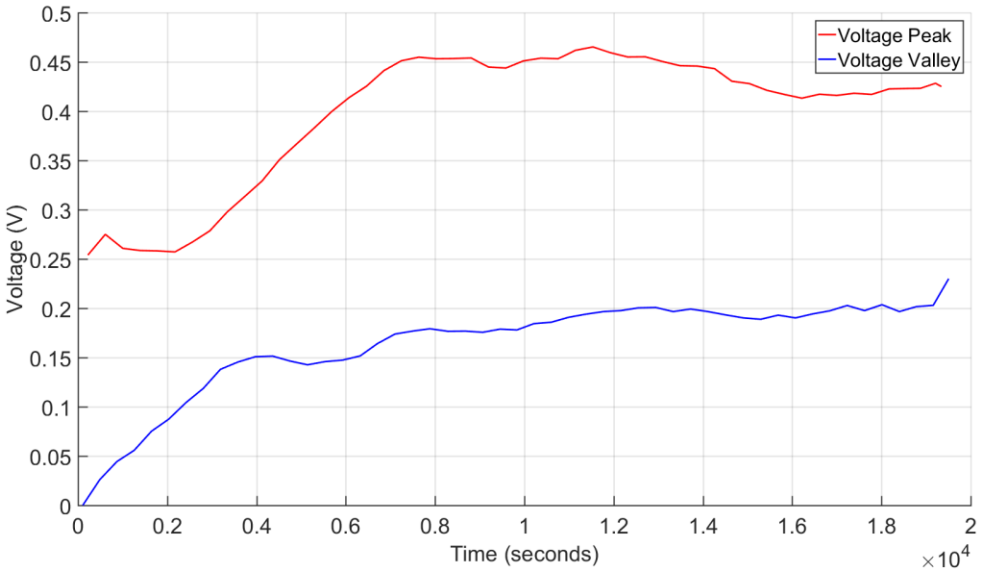

Figure 4.11 Peak and valley trend for 0.75 wt%

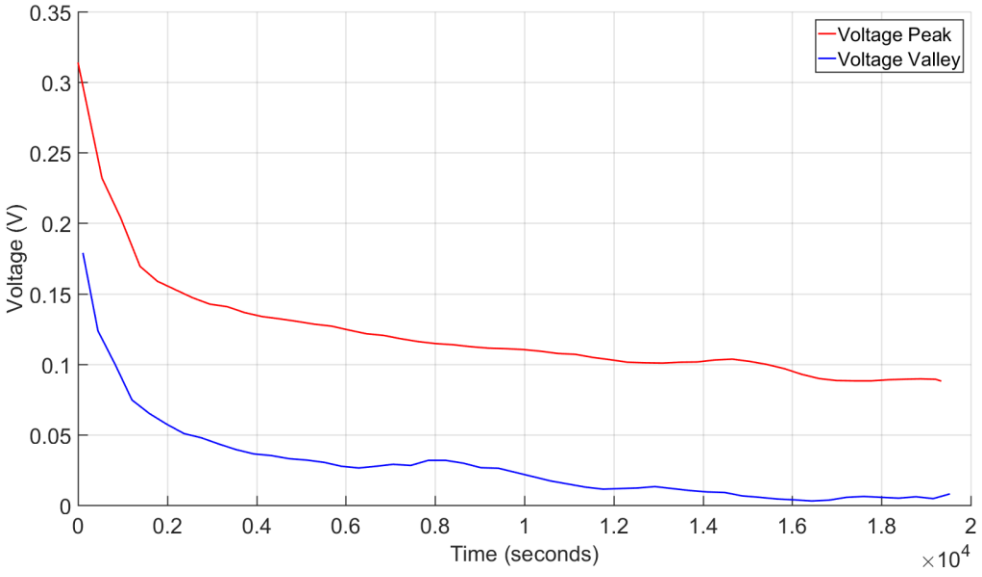

Figure 4.12 Peak and valley trend for 1.5 wt%

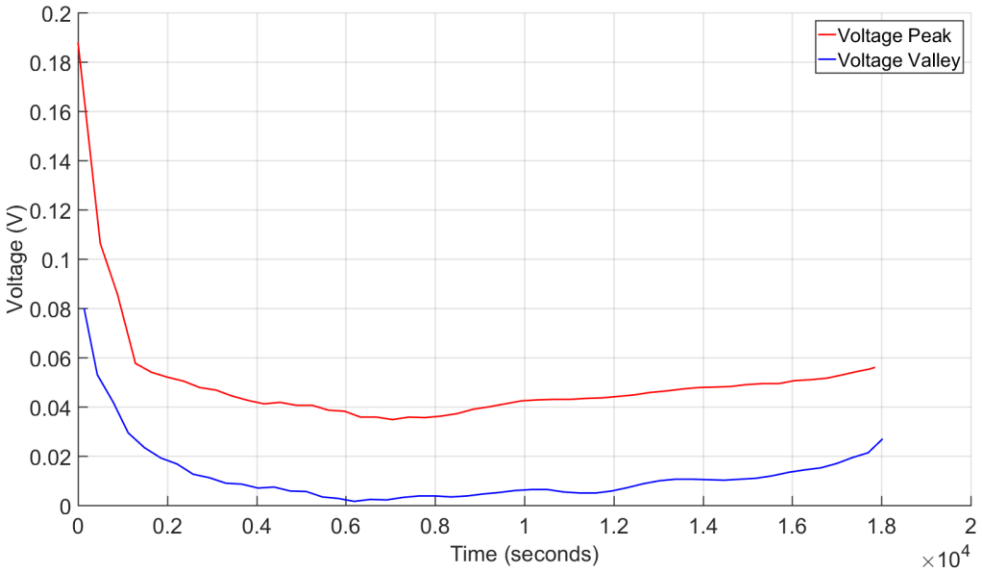

Figure 4.13 Peak and valley trend for 1.75 wt%

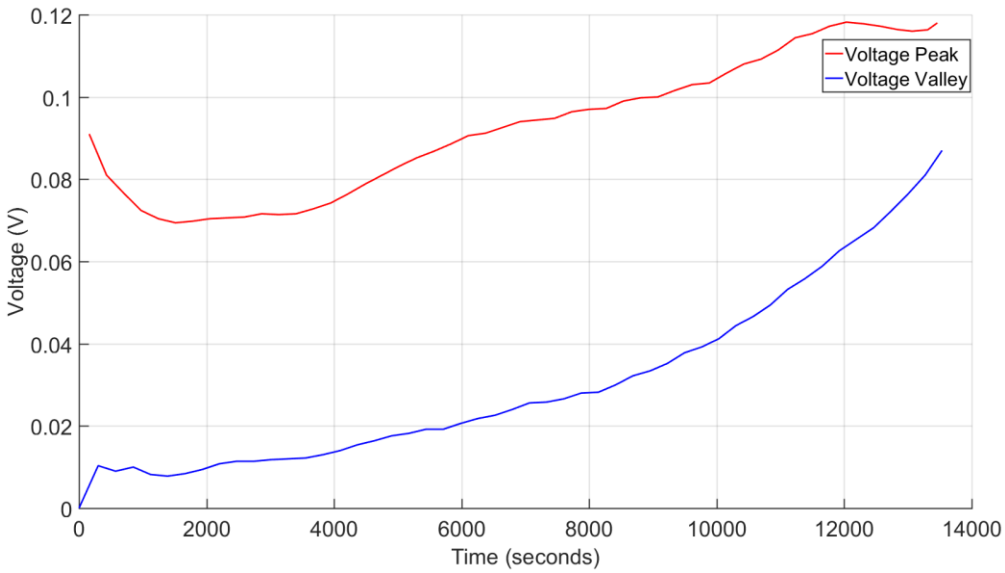

Figure 4.14 Type I: 2.0wt%: Flowing trend of peak-to-valley

The peak-to-valley signify the range of variation in the voltage signal. The linearity of this trend, as well as the difference between the peak and valley are consistent. The linearity of these two curves along with the constant separation show the sensor's stability.

4.3.2 Type II Samples

The Type II samples underwent compressive loading for 50 cycles. The electrical stability of the material was determined using similar analysis as for Type I samples.The conductivity responses over time for different samples are shown in Figure 4.15. Furthermore, we looked at the resistance to strain response over 50 cycles, where we

differentiated and analyzed key cycles. Finally, the trend of the peak-to-valley for the resistance to time response for different samples was analyzed.

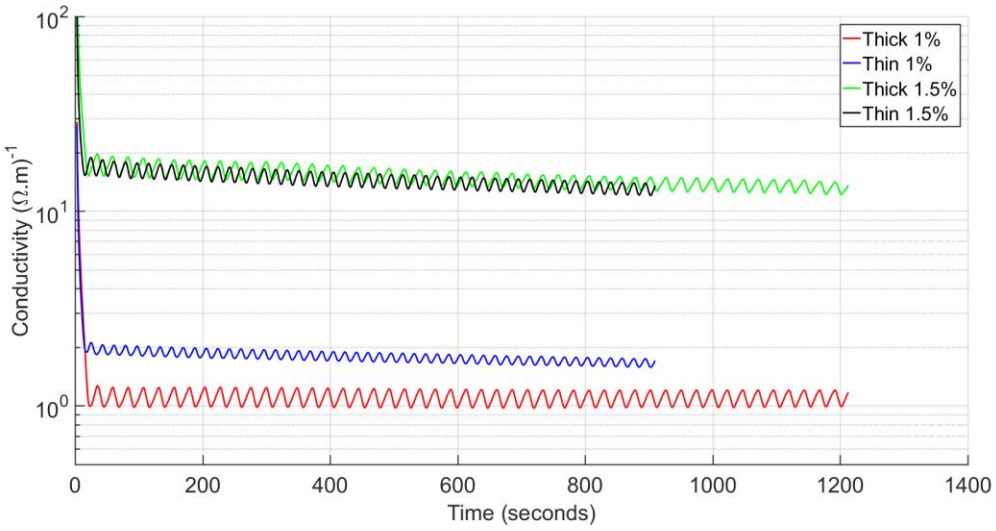

Figure 4.15 Conductivity response of different samples over time

The Thick and Thin samples of a particular weight percentage of MWCNT have comparable conductivities.The 1.5 wt%is more conductive than 1 wt%. The linear, near horizontal conductivity curve over time signifies that the material is electrically stable.

As with the Type I nanocomposite, Type II nanocomposite exhibited electrical hysteresis, which is seen in the resistance to strain relation. There are two different types of hysteresis, the first one is a hysteresis between the loading and unloading of a single cycle, the second one is between two cycles.The hysteresis exists due to the initial random orientation of MWCNTs and dissipates with the incremental alignment of MWCNT due to mechanical stretching. The electrical hysteresis between loading and unloading of a cycle decreases as the total number of cycles increases. This is evident

from the shrinking area enclosed by the loading and unloading curves. However, in majority of the samples, the overall resistance increased with each cycle of loading and unloading. Figure 4.16 to Figure 4.19 show the selective cycles of resistance to strain relation for different Type II samples.

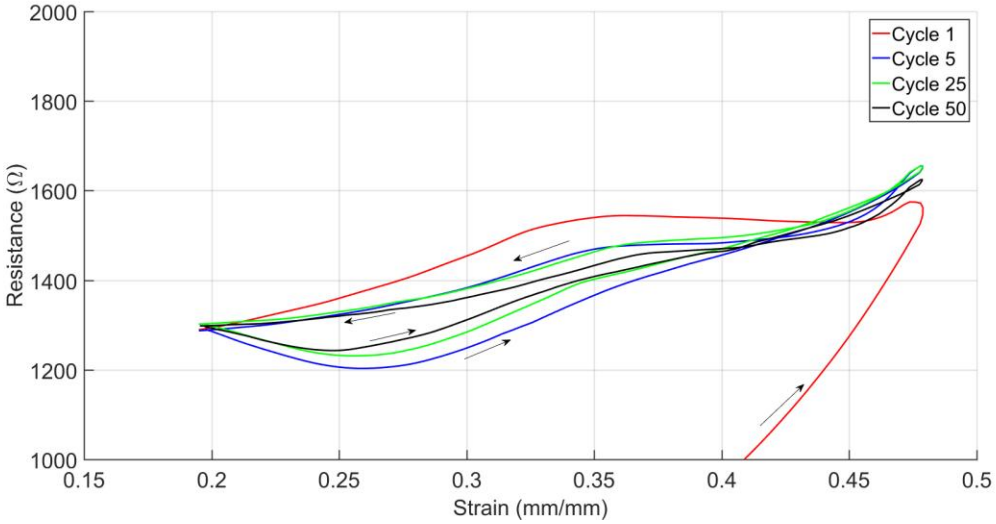

Figure 4.16 Resistance-Strain relation of 1% Thick for selective cycles

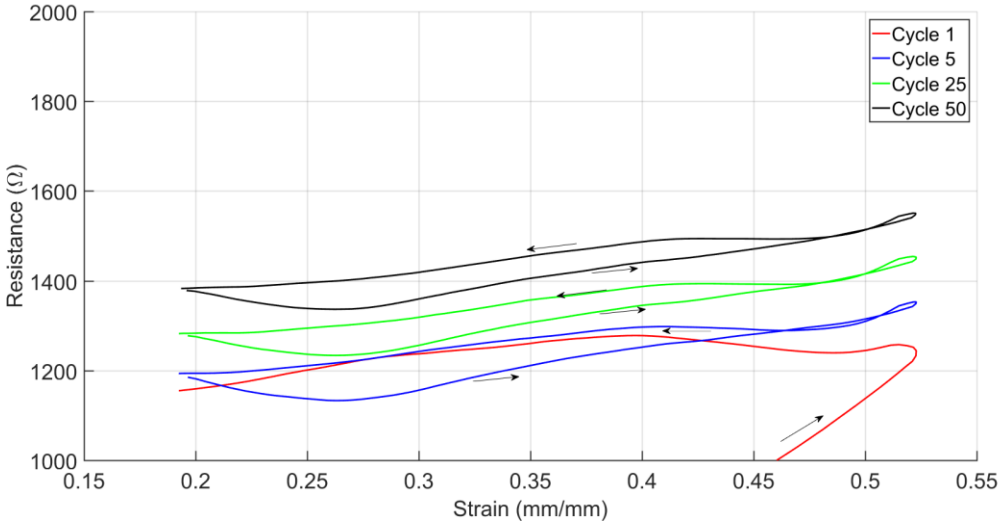

Figure 4.17 Resistance-Strain relation of 1% Thin for selective cycles

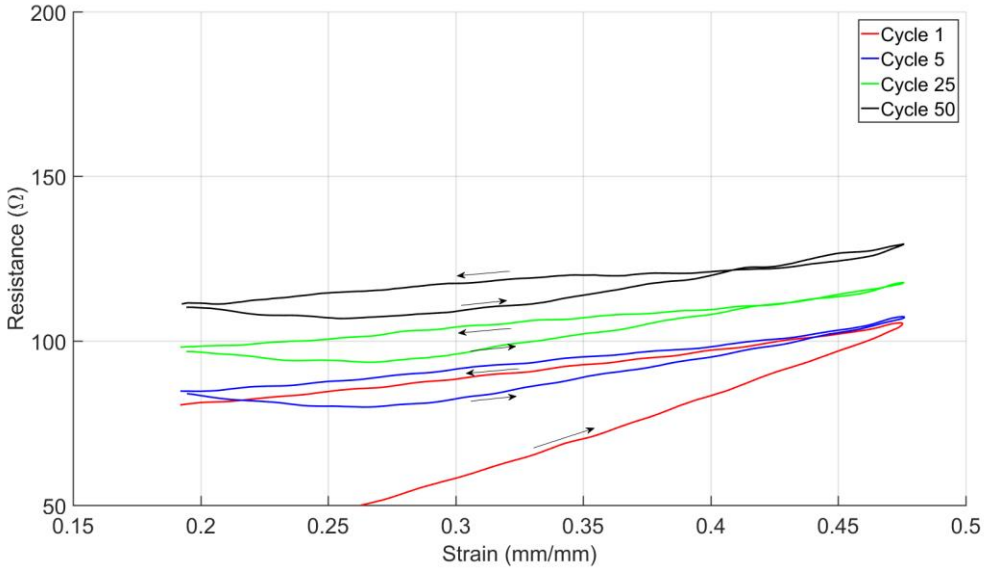

Figure 4.18 Resistance-Strain relation of 1.5% Thick for selective cycles

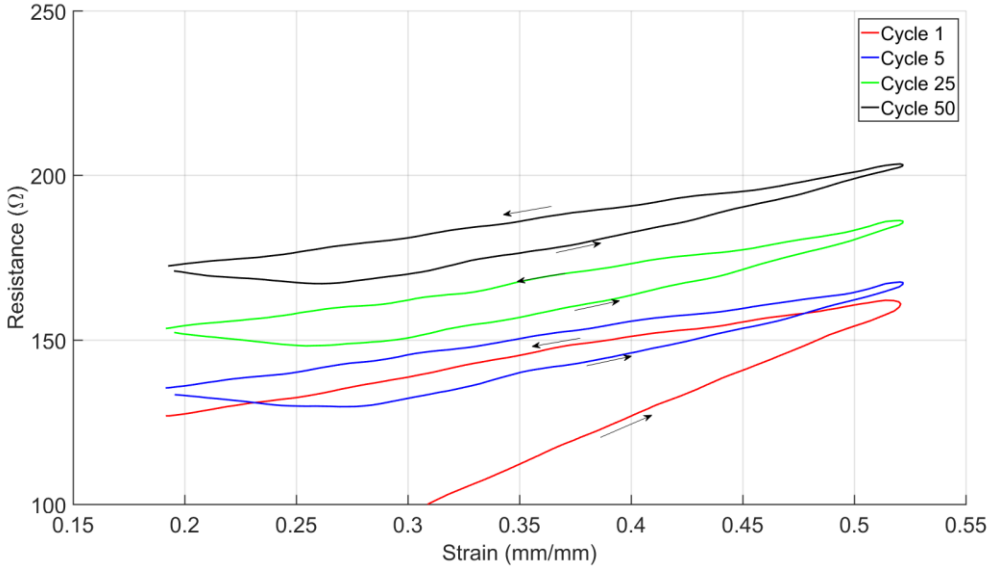

Figure 4.19 Resistance-Strain relation of 1.5% Thin for selective cycles

The resistance response is linear during the loading phase of a cycle (Figure 4.16 to Figure 4.19). Even though the overall resistance increases with increased number of cycles.The linearity is a good indicator of electrical stability as it allows for predictable behaviour, which is paramount for a sensor. The 1.5 wt% samples have lower resistance and are more linear than their 1 wt% counterparts. However,there is not a significant difference between the stability of Thick and Thin samples. The nanocomposite in compression experience an increase in conductivity when strained up to 30%, but experiences reduced conductivity when more strain is applied. This behaviour is explained by the increased proximity of MWCNT to each other, which causes an increase in conductivity at strains up to 30%. However, when the strain in increased any further, the thickness which effectively conducts is decreased, causing a decrease in the conducting pathways which leads to a decrease of conductivity at higher strain (Figure **4.20**).

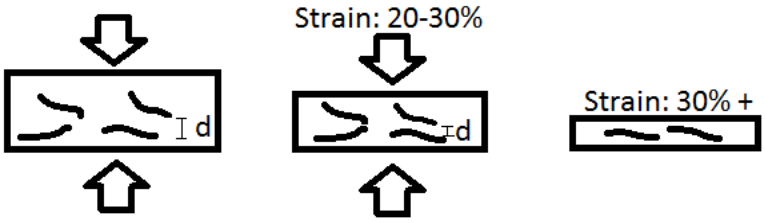

Figure 4.20 Structure change and conductivity (Type II)

The peak-to-valley trendof the resistance response was plotted and showed in Figure 4.21 to Figure 4.24.The peaks and valleys are the highest and lowest resistance

values for a particular cycle. The linearity of the trend overtime shows electrical stability of the nanocomposite.

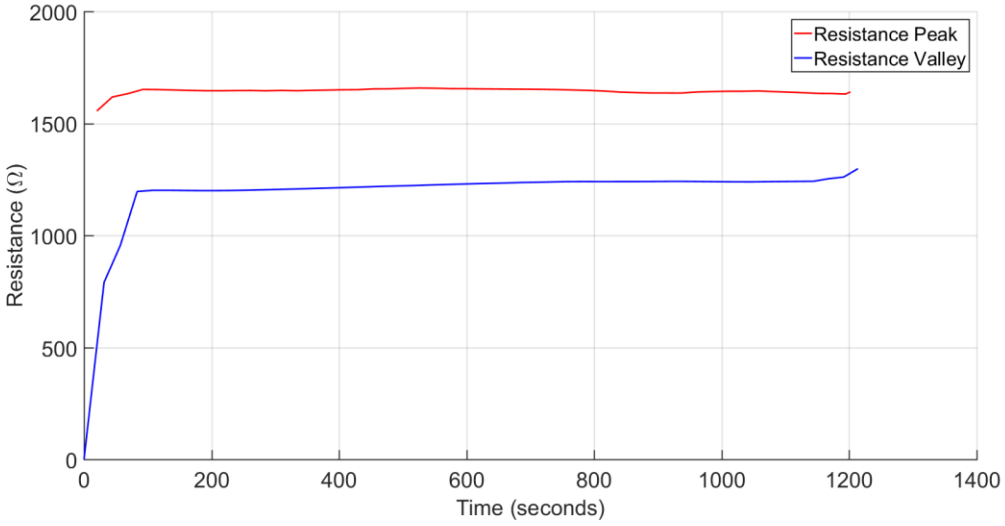

Figure 4.21 Peak and valley trend for 1% Thick

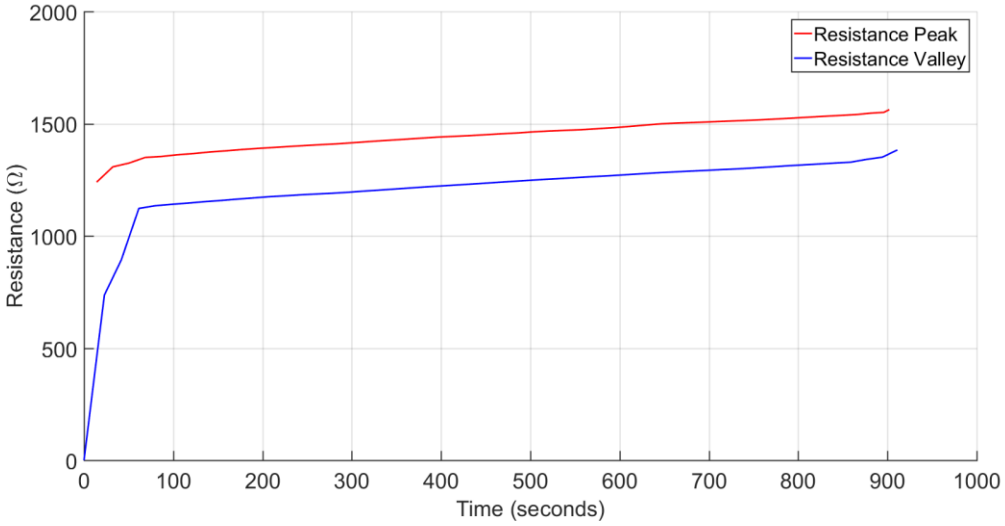

Figure 4.22 Peak and valley trend for 1% Thin

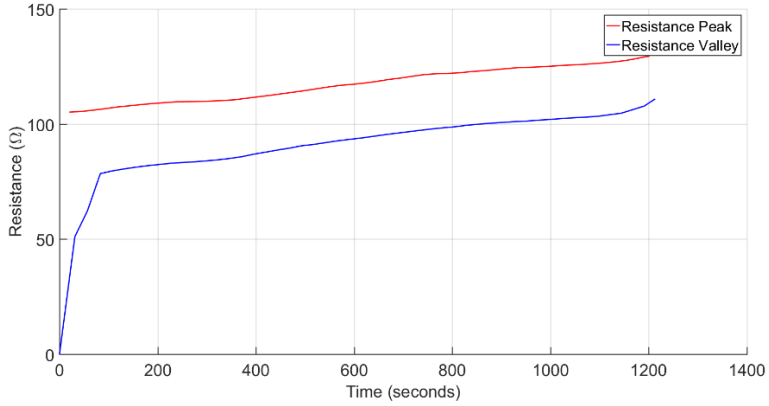

Figure 4.23 Peak and valley trend for 1.5% Thick

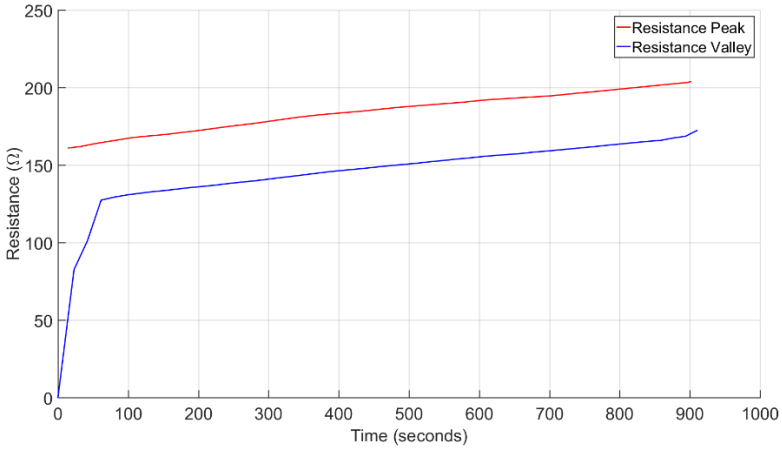

Figure 4.24 Peak and valley trend for 1.5% Thin

The peak-to-valley trends signify the range of sensitivity in the resistance signal. The trends are linear and are slightly increasing in resistance over time. It should be noted that the peaks and valleys increase simultaneously and remain parallel. The linearity of these two curves along with the constant separation,proves the sensors' stability. There is not a significant difference in the electrical properties of Thick and Thin samples for a specific weight percentage of MWCNT.

Chapter 5 MECHANICAL PROPERTIES AND DISCUSSION

Summary: In this chapter, we present our results for the mechanical properties of the PDMS-MWCNT nanocomposite.

5.1 Introduction

The mechanical properties were determined over 50 cycles of repeated loading and unloading. The rate of deformation was 2mm/min and the measurements were taken simultaneously with electrical property measurements. We characterised the (i) Elasticity of nanocomposite by determining the change in Young's modulus due to added wt% of filler MWCNTs. We further compared the stress-strain relation for samples with different wt% MWCNT. The (ii) Mechanical stability of the nanocomposite was identified by observing the mechanical hysteresis over different cycles.

The mechanical properties of the nanocomposites are influenced by the amount of added MWCNTs. The addition of MWCNTs causes increase in stiffness, which is represented by the increase in Young's modulus. The measurements for Type I samples were taken with the MTS Criterion and Laser Extensometer, for Type II, only the MTS

Criterion was used. For Type I, the Laser was used to find displacement in the active region, where as for Type II, the displacement was provided crosshead gripper.

5.2 Elasticity of Nanocomposite

In this section we determined the elastic properties of the nanocomposite, mainly the Young's modulus. We see a decrease in elasticity with an increase in added MWCNTs. A comparison of the stress-strain curves for selected samples is provided as well. The comparison also shows a difference in the stress-strain curves of the cycle 1 and cycle 50 for selected nanocomposite samples. This difference is representedas hysteresis and can be of concern when looking at stability of nanocomposite.

5.2.1 Type I Samples

The elastic properties of the nanocomposite for different weight percentage of MWCNTs were evaluated by uniaxial tensile tests. The Young's modulus (E), the slope of stress-strain curve for different weight percent of MWCNT is represented inFigure 5.2. The Young's modulus increases with an increase in the MWCNT loading. The stress-strain curves from the cycle 1 and cycle 50 of loading for different weight percentage of MWCNTs nanocomposite are plotted in Figure5.1.

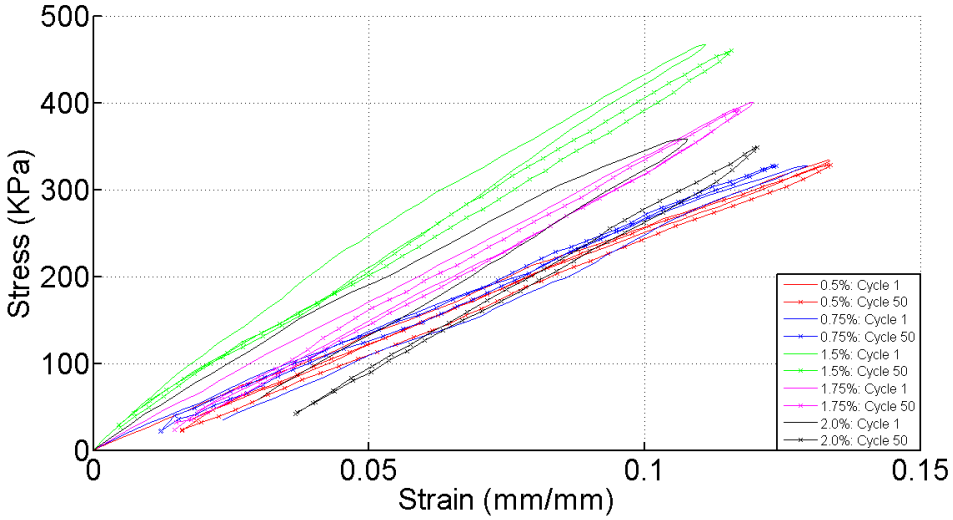

Figure 5.1 Stress-Strain of wt% Type Inanocomposite

The 1.5 wt% sample represented in Figure5.1has the highest slope, indicating a high Young's modulus. However, it must be noted that the Young's modulus provided in the Table 5.1 is the cumulative average of all the samples, where the 1.5 wt% is more flexible than its higher wt% counterparts.

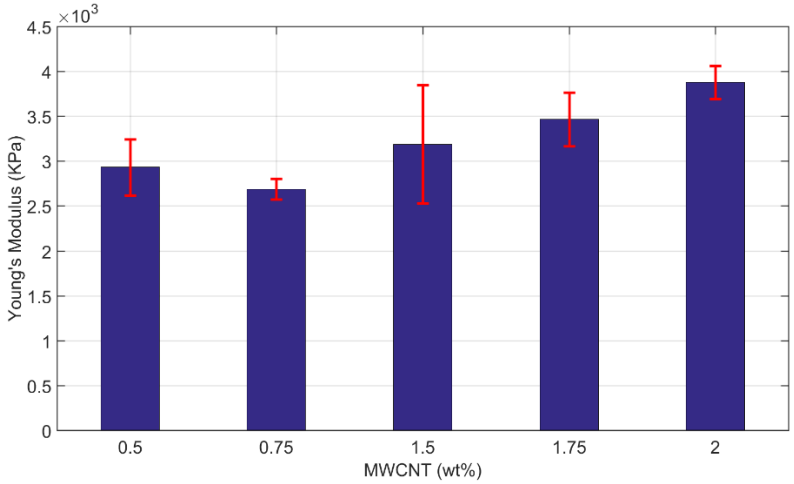

Figure 5.2 Young's Modulus of the Type I nanocomposite

The Figure 5.2 shows an increase in Young's modulus with an increase in MWCNT filler. The stiffnesses of 0.5 wt% and 0.75 wt% are similar due to relatively low amount of MWCNT's. On average, the addition of the MWCNT changes the material properties of the PDMS by increasing its stiffness, as represented by the increased Young's modulus.According to the results, for a flexible nanocomposite, it is prudent to have a low amount of added MWCNT.

Table 5.1 Type I Young's Modulus

MWCNT wt%	Young's Modulus (KPa)	Young's Modulus Standard Deviation (KPa)
0.5	2931.3	311.2
0.75	2687.6	116.3
1.5	3186.7	658.2
1.75	3466.3	298.2
2.0	3877.5	183.6

5.2.2 Type II Samples

The elastic properties of the Type II nanocomposite were evaluated by compression tests. The stress-strain curves of the first cycle of loading showing different Type II samples are plotted in the Figure 5.3.

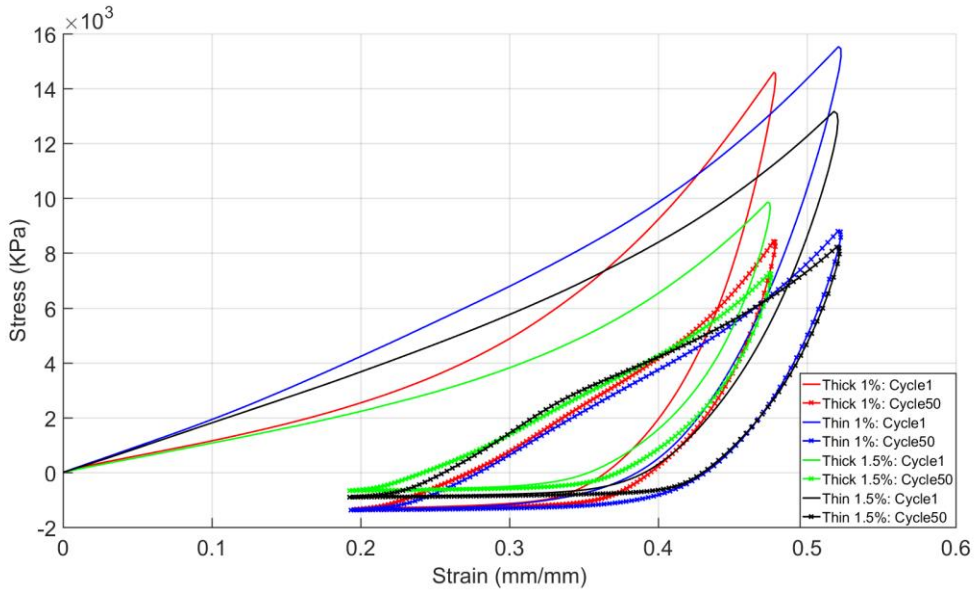

Figure 5.3 Stress-Strain of different samples in Type II nanocomposite

The stress-strain for Thick samples of both 1wt% and 1.5wt% MWCNT show a slight curvature during loading, whereas the Thin samples are more linear, Figure5.3. During unloading, the stress-strain curve has a negative value. This is because the samples were preloaded before testing and the unable to exert complete force after loading.

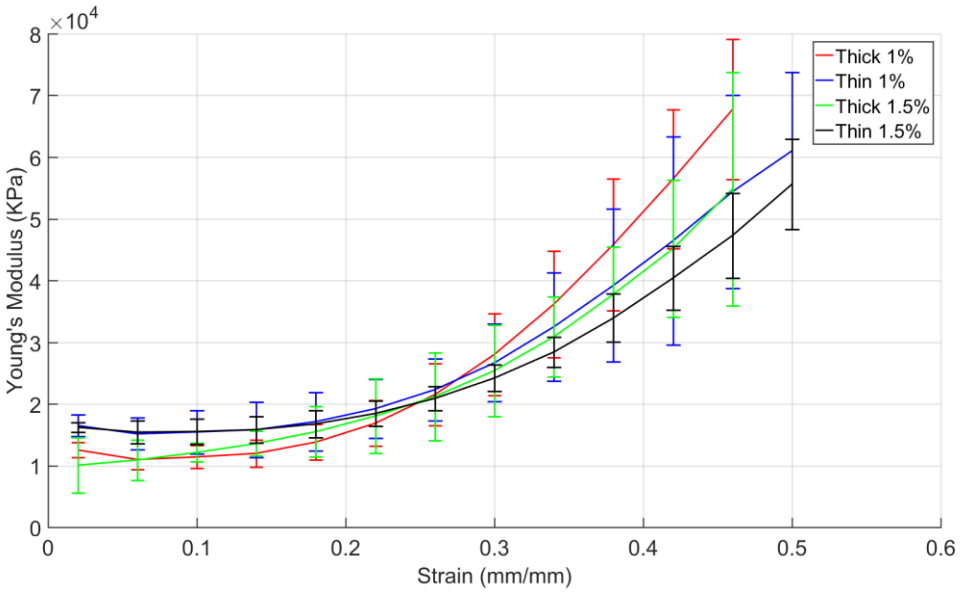

Figure 5.4 Young's Modulus of the Type II nanocomposite

The Young's modulus (E), slope of stress-strain curve for different samples is presented in Figure 5.4. The addition of the MWCNT changes the material properties of the PDMS by increasing its stiffness, represented by the increase in Young's modulus. The stiffnesses of 1wt% and 1.5 wt% of Type II nanocomposite samples are comparable due to similar amount of added MWCNT's. The Young's Modulus for 1wt%Thick sample is higher, but it also has an increased error. The Young's modulus represented in Figure 5.4 is the cumulative average of Type II samples and is not constant due to high loading strain. The Young's modulus increases with increased strain, which is a typical behavior of hyperelastic materials. The Table 5.2summarizes our findings for Type II Young's modulus.

Table 5.2 Type II Young's Modulus

Strain Range (mm/mm)	Young's Modulus ±Standard Deviation (KPa)			
	1.0 Thick	**1.0 Thin**	**1.5Thick**	**1.5Thin**
0.00-0.04	12.5±1.25 e3	16.4±1.76 e3	10.0±4.44 e3	16.1±0.77 e3
0.04-0.08	10.2±1.58 e3	14.5±2.58 e3	10.8±3.26 e3	15.2±1.88 e3
0.08-0.12	10.2±1.86 e3	14.4±3.53 e3	11.7±1.53 e3	14.8±2.08 e3
0.12-0.16	11.1±2.18 e3	15.3±4.51 e3	13.0±1.99 e3	15.0±2.15 e3
0.16-0.20	12.8±2.88 e3	16.4±4.73 e3	14.8±4.11 e3	16.2±2.17 e3
0.20-0.24	15.4±3.69 e3	18.3±4.75 e3	17.3±6.03 e3	17.7±2.08 e3
0.24-0.28	19.3±5.02 e3	21.0±2.01 e3	20.4±7.12 e3	19.8±1.97 e3
0.28-0.32	25.5±6.63 e3	24.8±6.31 e3	24.4±7.40 e3	23.2±2.14 e3
0.32-0.36	34.3±8.63 e3	30.7±8.78 e3	28.8±6.51 e3	27.2±2.44 e3
0.36-0.40	45.4±10.7 e3	38.2±12.3 e3	35.8±7.71 e3	32.7±3.89 e3
0.40-0.44	56.1±11.2 e3	47.6±16.8 e3	44.7±11.1 e3	38.8±5.19 e3
0.44-0.48	67.7±11.3 e3	54.5±15.6 e3	54.8±18.9 e3	47.4±6.89 e3
0.48-0.52		61.0±12.7 e3		55.6±7.32 e3

5.3 Mechanical Stability

A mechanically stable nanocomposite is necessary in order to have a sensor with long work life. A nanocomposite where the polymer matrix degrades after repeated loading is unsuitable. Overall, we found that if a nanocomposite had a trapped bubble cavity during fabrication, then it would fail within a few cycles. However, the samples which survive the initial phase are mechanically stable and have a converging hysteresis, where the

hysteresis reduces within the successive cycles as the number of cycles increases.

5.3.1 Type I Samples

The mechanical failure of the nanocomposite due to repeated stress is of concern. Thus, we looked at the stress-strain behavior of the nanocomposite samples over 50 cycles. This behavior for cycles 1, 5, 25 and 50 is represented in Figure 5.5to Figure 5.9.

The first cycle was pulled from 0 mm, however in every other cycle, the nanocomposite was kept under tension and was not allowed complete unloading. The later cycles had a minimum deformation of 1 mm at unloading.

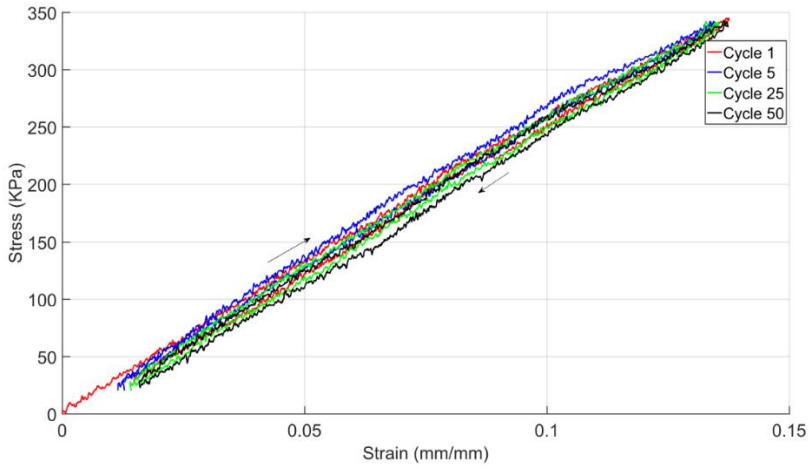

Figure 5.5 Stress-Strain behavior of 0.5 wt% nanocomposite

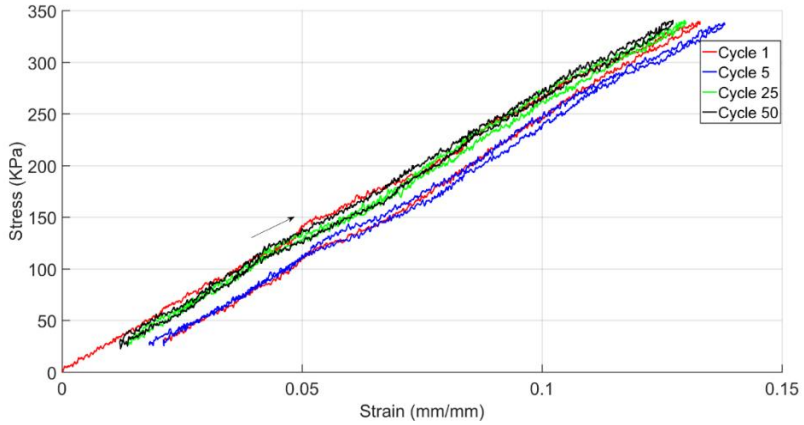

Figure 5.6 Stress-Strain behavior of 0.75 wt% nanocomposite

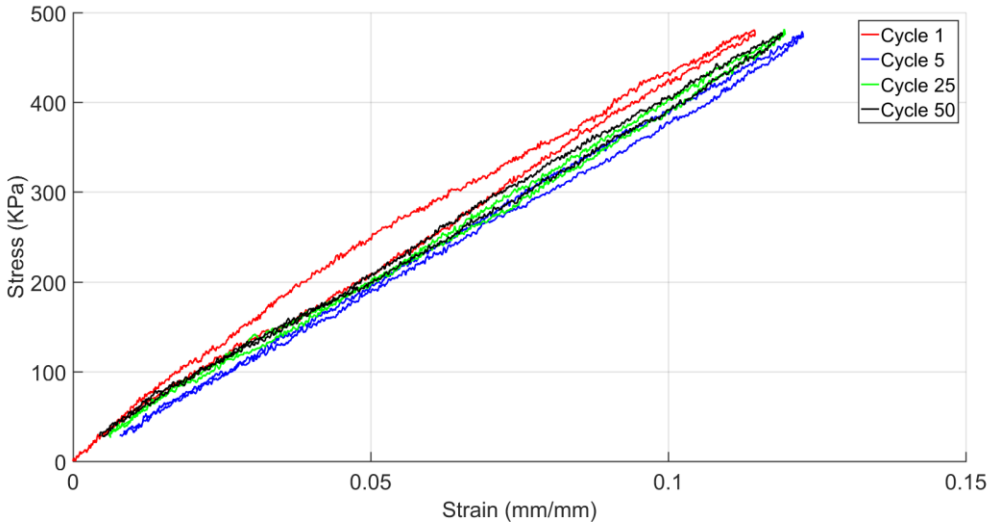

Figure 5.7 Stress-Strain behavior of 1.5 wt% nanocomposite

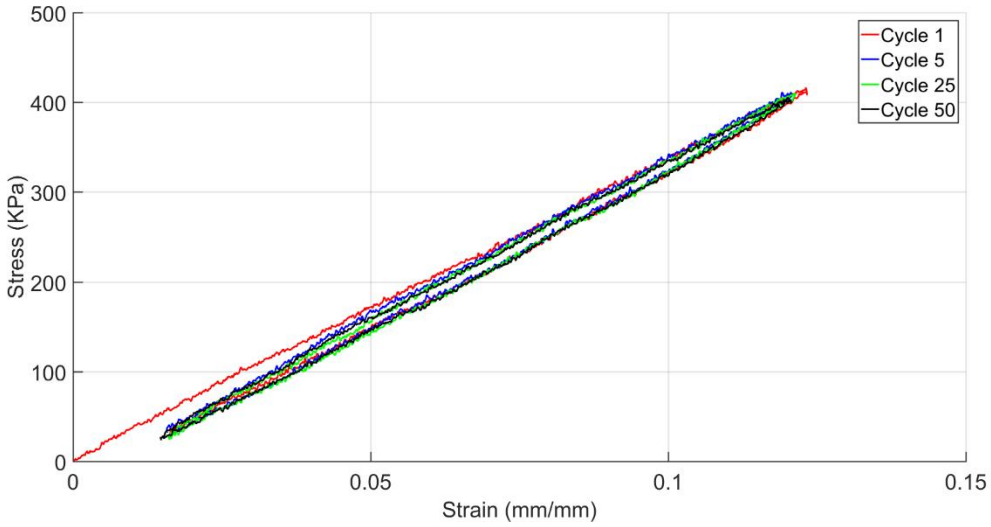

Figure 5.8 Stress-Strain behavior of 1.75 wt% nanocomposite

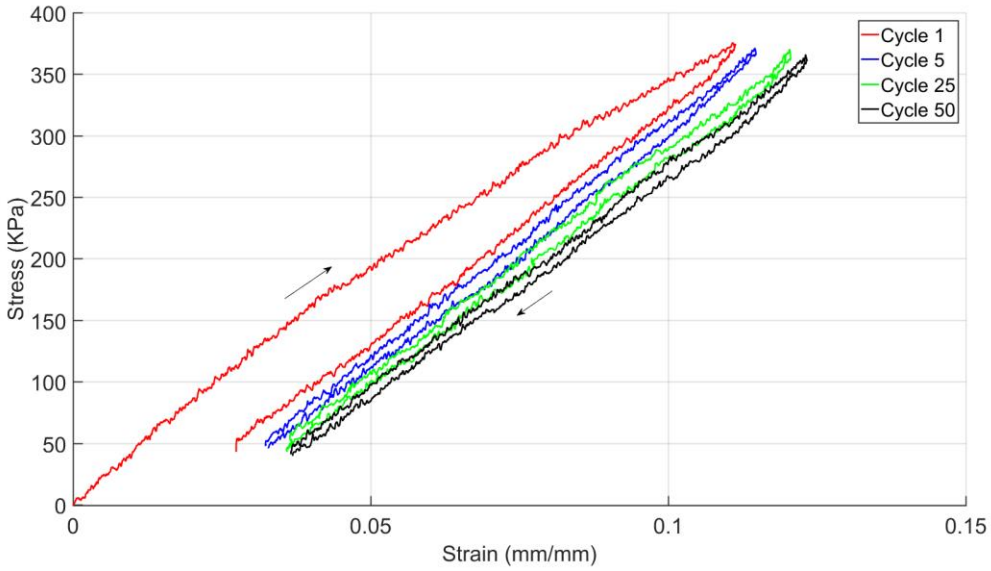

Figure 5.9 Stress-Strain behavior of 2.0 wt% nanocomposite

The nanocomposites undergo a strong hysteresis in the initial cycles and start to

become linear after fivecycles, as seen in Figure 5.5to Figure 5.9. This linearity is a good indicator of mechanical stability as it shows that the material does not undergo mechanical degradation over repeated loading. Moreover, the stress-strain curves overlap each other after cycle five, which signifies the settling of the material and reduced overall hysteresis between consecutive cycles. Furthermore, one important point of note; there exists hysteresis between the loading and unloading within each cycle, it is most pronounced for the first cycle and decreases over subsequent cycling.

5.3.2 Type II Samples

We analysed the behaviour of the nanocomposite over repeated loading and looked at the stress strain behavior for specific cycles. The behavior of the samples for cycles 1, 5, 25 and 50 is presented in Figure 5.10 to Figure 5.13.

Samples with two different thicknesses werecompressed, 1.4 mm (Thick) and 1.0 mm (Thin). The thick samples were pre-strained to 0.3 mm. In the successive cycles, the sample was always kept loaded by ranging the extension from 0.3 mm to 0.7 mm, with a total deformation of 0.4 mm. The thin samples were pre-strained to 0.2 mm. In the successive cycles, the sample was always kept loaded by ranging the extension from 0.2 mm to 0.5 mm, with a total deformation of 0.3 mm.

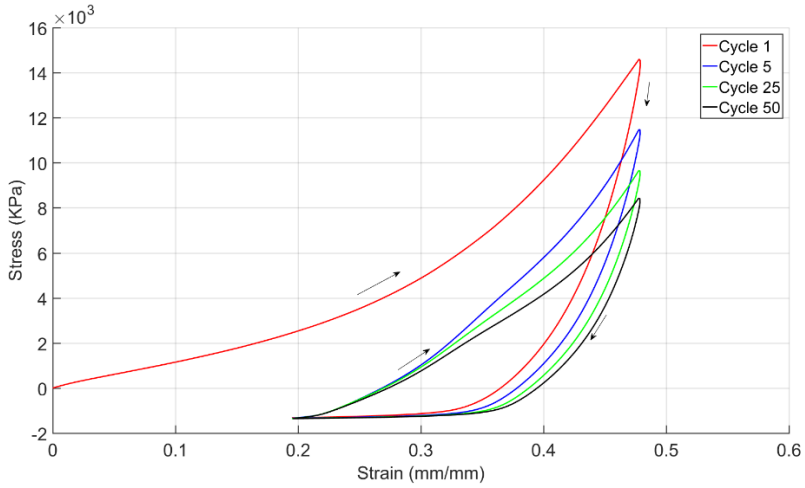

Figure 5.10 Stress-Strain behavior of 1% Thick nanocomposite

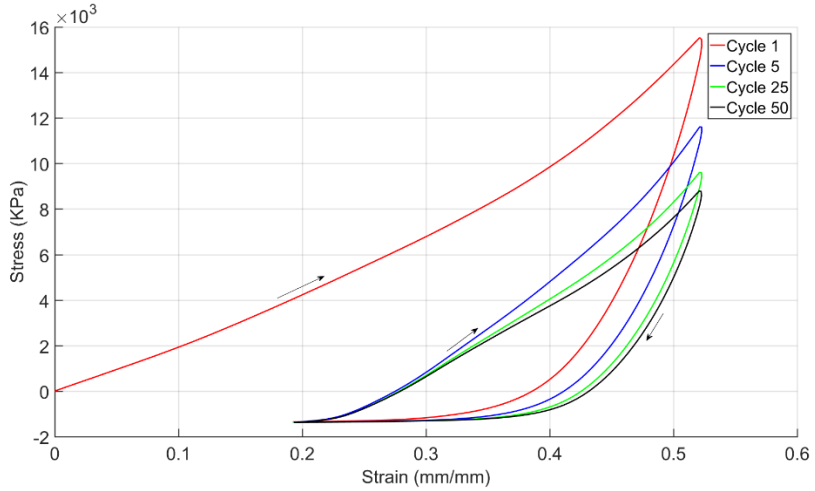

Figure 5.11 Stress-Strain behavior of 1% Thin nanocomposite

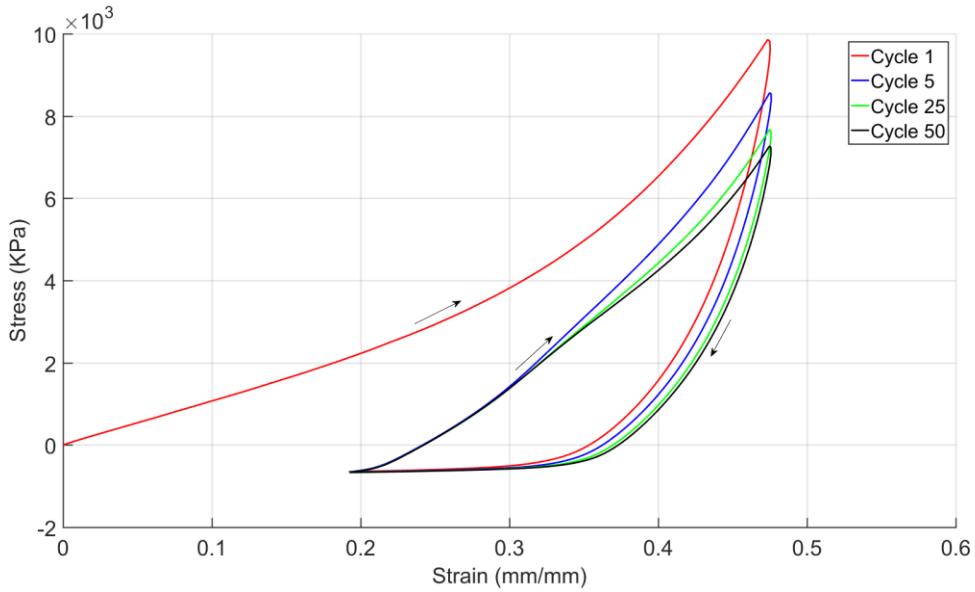

Figure 5.12 Stress-Strain behavior of 1.5% Thick nanocomposite

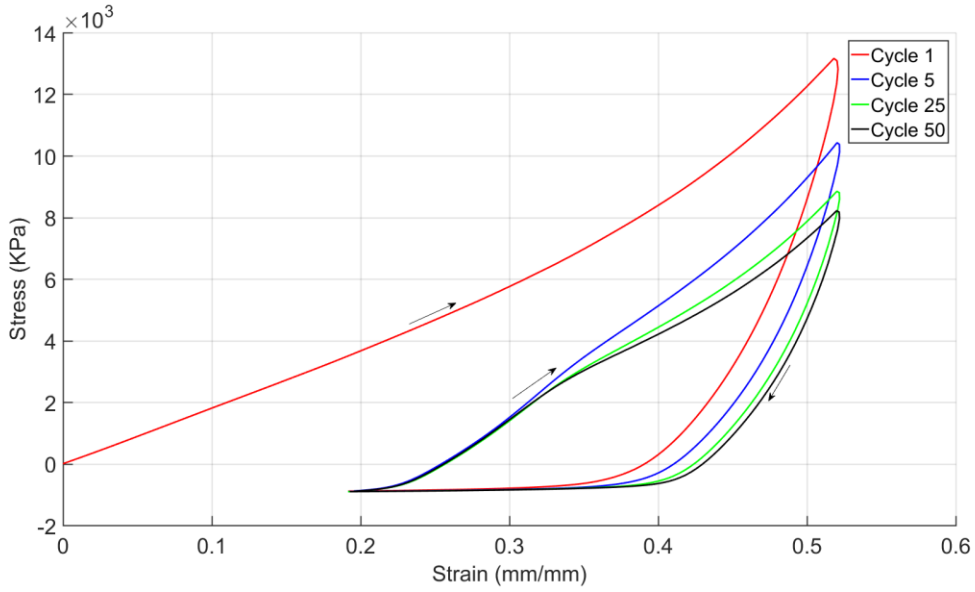

Figure 5.13 Stress-Strain behavior of 1.5% Thin nanocomposite

The hysteresis in the nanocomposites decreases as the samples undergo more cycles of loading and unloading. This decrease in mechanical hysteresis is represented by the shrinking area enclosed by the loading and unloading curves. The area covered by Cycle 50 is smaller than area of Cycle 5.

There is a constant decrease in the maximum stress of the nanocomposite because the rubber material takes longer to rebound with increasing cycles. This slower rebound can be due to the internal degradation of the material, where the polymer chains are damaged, causing the nanocomposite to lose its flexibility. However, rubbers in general undergo a stiffening effect, which is known as Mullins effect. Where the material has mechanicalhysteresis and settles overtime.In the presented analysis, the stress becomes negative as the strain decreases. This is because the samples were preloaded, where the force was set to zero during beginning of experiment and not due to loss of contact with the material, during loading. A sharp drop in stress would have represented a loss of contact during loading. The drop is not present in our finding.

In unloading section of the cycle, there was a slight loss of contact with material. The right side of any cycle is the return to initial position (unloading). The loss of contact is during the near horizontal stress line, from strain 0.2 to 0.3. This gap exists due to slow rebound time of the material and does not affect the measurements. The loss of contact during loading would have been of concern. The speed of unloading is a displacement controlled at 2mm/min, thus some loss of contact is unavoidable.

The Type I and Type II are both stable, but with hysteresis, thus improvements need to be made in processing technique to reduce the hysteresis. However, nanocomposite in tension experienced less change, thus less hysteresis because it was dimensionally constrained throughout deformation and relaxation, whereas Type II samples were only constrained during loading and were allowed to rebound freely during unloading. The rebound rate decreases as material experiences fatigue with increased number of cycles, causing the Type II to experience more hysteresis.

Chapter 6 PIEZORESISTIVITY AND DISCUSSION

Summary: In this chapter, we present our results for the piezoresistive properties of the PDMS-MWCNT nanocomposite.

6.1 Introduction

The properties were determined over 50 cycles of repeated loading and unloading at a deformation rate of 2 mm/min. During the setup and testing, it was observed that any forces acting on the electrodes (wires or shim) generated noise in the measured electrical signal. Thus, care was taken when connecting the electrodes to the measuring instruments and the possibilities of pushing or pulling on the electrodes were reduced. The piezoresistive properties were determined from mechanical and electrical properties, measured simultaneously. The MTS Criterionappliedcompressive deformation while the four probe method for Type I and two probe method for Type II were used to measure the electrical response. The piezoresistivity was inferred from these measurements using a computing processor. We observed the (i) cyclic piezoresistivity with special consideration to the last ten cycles. The (ii) Gauge Factor of the nanocomposite was

determined along with the (iiii) sensitivity stability.

6.2 Cyclic Piezoresistivity

The cyclic piezoresistivity dependents on the change in electric properties due to mechanical deformation. The piezoresistive materials require a power supply to measure electrical signal, Keighley 6517B Electrometer meter and Keighley 6220 Precision current source were used for Type I, the resistance response was measured using Keighley 2450 SourceMeter for Type II. The MTS Criterion along with Laser Extensometer were used to measure deformation. In the first cycle, the Type I samples were strained to 7.5mm and unloaded up to 1mm. In the successive cycles, the samples were kept loaded by ranging the extension from 1mm to 7.5mm, with a total deformation of 6.5mm. The Type II samples have two different thicknesses, 1.4 mm (Thick) and 1.0 mm (Thin). The thick samples were pre-strained to 0.3 mm and in the successive cycles, the samples were compressed from 0.3 mm to 0.7 mm, with a total deformation of 0.4 mm. The thin samples were pre- strained to 0.2 mm and in the successive cycles, the samples were compressed from 0.2 mm to 0.5 mm, with a total deformation of 0.3 mm.

In this section, we explore the nanocomposite piezoresistivity, presented in the change of electrical signal over time while undergoing deformation. The electrical signal to strain correlation is also of interest and is shown as well. We found a strong relation between the electrical signal and deformation.

6.2.1 Type I Samples

The nanocomposites with different weight percentage were subjected to cyclic uniaxial tensile loading, while the electric response was measured via four-point probe method. The nanocomposites were loaded and unloaded 50 times at a rate of 2mm/min. The strain wasmeasured at the narrow middle section of the sample via placing two pieces of reflective tape, roughly 23mm apart. The voltage response to tensile loading and unloading over time for varying weight percent of MWCNT was characterized. The voltage response for weight percentage of 0.5%, 0.75%, 1.5%. 1.75% and 2.0% are shown in Figure 6.1 to Figure 6.5. 6.16.16.16.1

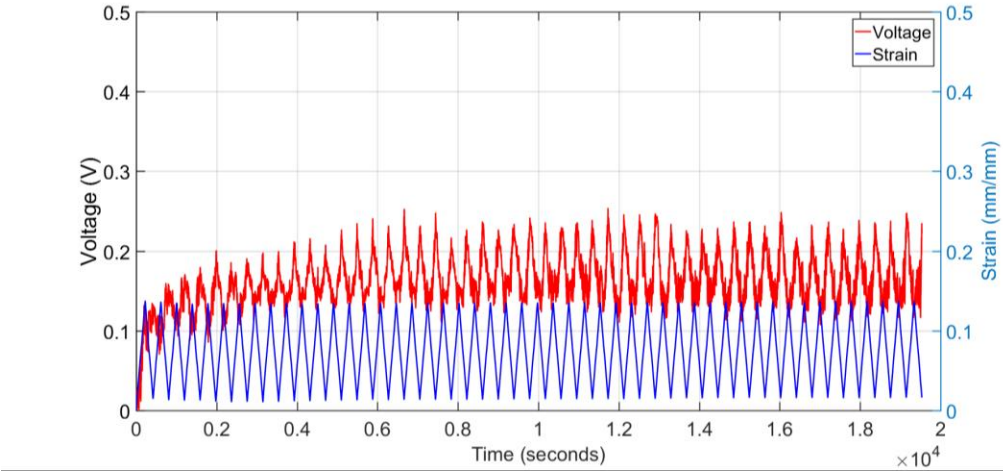

Figure 6.1 Voltage response of 0.5wt% MWCNTs to cyclic loading

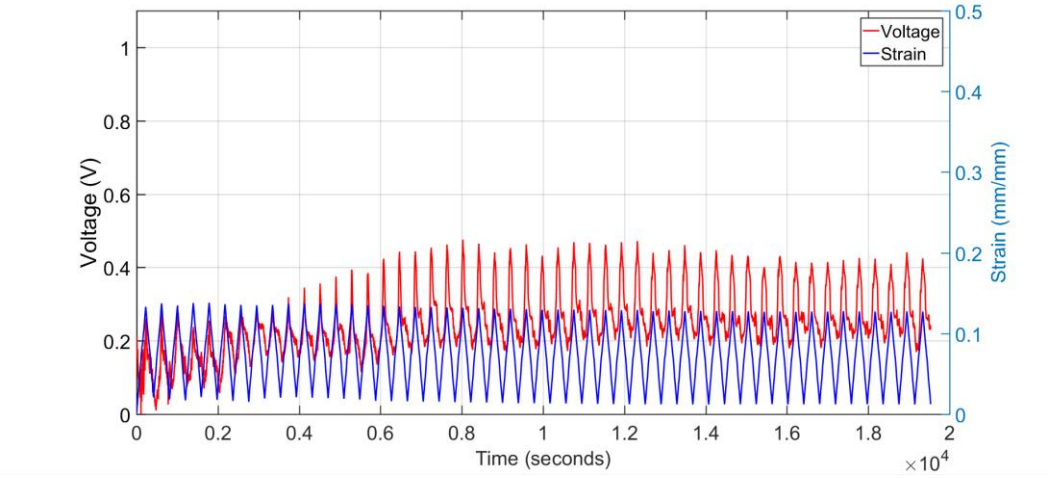

Figure 6.2 Voltage response of 0.75wt% MWCNTs to cyclic loading

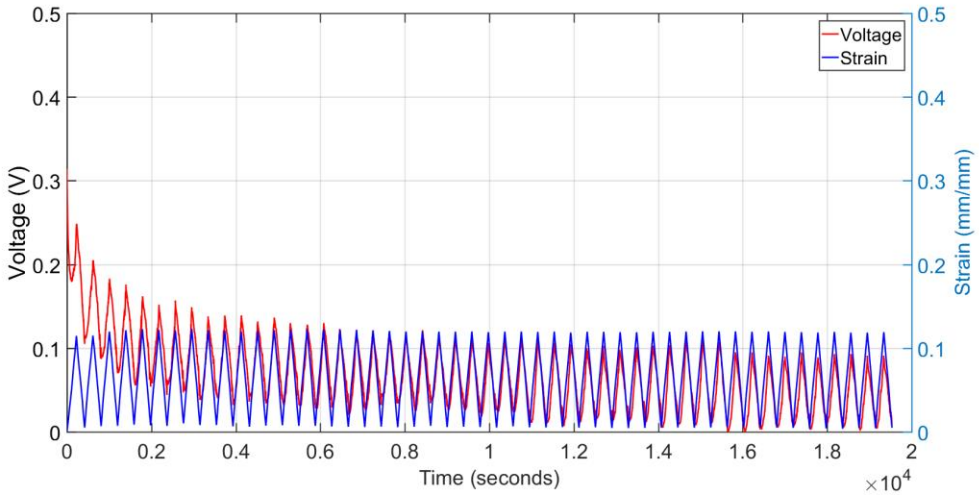

Figure 6.3 Voltage response of 1.5wt% MWCNTs to cyclic loading

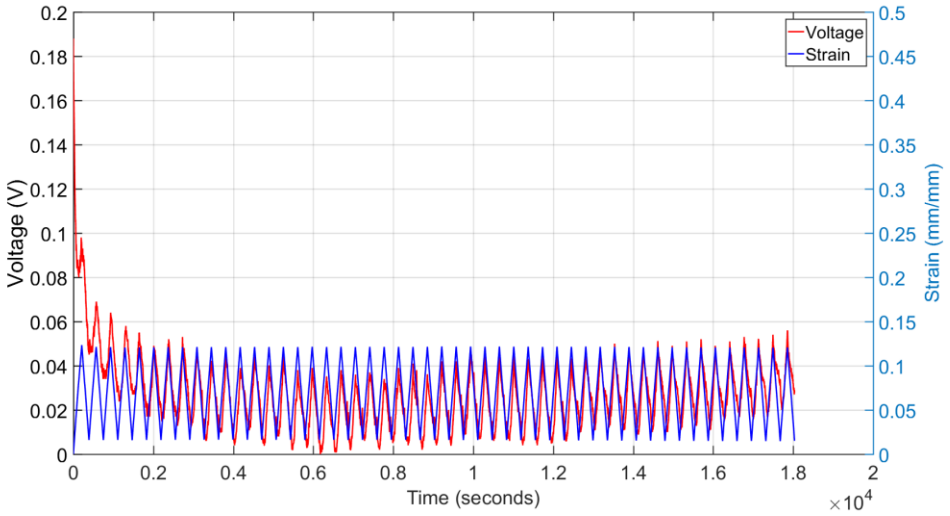

Figure 6.4 Voltage response of 1.75wt% MWCNTs to cyclic loading

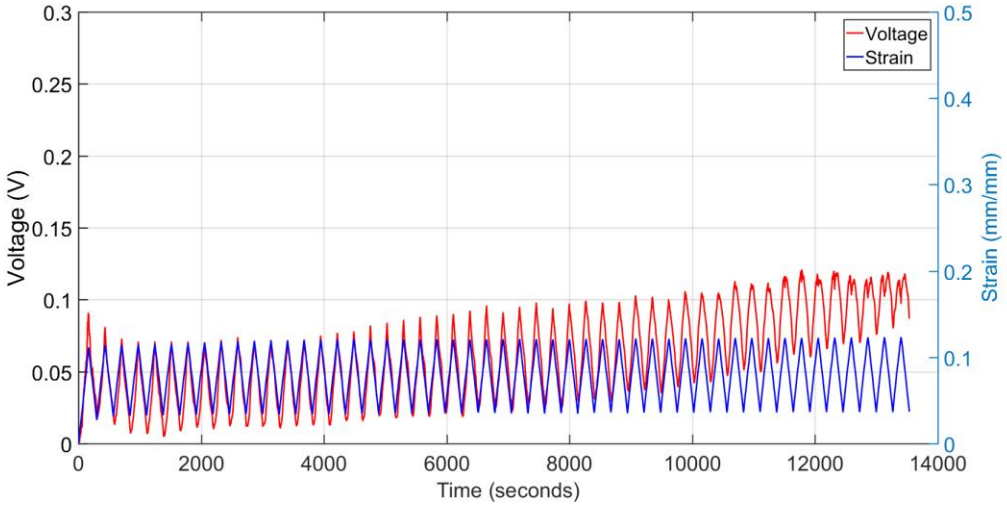

Figure 6.5 Voltage response of 2.0wt% MWCNTs to cyclic loading

An in-depth correlation between the sensor's electrical response and strain is

rarely reported in the literature. We observed that the voltage response to strain relation is linear. Moreover,the sensitivity and the stability of material does not degrade over repeated loading.

The voltage response for all the weight percentages have a settling time, after which the change in peak to peak voltage due to cyclic strain becomes linear. The lower weight percentage nanocomposite of 0.5% and 0.75% has the most elasticity, however their peak to peak voltage response in not fully defined during unloading. Moreover, during unloading, these weight percentages have an almost noise like behavior which is not ideal for a sensor. The high weight percentage nanocomposite on the other hand have sharper peaks during loading and unloading but are stiffer due to the addition of higher amount of MWCNTs. This as well is not suitable for a sensor as not only does the sensitivity or the delta peak to peak voltage decrease, it also loses some flexibility.

A sensor needs to have a linear relation between voltage and strain (especially at the point of maximum loading and unloading) as well as large sensitivity, i.e. peak to peak voltage. However, these two properties are in conflict with each other as you need to add more CNTs to have less noise, but addition of more CNTs reduces the elasticity and the sensitivity of the nanocomposite, which in turn reduces delta peak to peak voltage. Thus, a trade-off is necessary between the low signal noise and the high sensitivity. The 1.5 wt% nanocomposite samples are the best fit for this scenario. The 1.5 wt% nanocomposite have sharp peaks at loading and unloading as well as its delta voltage is

0.1 V on average.

Moreover, there is strong correlation between strain and voltage response of 1.5 wt%. Figure 6.3 illustrates initial settling of the composite, after which there is strong linearity of the voltage response to strain during loading and unloading, especially at the peaks . The voltage response in all cases needed time to settle, this is most likely due to the materials' properties of PDMS polymer and can be described by Mullins effect. Also, the MWCNT become more aligned over time due to mechanical stretching, which gives a stable response[40]. Another obtained observation is that the material may undergo fatigue and the internal defects during fabrication, whichmay become more pronounced over time. This can be seen in the response of 2 wt% near the later cycles. The nanocomposite starts to become unstable until it breaks.

The voltage to strain relation provides a direct account of the nanocomposite piezoresistivity. The nanocomposite undergoes an internal settling that effects the electrical signal, causing hysteresis. A detailed look at this hysteresis is provided in Chapter 4, where key cycles from the voltage to strain relation are presented. The electrical hysteresis exists due to the initial random orientation of MWCNTs and their gradual alignment due to mechanical stretching. It can also exist due to buildup of charge within the composite, where the nanotubes within the polymer act as nanocapacitors. The complete piezoresistive behaviour of strain dependent voltage can be seen in Figure 6.6 to Figure 6.10.

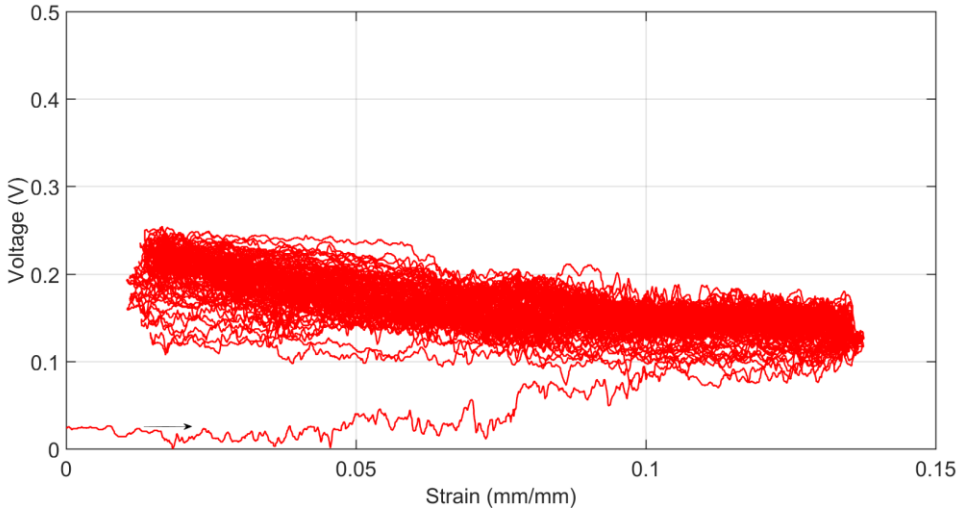

Figure 6.6 Voltage-Strain relation over 50 cycles for 0.5 wt%

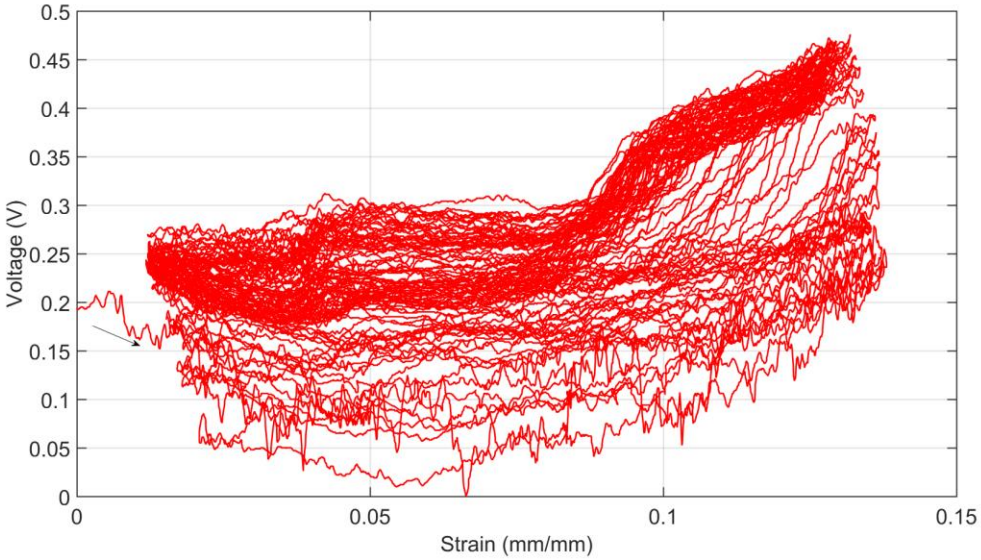

Figure 6.7 Voltage-Strain relation over 50 cycles for 0.75 wt%

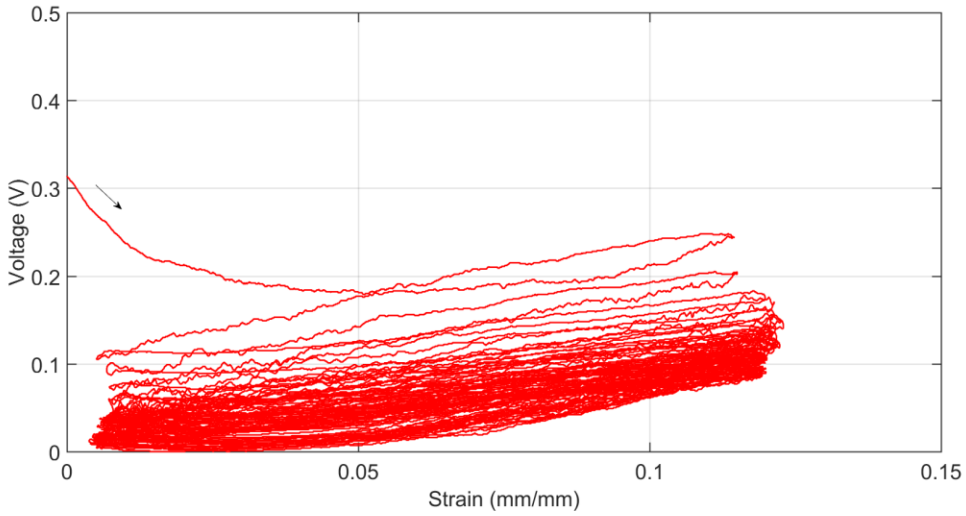

Figure 6.8 Voltage-Strain relation over 50 cycles for 1.5 wt%

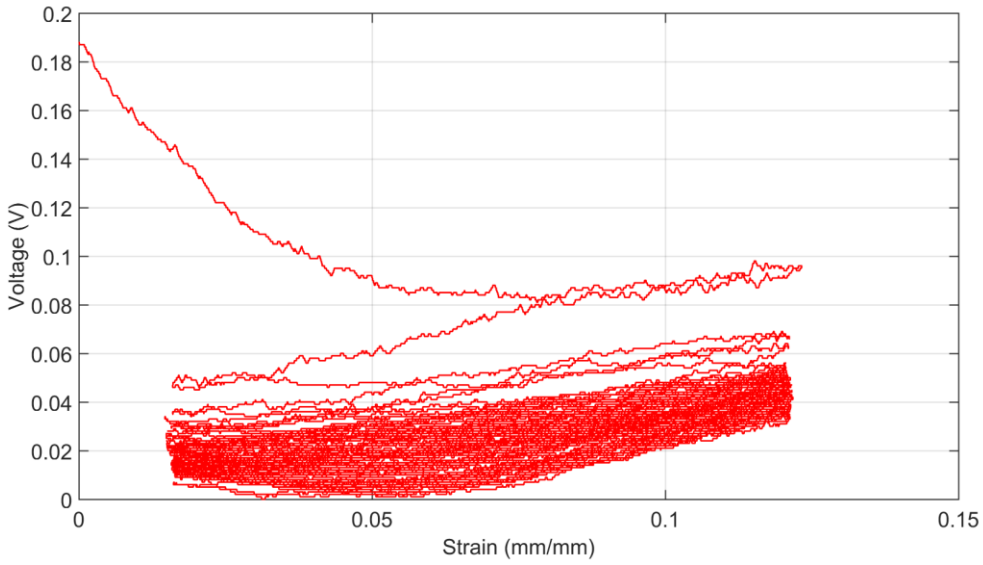

Figure 6.9 Voltage-Strain relation over 50 cycles for 1.75 wt%

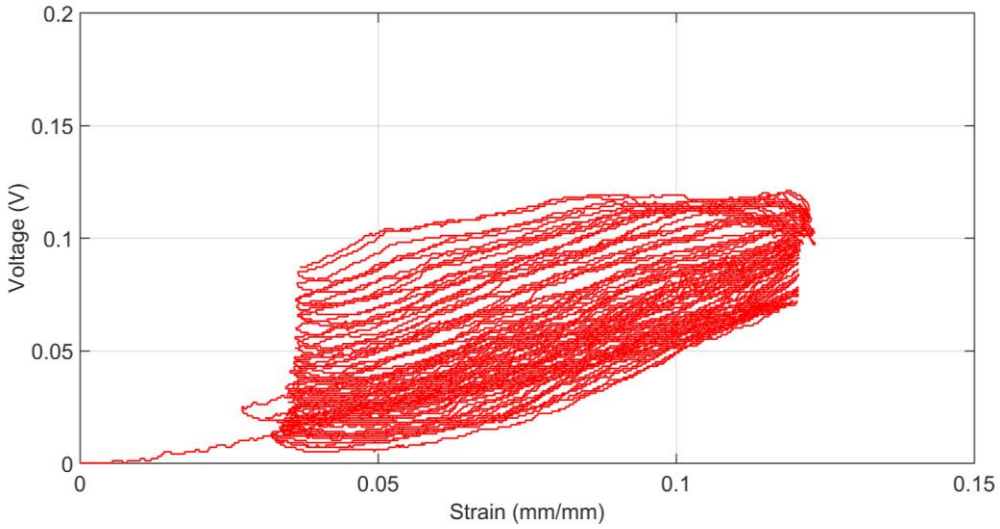

Figure 6.10 Voltage-Strain relation over 50 cycles for 2.0 wt%

The nanocomposites have a change in their conductivity with repeated loading and unloading. In most cases, the conductivity decreases slightly as shown by the upward shift on voltage to strain graphs. The 0.5wt%however, has the opposite trend, its conductivity increases as shown by the downwards shift. This shift happens due to change in conducting mechanism. The 0.5wt% is near the percolation threshold, where the conductivity mechanism is primarily due to tunneling, but as the stress softening happens, the nanocomposites develops more CNT networks which causes an overall increase in the conductivity. The increase can also be caused by the MWCNTs' alignment due to mechanical stretching. For other weight percentages, the primary mode of conductivity is due to CNT networks, the softening increases the distance, thus breaking the networks and increasing the resistance.

6.2.2 Type II Samples

The Type II nanocomposite samples were subjected to cyclic compression for 50 cycles, at a rate of 2mm/min. The two probe method was used to measure the electric response. The MTS criterion gripper displacement was used to calculate the strain. The resistance response to compressive loading and unloading over timefor different samples is show in Figure 6.10 to Figure 6.14.

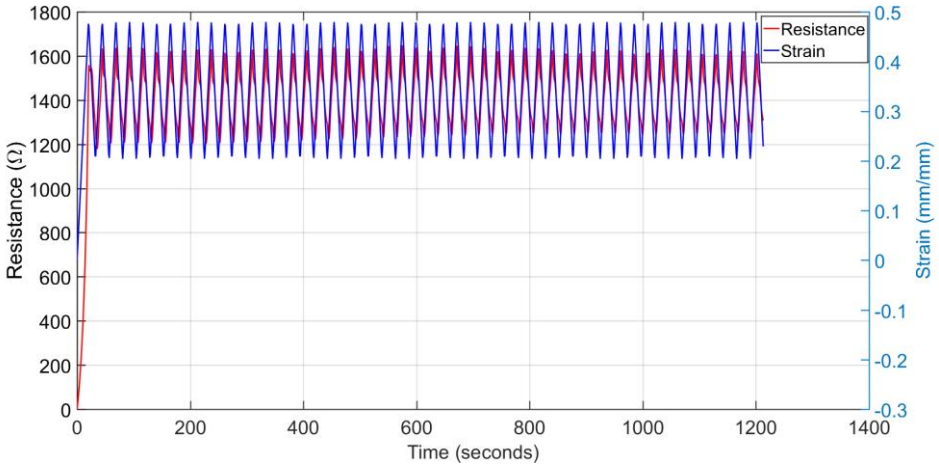

Figure 6.11 Resistance response of 1% Thick to cyclic loading

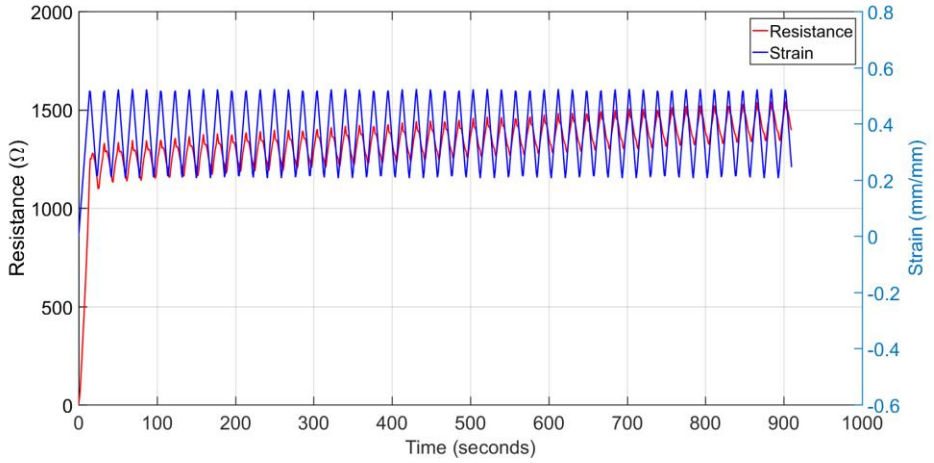

Figure 6.12 Resistance response of 1% Thin to cyclic loading

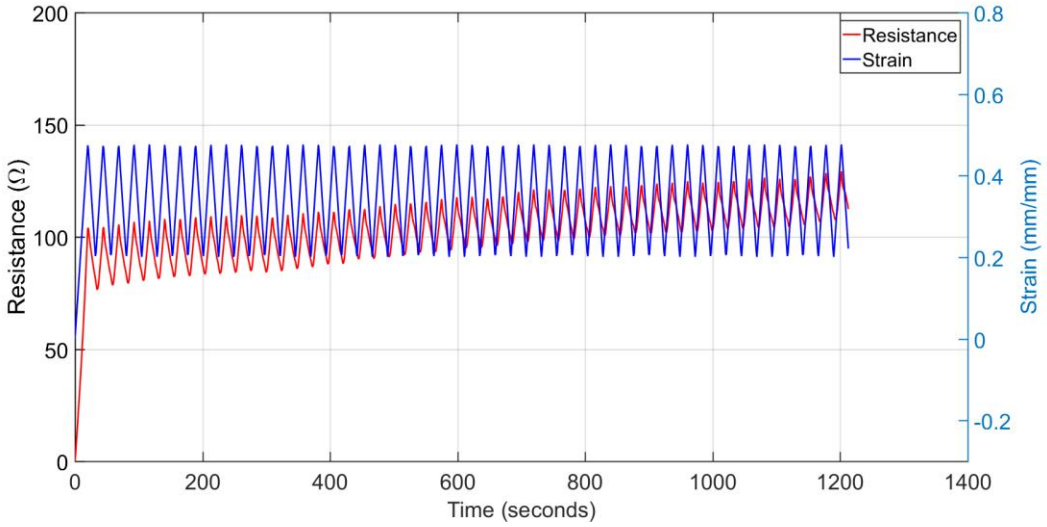

Figure 6.13 Resistance response of 1.5% Thick to cyclic loading

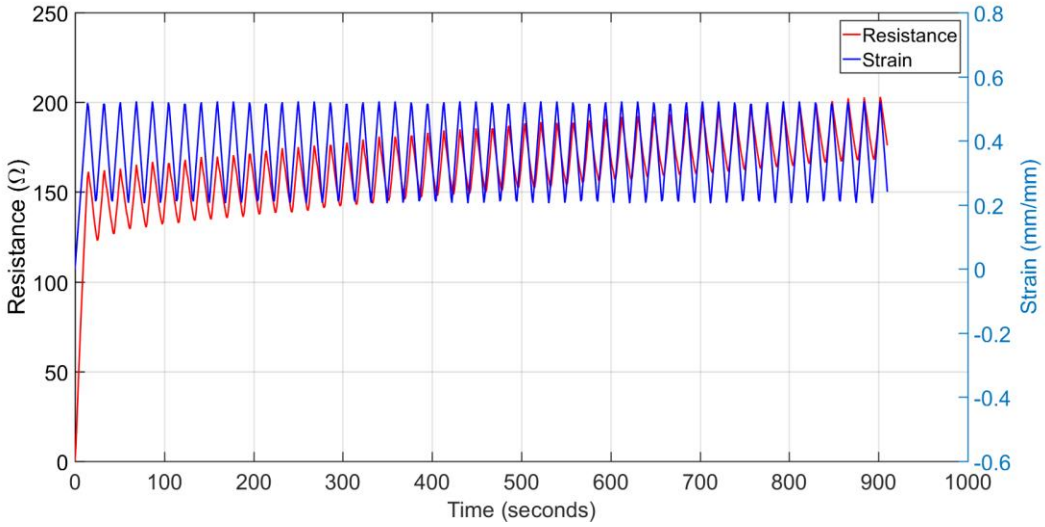

Figure 6.14 Resistance response of 1.5% Thin to cyclic loading

The Type II samples have a strong relation with strain as seen in Figure 6.10 to Figure 6.14. The resistance signal of Thick and Thin samples for both wt% of MWCNTs are linearly affected by strain. The overall resistance increases with repeated loading. However, the range difference between maximum and minimum resistance for each cycle remains consistent.The 1 wt% and 1.5 wt% used for Type II have low noise and provide a smooth signal.Generally, the nanocomposite loses its flexibility with addition of MWCNT. However, a decrease in thickness of Type II samples counters this and retains its flexibility. The wt% for the Type II were chosen based on the trade-offs conducted between high flexibility and low noise in signals for Type I.

The piezoresistivity of Type II nanocomposite is also represented by the resistance to strain relation. The nanocomposite is affected by hysteresis, which decreases over

successive cycles, a detailed analysis is provided in Chapter 4 using key cycles from the resistance to strain relation. The complete piezoresistive behaviour of strain dependent resistance is given in Figure 6.15to Figure 6.18.

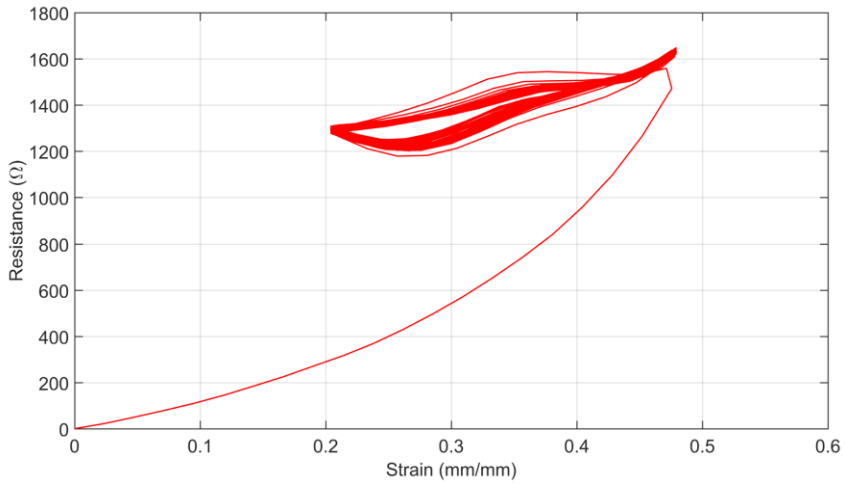

Figure 6.15 Resistance-Strain relation over 50 cycles for 1% Thick

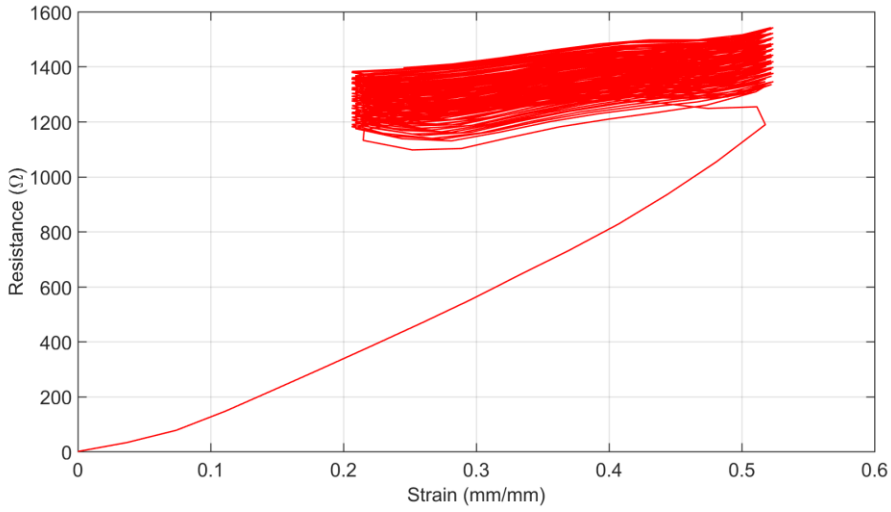

Figure 6.16 Resistance-Strain relation over 50 cycles for 1% Thin

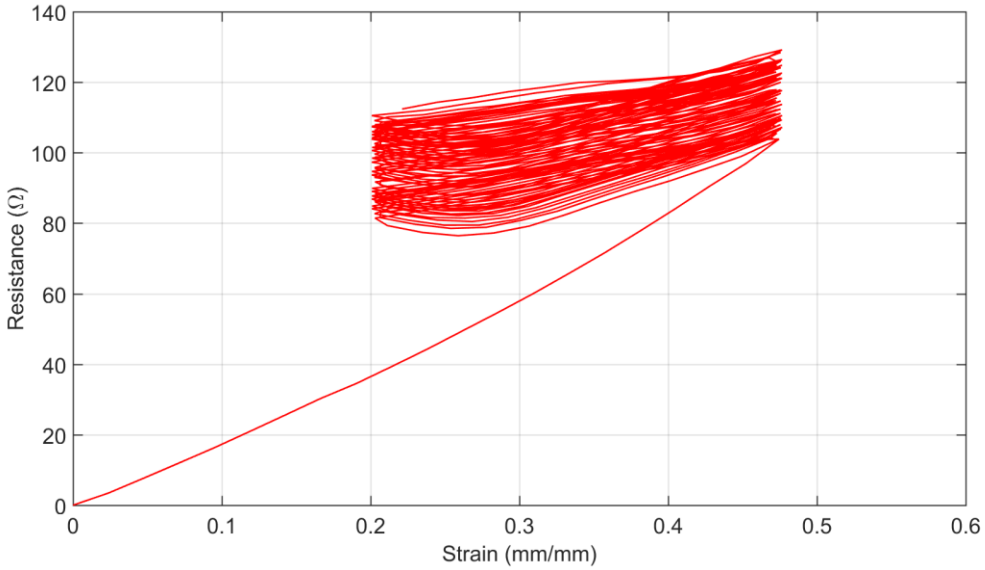

Figure 6.17 Resistance-Strain relation over 50 cycles for 1.5% Thick

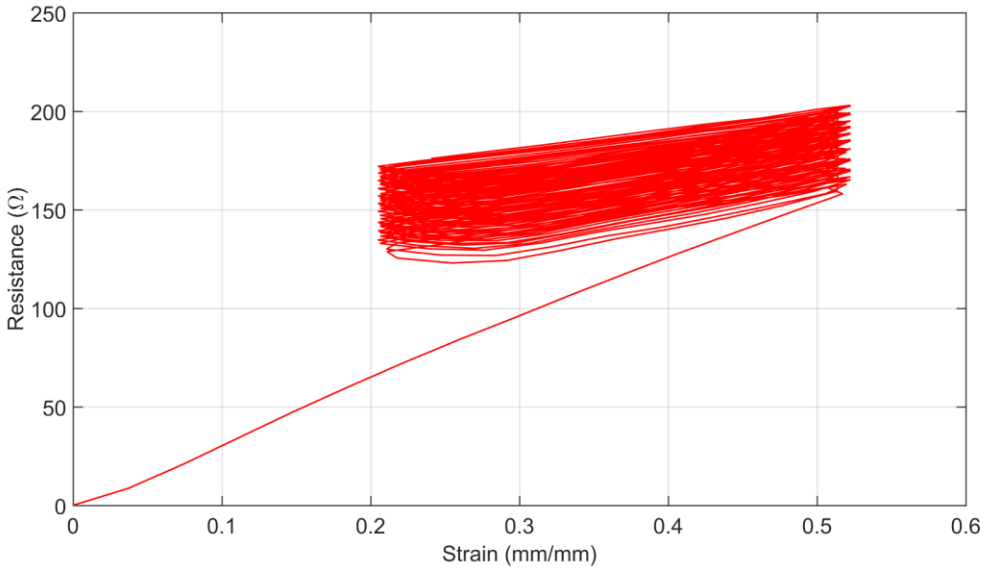

Figure 6.18 Resistance-Strain relation over 50 cycles for 1.5% Thin

The overall resistance of the nanocomposites changes with repeated loading and unloading, Figure 6.15to Figure 6.18. In most cases, the resistance increases with repeated loading but the hysteresis within each cycle decreases. The resistances of Thick and Thin samples for a particular wt% of MWCNT are comparable. The resistance increases linearly with strain, with 1.5 wt% samples being more linear than their 1 wt% counterparts.

6.3 Sensitivity/Gauge Factor

The sensitivity or the Gauge Factor is one of the most important parameters for piezoresistive materials. The sensitivity of both Type I and Type II samples is determined in this section. The effects of MWCNT as well as sample thicknesses on the gauge factor are explored.

6.3.1 Type I Samples

The electro-mechanical properties of the material were examined using the MTS along with the laser displacement measure. The electrical response of the composite was measured in tandem with the mechanical behavior to determine the piezoresistive response, using the four-point probe method.

The piezoresistive sensitivity (GF) of the nanocomposite is based on the voltage response for each cycle of loading and unloading. The current applied was constant over time, thus the resistance was effectively based on the voltage. Therefore, the GF for Type

I samples was computed as:

$$GF = \frac{\Delta V}{\varepsilon . V_{\min}} \tag{6.1}$$

where the ΔV is the difference between the maximum and the minimum voltage within a cycle and the $V_{\min}$ is the of minimum voltage, ε is the strain. In order to compute the GF, each cycle was divided into two halves, to accommodate for the two points of unloaded stress. However, the maximum voltage for these two halves is still the same. Thus, each cycle has one maximum and two minimums.

The sensitivity of the nanocomposite was determined by the Gauge factor. The Gauge factor is highest near the percolation threshold of 0.5 wt%, with a value of 16.7 and drops significantly as more MWCNTs are added. The 1.5 wt% of MWCNT has a factor of 0.93. The high sensitivity of the nanocomposite is crucial in order to measure minor variations in applied stress. The Gauge factor for Type I samples is plotted in Figure 6.19.

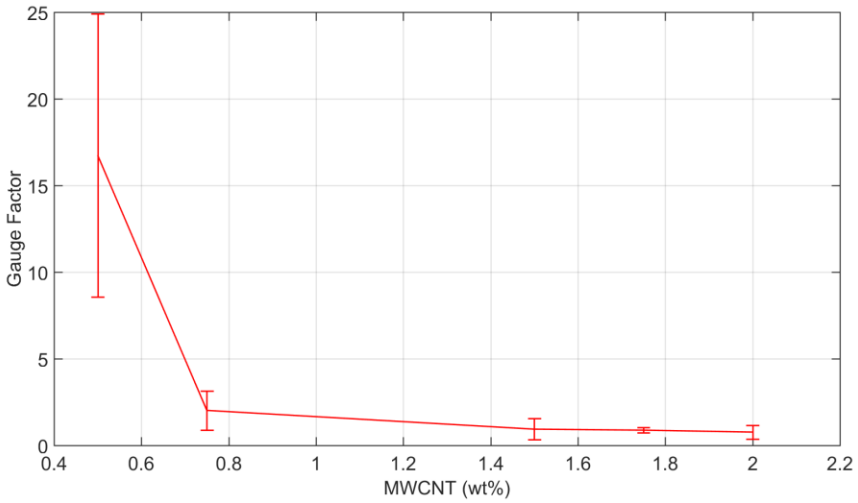

Figure 6.19 Gauge Factor for the PDMS-MWCNT composite

Table 6.1 Type IGauge Factor

MWCNT wt%	Gauge Factor	Gauge Factor Standard Deviation
0.5	16.741	8.1722
0.75	2.018	1.1352
1.5	0.935	0.6083
1.75	0.876	0.1579
2.0	0.766	0.4003

It should be noted that the PDMS-MWCNT mixture was ultra-sonicated for at least 80 hours, which is quite extensive and may have caused reduced sensitivity.

The percent change in voltage over a percent change in strain is also crucial when

evaluating the sensitivity of nanocomposites. The change in voltage ratio to strain for Type I samples is plotted in Figure 6.20 to Figure 6.24.

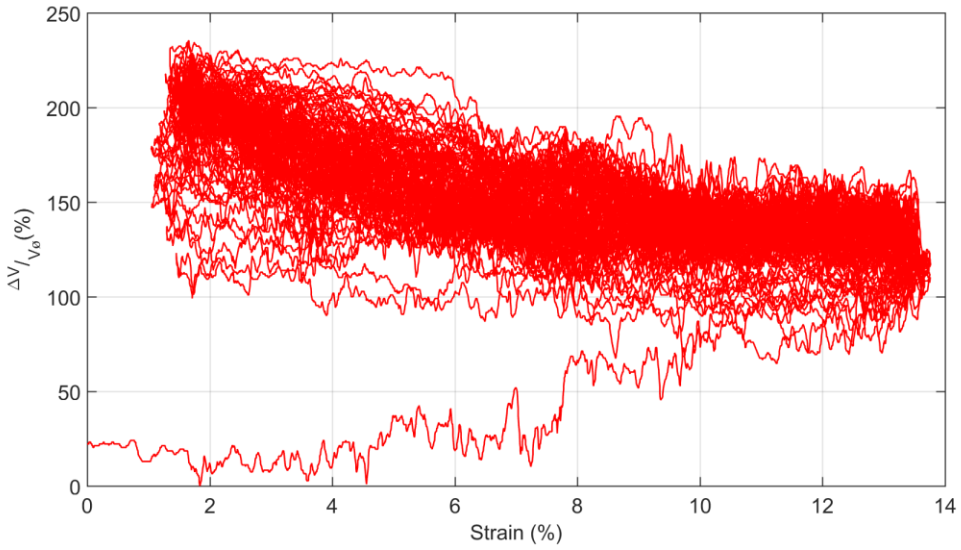

Figure 6.20 Voltage ratio to strain for 0.5 wt%

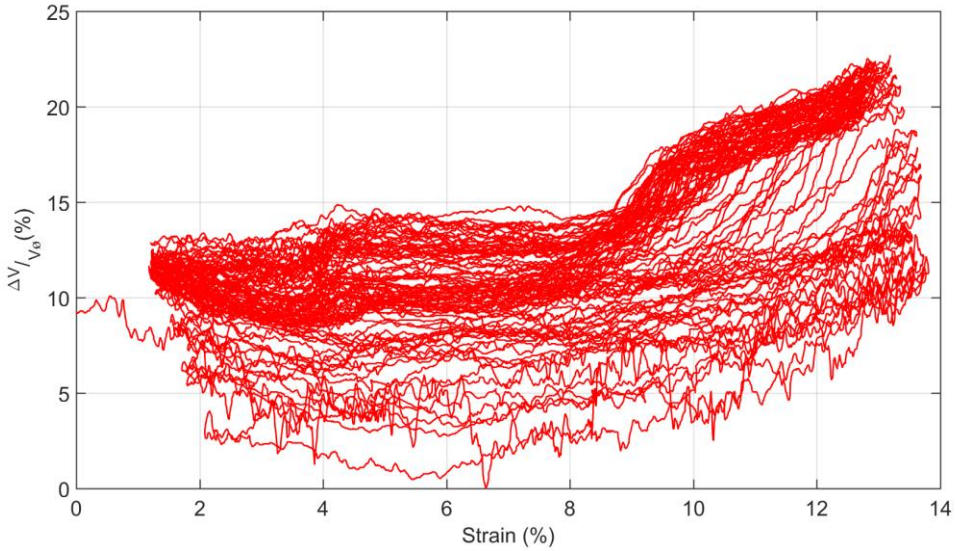

Figure 6.21 Voltage ratio to strain for 0.75 wt%

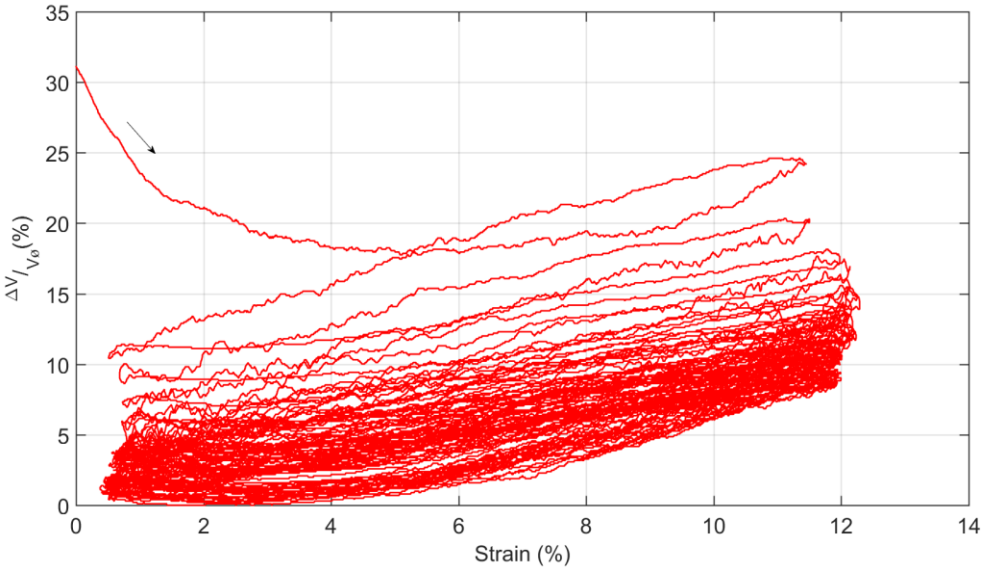

Figure 6.22 Voltage ratio to strain for 1.5 wt%

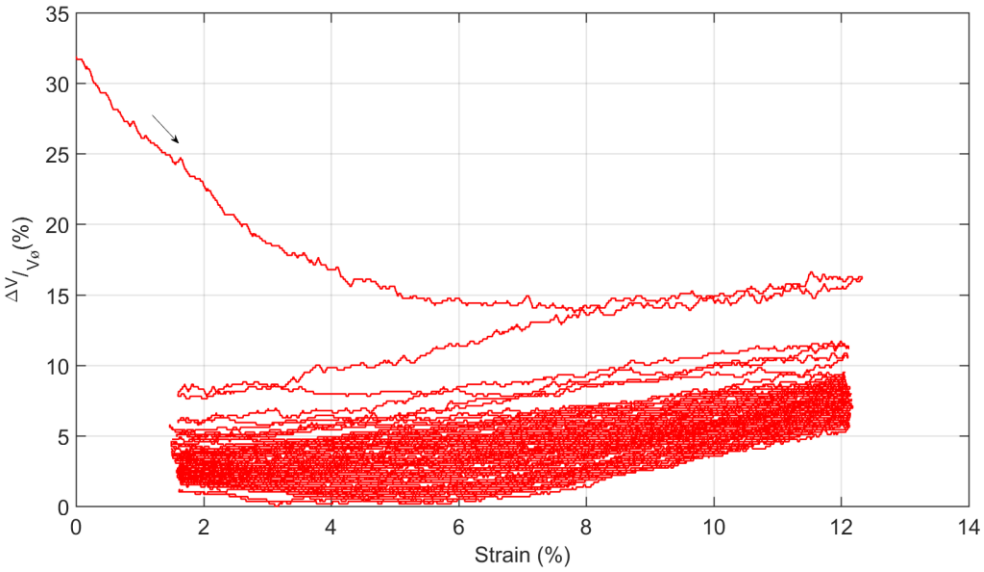

Figure 6.23 Voltage ratio to strain for 1.75 wt%

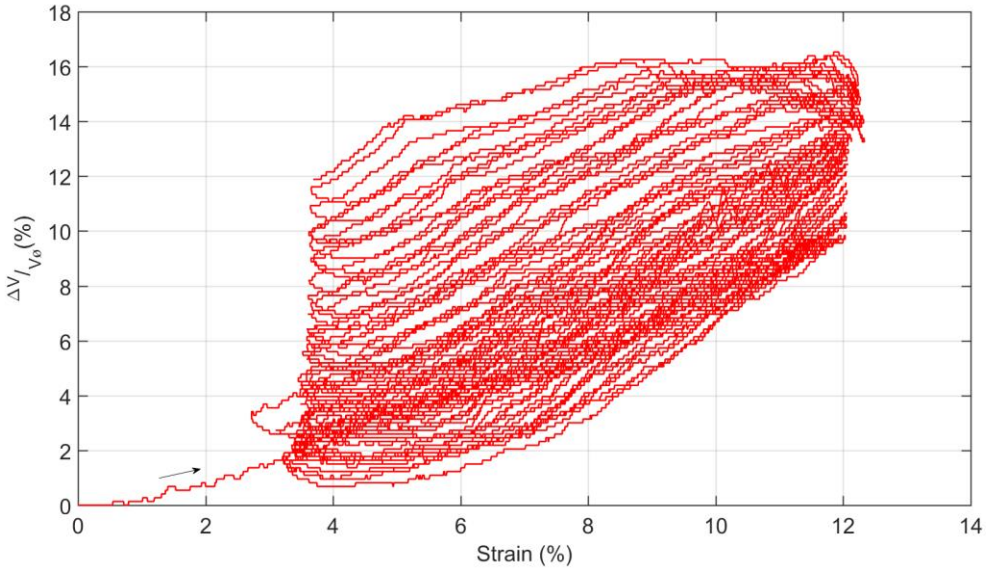

Figure 6.24 Voltage ratio to strain for 2.0 wt%

The change in percent voltage ratio decreases with an increase in MWCNT for a cycle of deformation. The 0.5 wt% samples have an approximate change of 75% in voltage over a 10% strain, whereas the 1.5 wt% has an approximate change of 7% in voltage over a 10% strain. This significant reduction in sensitivity is the trade-off for lower noise.

6.3.2 Type II Samples

The piezoresistive response of Type II samples was measured using two probe method. The Gauge factor of the nanocomposite is based on the resistance response for each cycle of loading and unloading. The GF for Type II samples was computed as:

$$GF = \frac{\Delta R}{\varepsilon . R_o} \tag{6.2}$$

where the ΔR is the difference between the maximum and the minimum resistance within a cycle and the R_o is the initial resistance for each cycle and ε is the strain.

The sensitivity of the nanocomposite was determined by the Gauge factor. The Gauge factor is highest near the percolation threshold of 0.5 wt%, which was determined from the Type I samples. The Type II samples explored the effect of sample thickness on the Gauge factor. We found that the 1 wt% samples have a higher gauge factor than the 1.5 wt% samples, and the thickness of a sample does not have a major effect on sensitivity. The Type II compressive samples seem to have a higher gauge factor than their Type I counterparts. However, this can be due to the difference between the formulas used to calculate the sensitivity for each type. Thegauge factor for Type II samples is plotted in Figure 6.25.

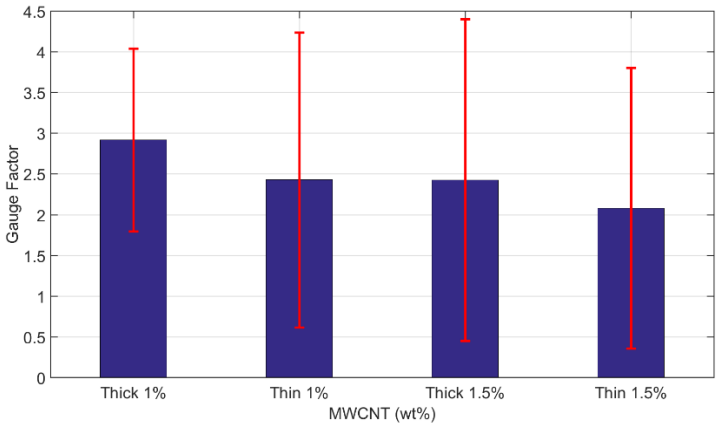

Figure 6.25 Gauge Factor of Type II

Table 6.2 Type II Young's Modulus

MWCNT wt%	Gauge Factor	Gauge Factor Standard Deviation
1.0 Thick	2.92	1.12
1.0 Thin	2.43	1.81
1.5Thick	2.43	1.98
1.5Thin	2.08	1.72

The Thick samples have slightly higher gauge factor than the thin samples, but this difference is negligible. The gauge factor for Type I and Type II have high standard deviation because the nanocomposite samples have differentindividual initial conductivity values. These values are stable overtime, which causes an increased standard deviation when taking the average over multiple samples for a particularwt%.This difference in conductivity is based on the homogeneity of dispersed MWCNT within the nanocomposite, causing a need for improvement in the processing technique.

The change in resistance ratio to strain for Type II samples is compared and plotted in Figure 6.26 to Figure 6.29.

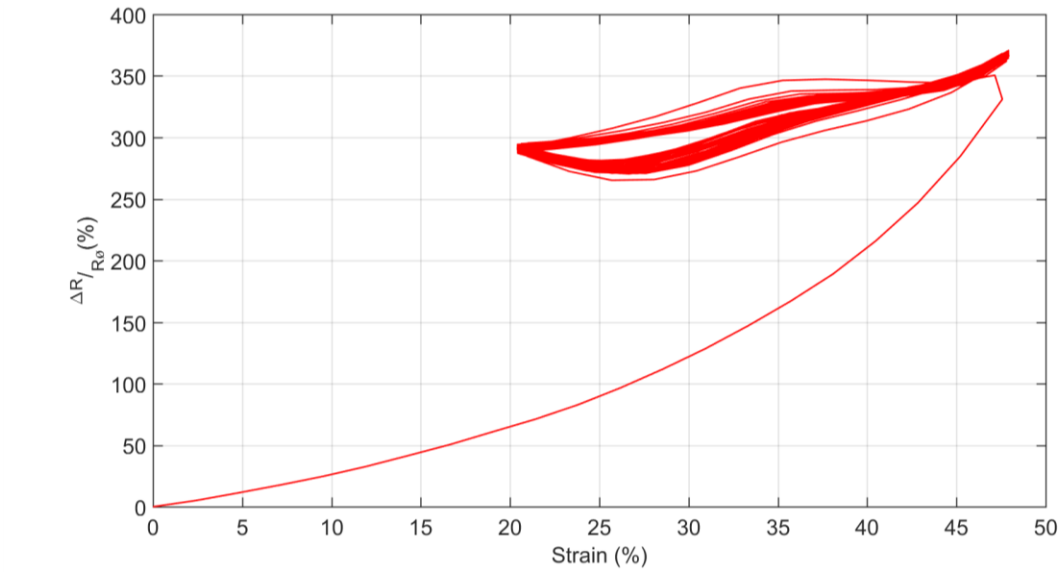

Figure 6.26 Resistance ratio to Strain 1% Thick

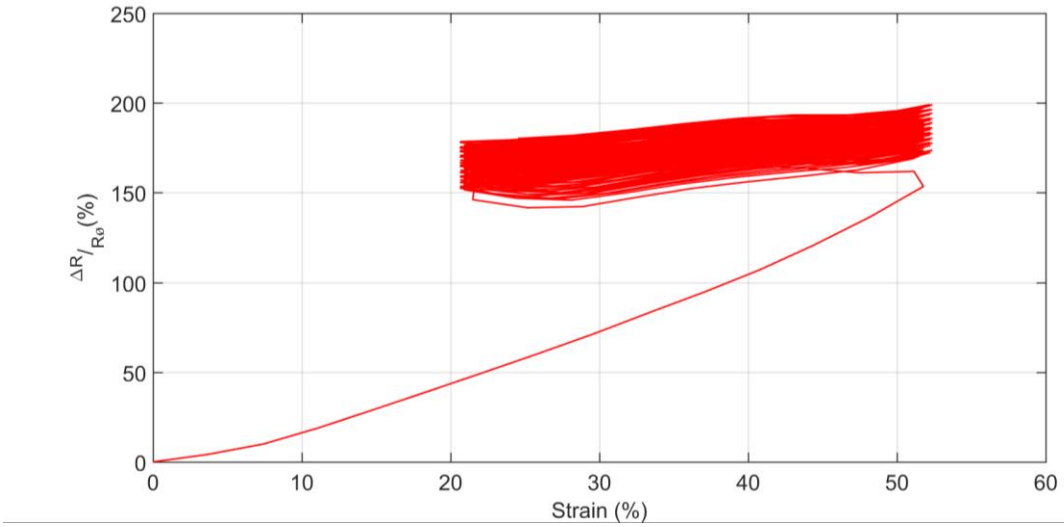

Figure6.27 Resistance ratio to Strain 1% Thin

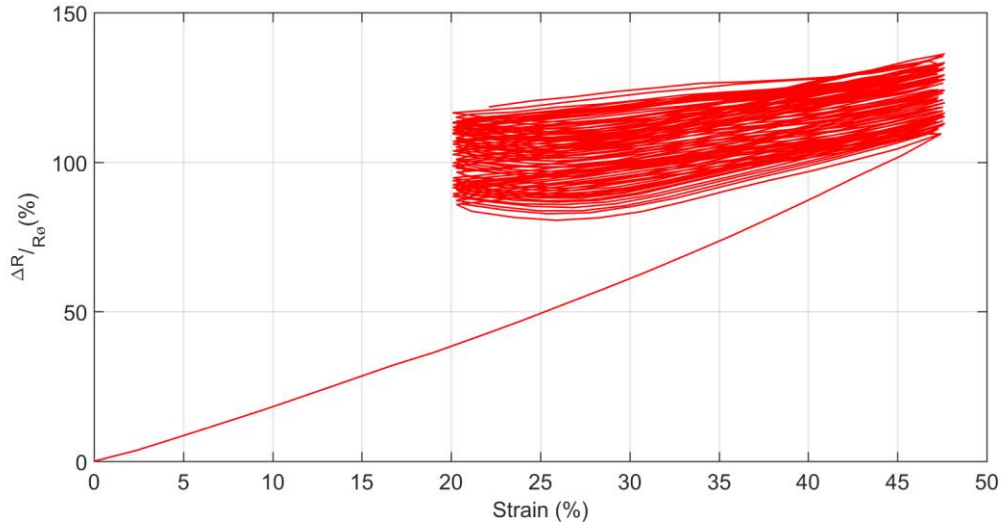

Figure 6.28 Resistance ratio to Strain 1.5% Thick

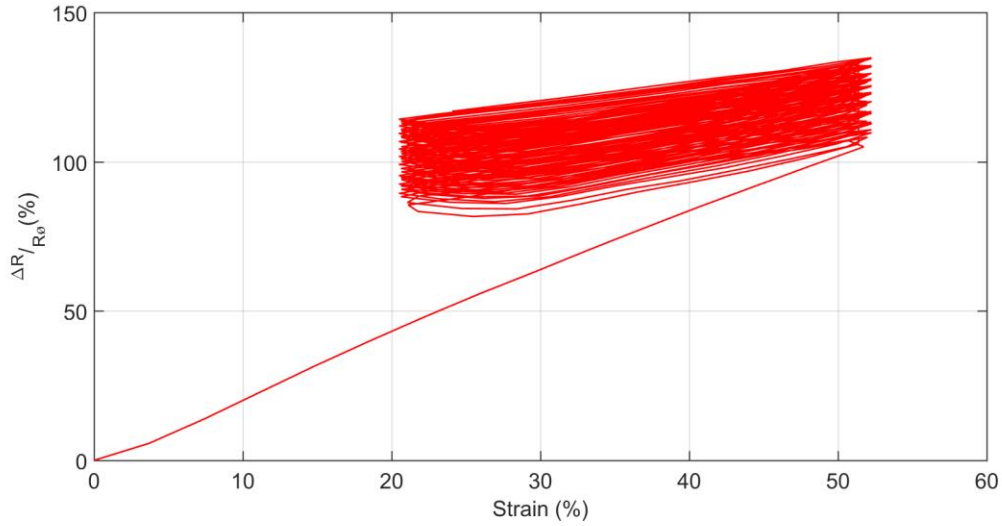

Figure 6.29 Resistance ratio to Strain 1.5% Thin

The samples for same wt% of MWCNT have similar change in percent resistance. The Type II 1.0 wt% samples have an approximate change of 30% in resistance over a

30% strain, with 1.5 wt% samples having an approximate change of 20% in resistance over a 25% strain.

6.4 Sensitivity Stability

The stability of the nanocomposite sensitivity over time and under repeated loading is necessary for the development of a good sensor. The stability of sensitivity has been characterized based on the relationship between Gauge factor and strain, the electrical properties to strain for the last 10 out of 50 cycles deformation.

6.4.1 Type I Samples

The sensitivity is represented as Gauge factor, and its response over strain is plotted in Figure 6.30 to Figure 6.34. In order to develop a reliable sensor, the sensitivity should not fluctuate over time and should correlate to the increase and decrease of the load. This is most prevalent in the nanocomposites with 1.5 wt% and 1.75 wt% MWCNTs.

The Figure 6.34 show the response of a deteriorating nanocomposite and it can be seen that the Gauge factor increases overtime as the conductive pathways are reduced.

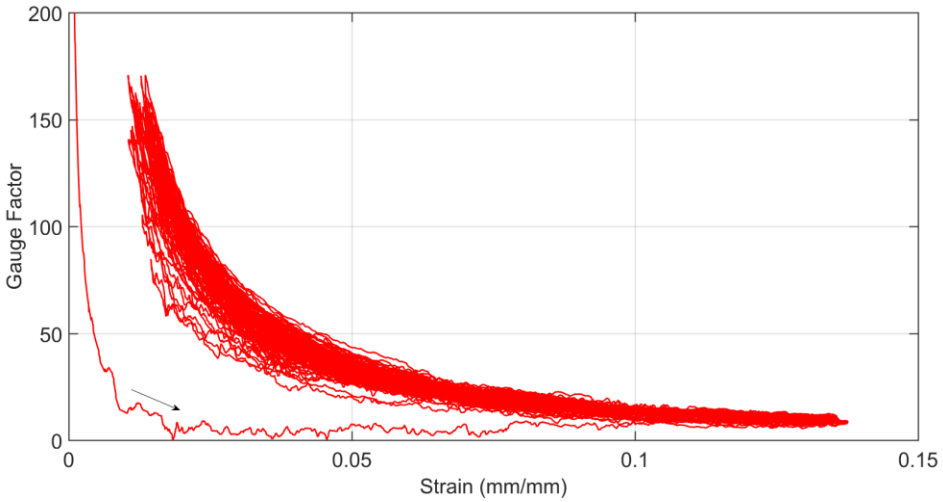

Figure 6.30 Gauge factor to strain for 0.5 wt%

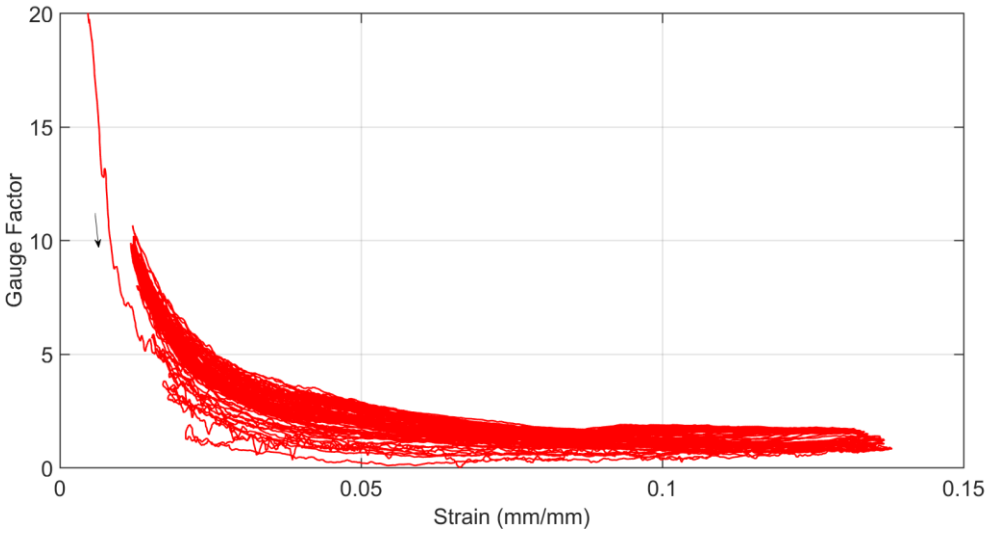

Figure 6.31 Gauge factor to strain for 0.75 wt%

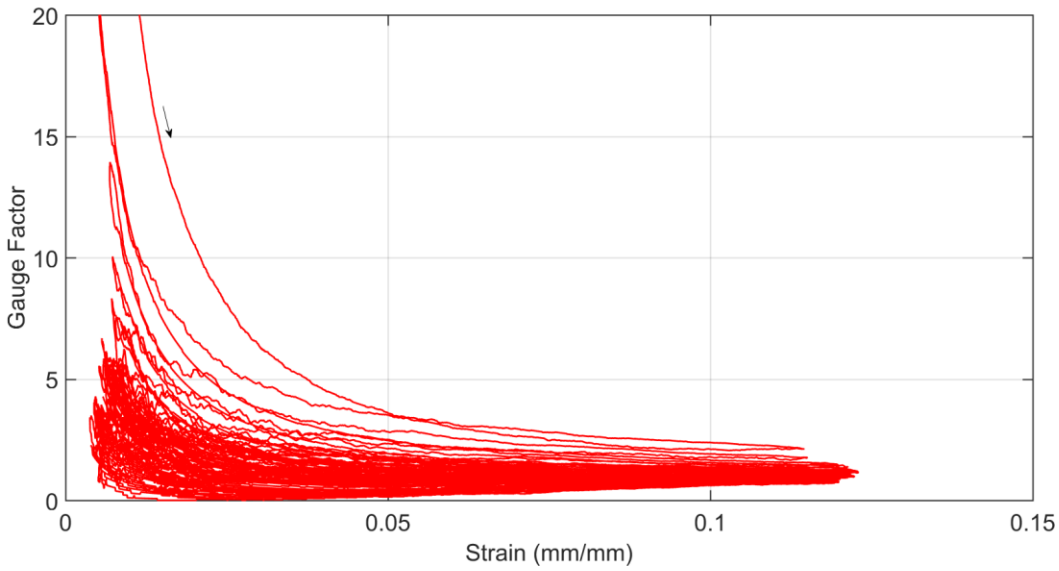

Figure 6.32 Gauge factor to strain for 1.5 wt%

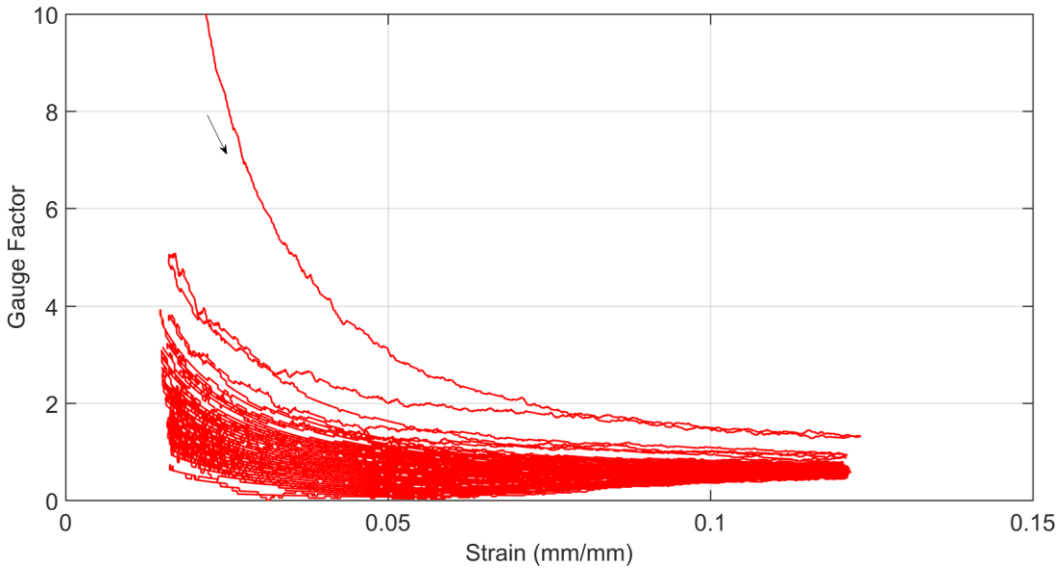

Figure 6.33 Gauge factor to strain for 1.75 wt%

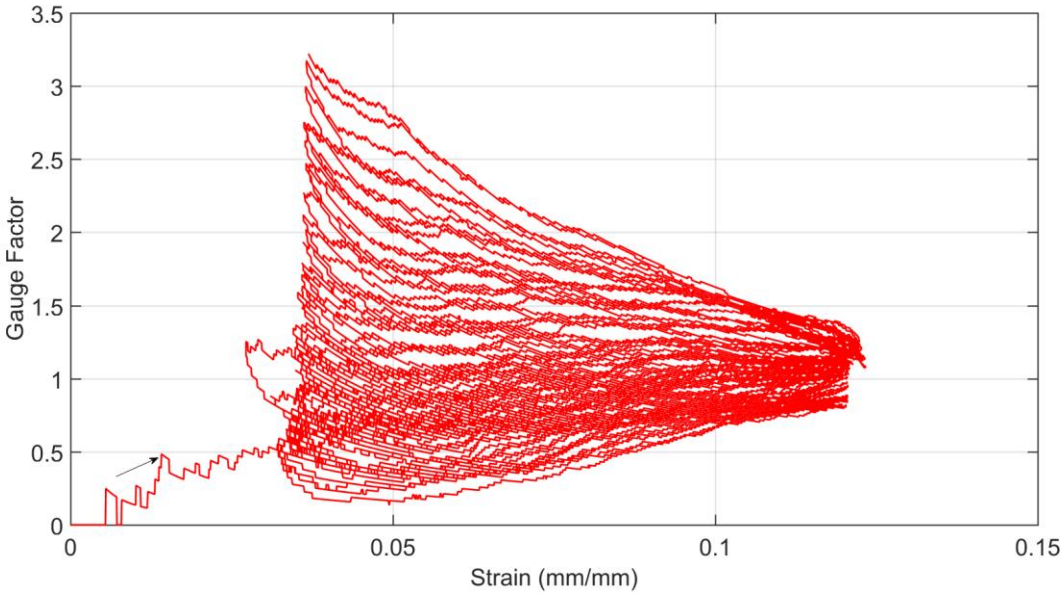

Figure 6.34 Gauge factor to strain for 2.0 wt%

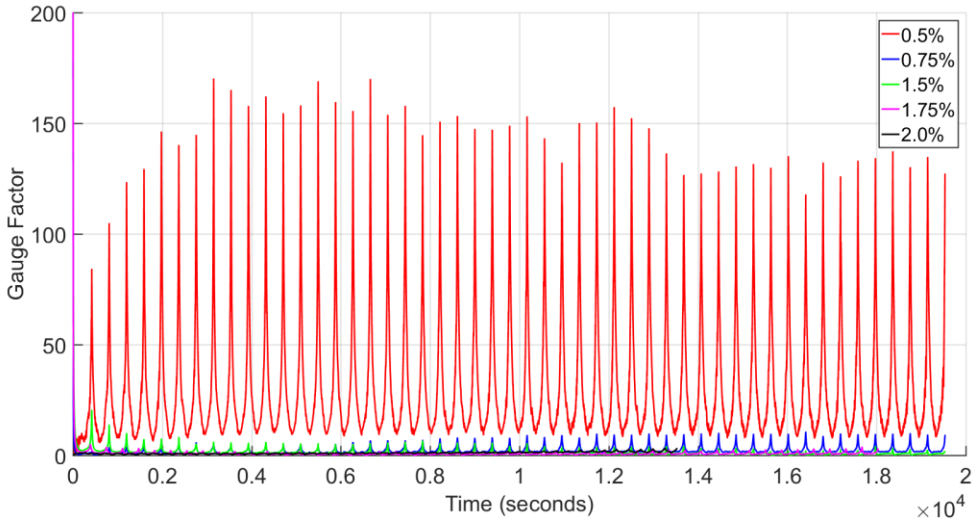

Figure 6.35 Type I samples gaugefactor over time

The stability of sensitivity is illustrated by the behavior of gauge factor to cyclic deformation. When the gauge factor remains constant through out the cycles of

deformation, the sensitivity is determined to be stable. The Figure 6.35 illustrates that the gauge factor is highest for 0.5 wt% but it fluctuates significantly. The 1.5 wt% has the most constant gauge factor, which makes this wt% to be the most suitable for a sensor operating under tension. The general trend is that the sensitivity is reduced, but becomes stabilized with increase in MWCNT

In order to determine the settled piezoresistive response of the nanocomposite, the last 10 cycles for each wt%are plotted and shown in Figure 6.36 to Figure 6.40. The voltage response over time to repeated loading for 0.5 wt% and 0.75wt% is noisy especially at the peaks and valleys. The response for 1.75 wt% and 2.0 wt% drifts, because the loading is near the failure stress and causes changes in the internal structure of the material. The 1.5 wt% response is good as it has sharp peaks and valleys, moreover, the voltage trend does not drift.

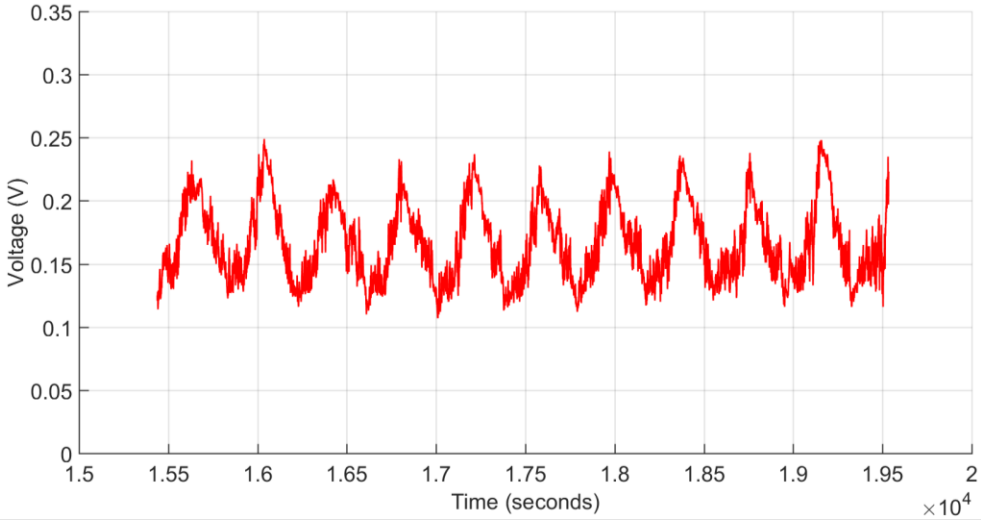

Figure 6.36 Last 10 cycles of 0.5 wt%

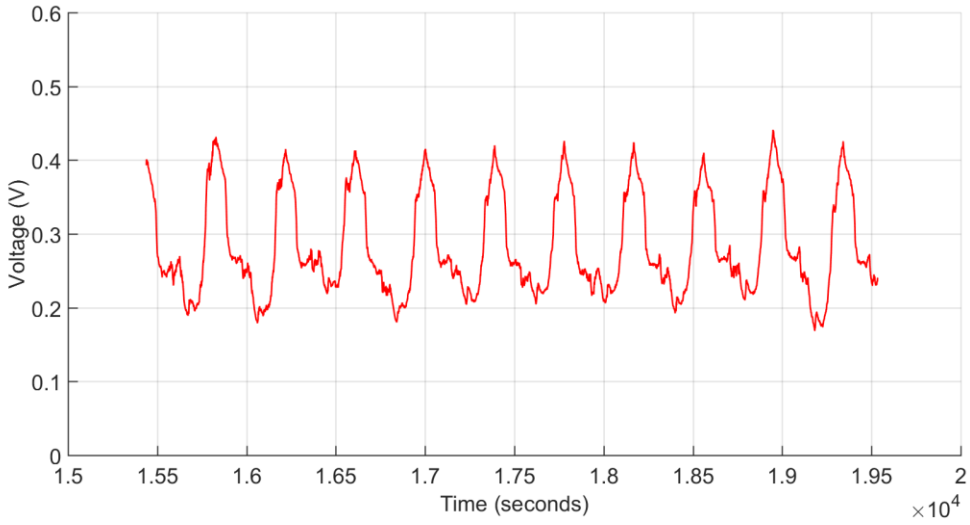

Figure 6.37 Last 10 cycles of 0.75 wt%

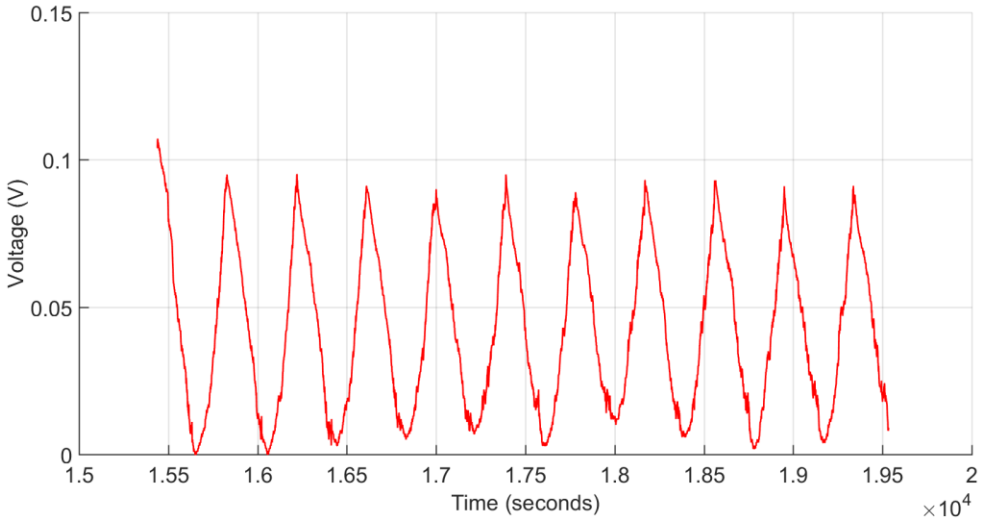

Figure 6.38 Last 10 cycles of 1.5 wt%

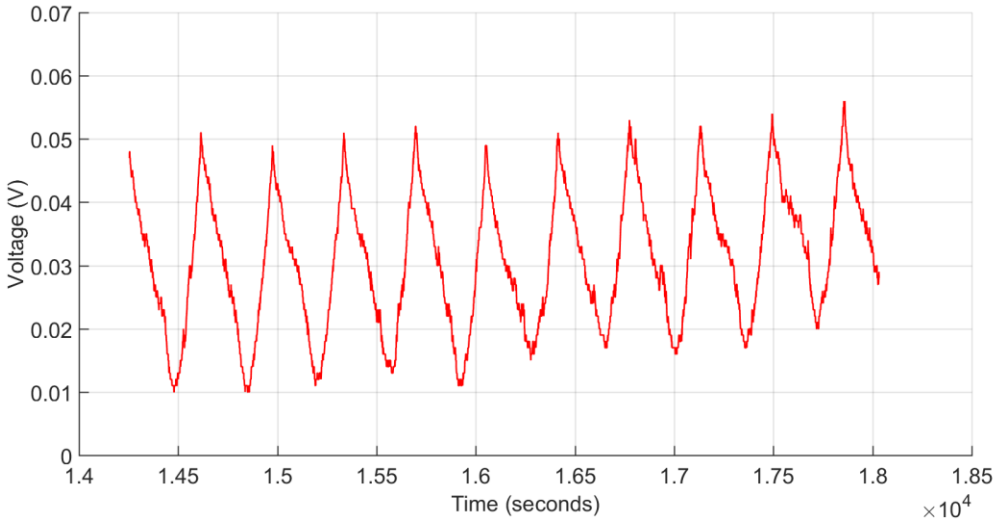

Figure 6.39 Last 10 cycles of 1.75 wt%

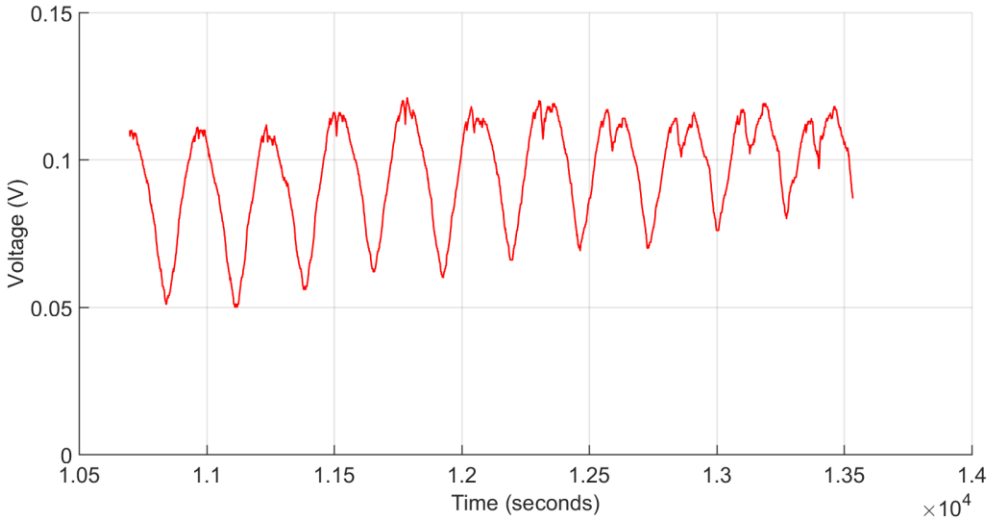

Figure 6.40 Last 10 cycles of 2.0 wt%

The nanocomposite with 2 wt% MWCNT undergoes material deterioration which can be seen in its last cycles, Figure 6.40. The 2 wt% has the highest stiffness and is more likely to deteriorate overtime. This sample was chosen to illustrate the response of a

deteriorating nanocomposite.

6.4.2 Type II Samples

The stability of the nanocomposite sensitivity is represented by the predictable gauge factor to strain response and is plotted in Figure 6.41 to Figure 6.44. In order to develop a reliable sensor, the sensitivity should not fluctuate over time and should correlate to the increase and decrease to the load.

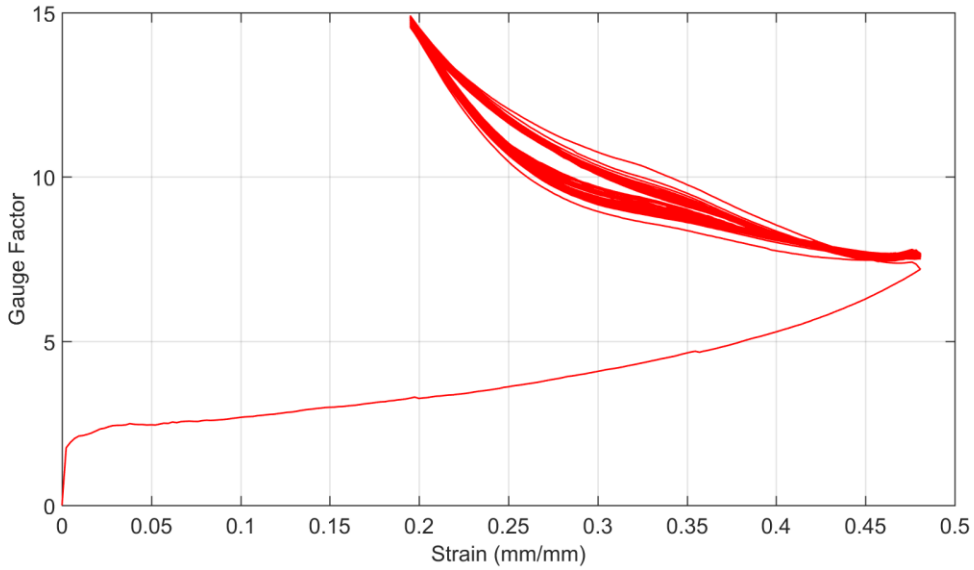

Figure 6.41 Gauge Factor to Strain 1% Thick

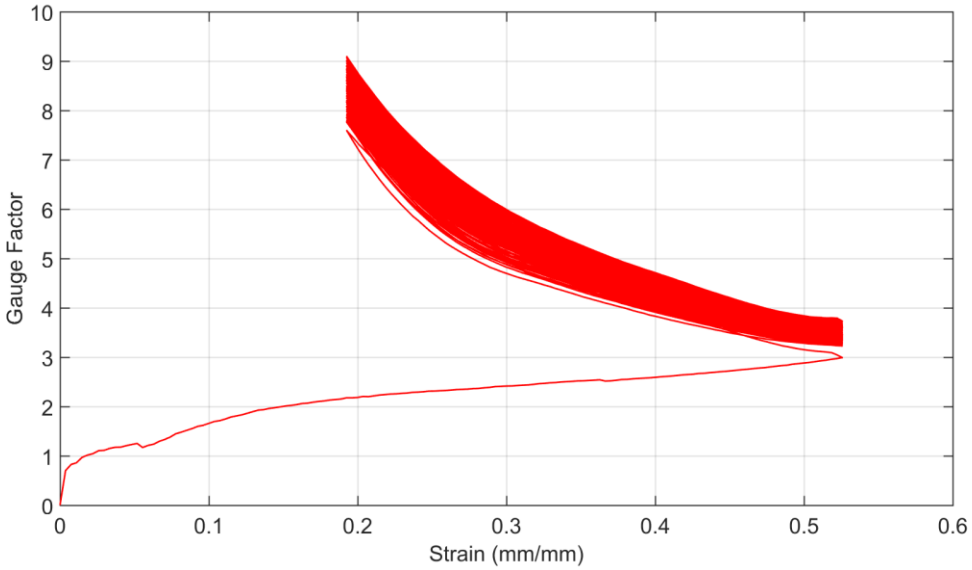

Figure 6.42 Gauge Factor to Strain 1% Thin

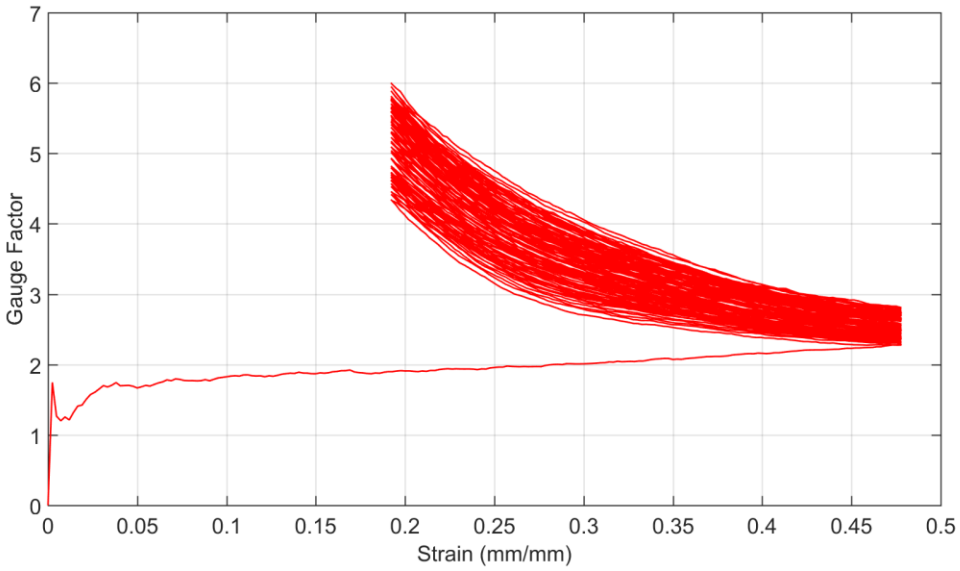

Figure 6.43 Gauge Factor to Strain 1.5% Thick

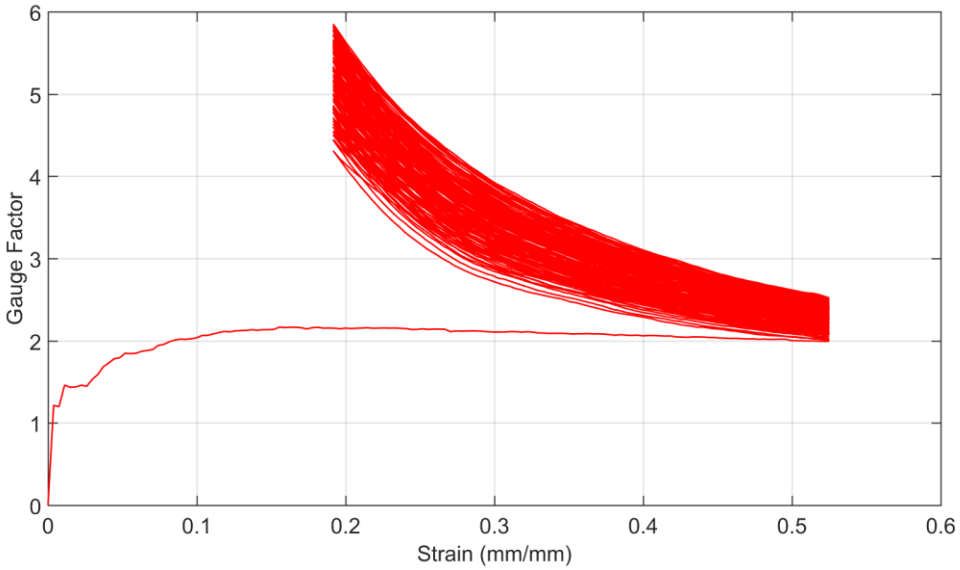

Figure 6.44 Gauge Factor to Strain 1.5% Thin

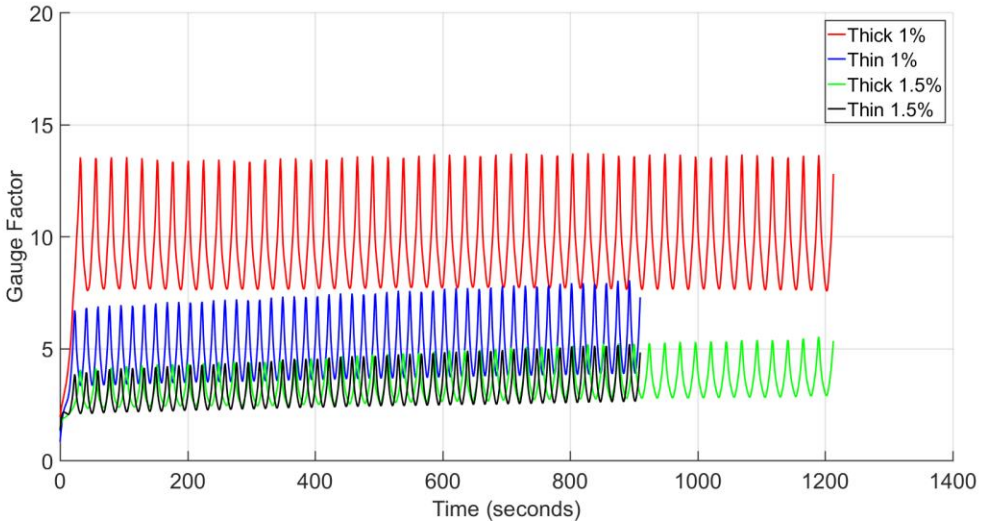

Figure 6.45 Sensitivity stability of the nanocomposite

The Type II samples underwent significant strain. Figure 6.41 to Figure 6.44 show that the gauge factor is curved for lower strains and linear for larger strains. Also, the

sensitivity is higher during lower strain loading and significantly drops at higher loading. There is not a significant difference between the Thick and Thin samples for respective loadings of MWCNT. The gauge factor is stable overtime as seen in Figure 6.45 The linearity of the gauge factor response over time increases with repeated loading. The 1 wt% and 1.5 wt% are both suitable for a sensor.

In order to determine the settled piezoresistive response of the nanocomposite, the last 10 out of 50 cycles are plotted and shown from Figure 6.46 to Figure 6.49. The resistance response over time to repeated loading is stable for all Type II samples, with a slight increase in resistance over time.

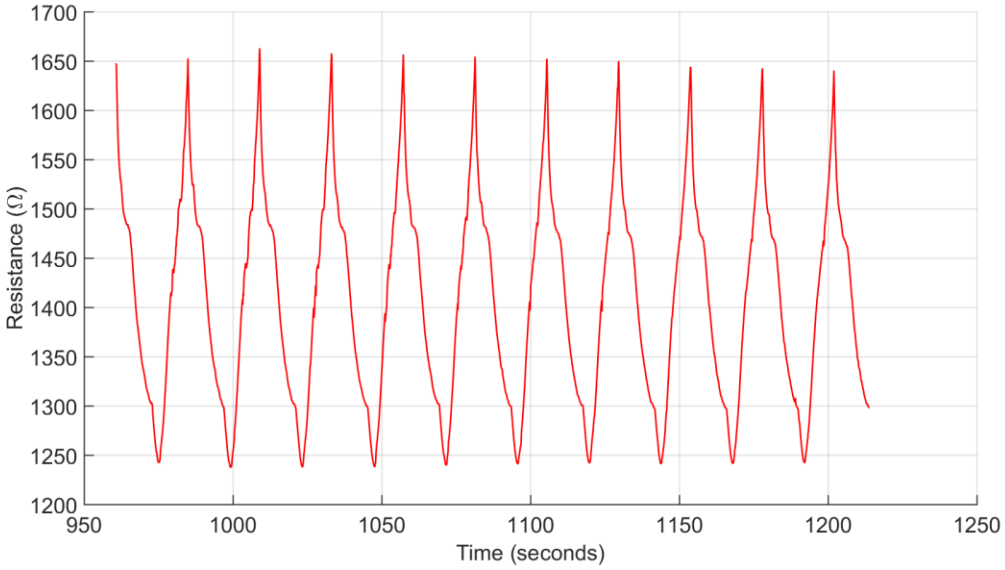

Figure 6.46 Last 10 cycles of 1% Thick

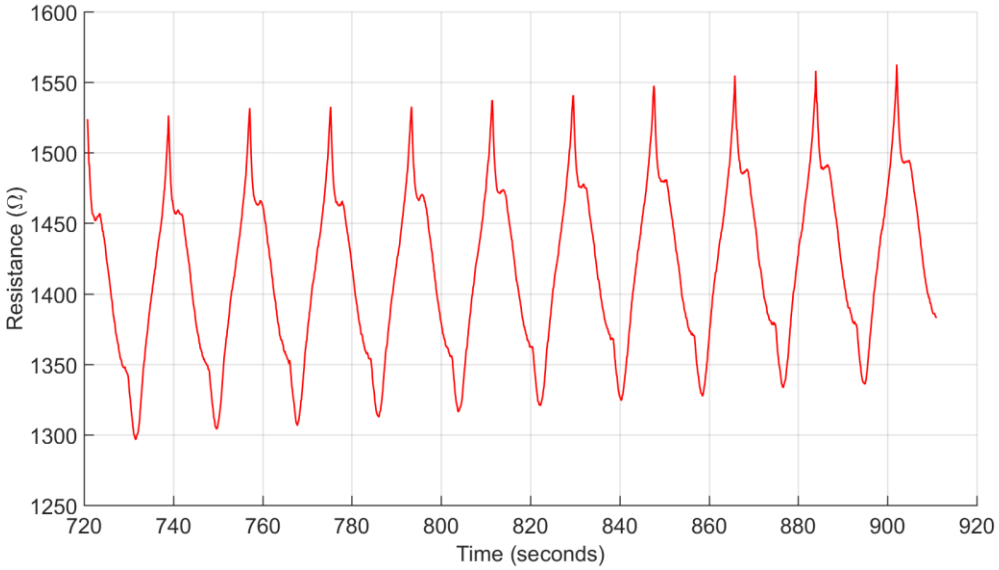

Figure 6.47 Last 10 cycles of 1% Thin

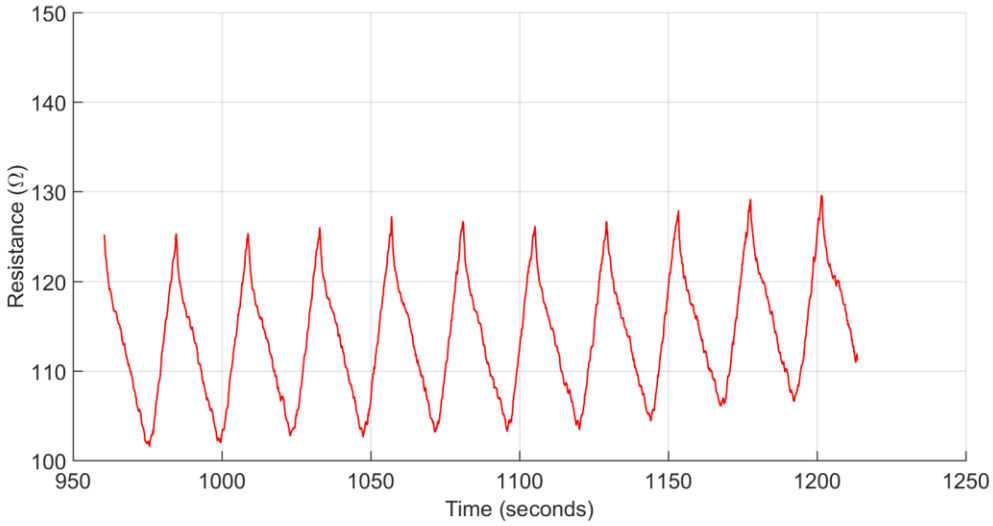

Figure 6.48 Last 10 cycles of 1.5% Thick

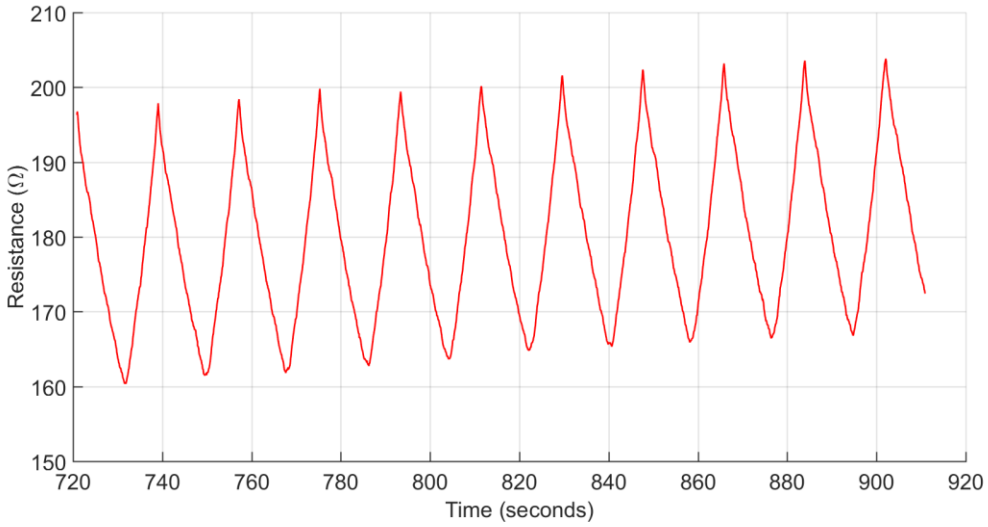

Figure 6.49 Last 10 cycles of 1.5% Thin

The nanocomposite has well defined peaks at loading and unloading and a predictable increase in resistance over time. Moreover, the resistance changes linearly with applied strain, further increasing the viability of the nanocomposite to be used as a sensor.

Chapter 7 CONCLUSIONS AND FUTURE WORK

Summary: We conducted tests where we characterized the effect of MWCNT using tensile Type I samples and effects of the Thickness with compressive Type II samples.The tests were performed at a deformation rate of 2mm/min. Our findings can be broadly characterized into Electrical, Mechanical and Piezoresistive properties of the nanocomposite.

7.1 Electrical Properties

7.1.1 Conductivity

The electrical properties of the nanocomposites are influenced by the amount of added MWCNTs. The conductivity increases and decreases directly with the amount of added carbon nanotubes. The nanocomposite started to conduct electricity at 0.5 wt% MWCNT, with its conductivity rising rapidly until 1.75 wt%, where the increase in conductivity starts to level off. This trend is characterized by the tensile tests of Type I samples in Figure 4.1.

The percolation threshold is deemed to occur at 0.5 wt% for the PDMS-MWCNT

nanocomposite, with a conductivity of 0.0035[$\Omega.m^{-1}$]. The conductivity of the tensile Type I samples is comparable to the compressive Type II samples for similar wt%of MWCNT. However, the Type II samples have a higher deviation error, which may be due to the contact resistance in the two probe method.

Moreover, the thickness of the nanocomposite has a negligible difference on conductivity, as shown the Type II Thick and Thin samples for 1 wt% and 1.5 wt%.

7.1.2 Electrical Hysteresis

The Type I and Type II samples are stable.However, they experience electrical hysteresis. This hysteresis is presentedby the initial value of electrical signal for different cycles of strain as well as by the area enclosed by those curves.We picked key cycles to represent the change in electrical signal over 50 cycles ofdeformation, where we observed the voltage-strain relation (Figure 4.4- Figure 4.8) for Type I and resistance-strain (Figure 4.16- Figure 4.19) for Type II samples.The initial value of each cycle for these electrical signals is drifting, showing hysteresis. However, the overall area enclosed by the electrical response curves formed during deformation and relaxation changes negligibly, showing stability.

The change in initial electric value can be clearly seen from the difference in beginnings of cycle 5 and cycle 25. However, thechange in the amount of shift between consecutive cycles decreases as the total number of cycles increases.The hysteresis in the nanocomposite is more in the first few cycles and gradually tapers off in the latter cycles.

This settling is clear from the closer proximity of the initial values (Figure 4.6) of cycle 25 and cycle 50, when compared with that of cycle 1 and cycle 5 initial electric values. Moreover, different wt% of MWCNT will settle differently and at different rates. The change in initial voltage value for Type I and resistance value for Type II can also be seenin the steady increase of the Peak-to-Valley signals.

7.1.3 Electrical stability

The nanocomposite was electrically stable when undergoing cyclic tension or compression. The stability is represented in the linear relation of conductivity to applied strain,where the trend remains horizontally stable overtime. The horizontal trend of the conductivity overtime for different wt% of MWCNT in Type I (Figure 4.3) and Type II (Figure 4.15).

Furthermore, the peak-to-valley trend was plotted and presented from Figure 4.10 to Figure 4.14 for Type I and Figure 4.21 to Figure 4.24 for Type II. The linearity of the trend overtime shows electrical stability of the nanocomposite and is paramount in 1.5 wt% and 1.75wt%. The trends are linear and remain parallel with a constant difference between the peaks and valleys.This constant separation allows for predicting the strain for a given voltage for Type I and resistance for Type II. Moreover, the thickness of samples does not affect the stabilityas shown by Type II testing.

The stability improves as the number of cycles increases or the wt% of added MWCNT increases. However, the increase in linearity due to added MWCNT causes a

reduction in sensing sensitivity.

7.2 Mechanical Properties

7.2.1 Young's Modulus

The mechanical properties of the nanocomposite are affected by the amount of added MWCNT, where the Young's modulus increases with an increase in the MWCNTs. The Type I tensile Young's modulus increases from 2931.3 KPa for 0.5 wt% to 3877.5 KPa for 2.0 wt% and can be seen in Figure 5.2. The Type II compression Young's modulus is one magnitude higher than the Type I tension Young's modulus. The Type II samples are thin film which characterize the effect of thickness, where the thicker samples have a slightly higher Young's modulus than the thinner samples. Due to high strain range of 18% to 52%, the Young's modulus in Type II is not constant and changes with the strain.

7.2.2 Mechanical Hysteresis

The nanocomposites have mechanical hysteresis in shifts between consecutive cycles and linearity within the loading and unloading of a single cycle. The hysteresis between the loading and unloading of a single cycle, is most pronounced for the first cycle and decreases over subsequent cycling. This decrease in mechanical hysteresis is represented by the shrinking area enclosed by the loading and unloading curves, where the area covered by cycle 50 is smaller than area of cycle 5. The mechanical response of stress strain curves starts to becomemore linear after five cycles, as seen in Figure 5.5 to Figure

5.9, for Type I and Figure 5.10 to Figure 5.13 for Type II. This linearity is a good indicator of a stable sensor as it shows that the material does not undergo mechanical degradation over repeated loading.

When comparing consecutive cycles, we observed the nanocomposite shifting its initial position with each cycle. The shift is stronger in the initial cyclesand becomes smaller with increase in number of cycles.

Overall, we found that if a nanocomposite had a trapped bubble cavity during fabrication, then it would fail within a few cycles. However, the samples which survive the initial cycles are mechanically stable. The Type I and Type II are both stable, thus improvement need to be made in processing thus to reduce the hysteresis.

7.2.3 Material rebound

Type I samples being constrained through deformation and relaxation, whereas Type II were constantly constrained during loading and were allowed to rebound themselves during unloading. The rebound rate decreases as material experiences fatigue with increased number of cycles.This slower rebound can be due to the internal degradation of the material, where the polymer chains are damaged, causing the nanocomposite to lose its flexibility. In unloading section of the cycle, there is a slight loss of contact with material. The right side of a cycle is the return to initial position (unloading). The loss of contact is during the near horizontal stress line, from 0.2 to 0.3 strain.

7.3 Piezoresistive Properties

7.3.1 Cyclic Piezoresistivity

The nanocomposite piezoresistivity is dependent on the change in electric properties due to mechanical deformation.The electrical signal overtime directly co-relates to applied deformation, where an increase in strain causes an increase in resistivity, with a decrease in strain, there is a decrease in resistivity.

The Type I tensilesamples are shown in Figure 6.1 to Figure 6.5 and the Type II samples in compression are shown in Figure 6.11 to Figure 6.14.The voltage of Type I samples drifts overtime, with the initial value of a cycle being different than the previous, showing some hysteresis. The resistance of Type II experiences a steady increase due to electrical and mechanical hysteresis, with the material rebounding slowly.

In Type I, the lower weight percentage nanocomposite of 0.5% and 0.75% has the most elasticity, however their peak to peak voltage response in not fully defined during unloading. During unloading, these weight percentages have an almost noise like behavior which is not ideal for a sensor. The higher wt%nanocomposites on the other hand have sharper peaks during loading and unloading but are stifferand have a reduced sensitivity. The Type II samples show that there is no significant difference in the piezoresistive behaviour due to thickness of sample.

7.3.2 Sensitivity/Gauge factor

The sensitivity of the nanocomposite is affected by the amount of MWCNT within the composite. The sensitivity or the gauge factor is highest near the percolation threshold of

0.5 wt%, with a value of 16.7 and drops as more MWCNTs are added, as characterized by Type I samples Figure 6.19. The Type II samples explored the effect of sample thickness on the gauge factor. We found that, for a particular wt% MWCNT, the thickness of a sample does not have a major effect on its sensitivity, Figure 6.25. The Type II compressive samples have a higher gauge factor than their Type I counterparts.

The sensitivity of the nanocomposite is also reflected in the percent change of electrical signal to a change in percentage of strain. Where the sensitivity decreases with an increase in MWCNT. The change in voltage ratio to strain for Type I samples is plotted in Figure 6.20 to Figure 6.24. The 0.5 wt% samples have an approximate change of 75% in voltage over a 10% strain, whereas the 1.5 wt% has an approximate change of 7% in voltage over a 10% strain, when comparing the last cycles. The change in resistance ratio to strain for Type II samples is compared and plotted in Figure 6.26 to Figure 6.29. The thickness of the nanocomposite does not play a significant role. The Type II 1.0 wt% samples have an approximate change of 30% in resistance over a 30% strain, with 1.5 wt% samples having an approximate change of 20% in resistance over a 25% strain. The nanocomposite in tension (Type I) seems to have lower sensitivity than in compression (Type II), evident when comparing the 1.5 wt% for both types.

7.3.3 Piezoresistive Stability

The nanocomposite piezoresistivity is stable under repeated loading, with the electrical response to mechanical stimuli remaining linear, as shown in the last 10 out of 50 cycles.

The tensile Type I are shown inFigure 6.36 to Figure 6.40 and the Type II compression are from Figure 6.46 to Figure 6.49.

The nanocomposite has a stable gauge factor, because the gauge factor response tocyclic strain is predictable.The gauge factor remains relatively constant for different cycles and has horizontal trend overtime.The linearity of the gauge factor's horizontal trend increases with an increase in MWCNTand is most prevalent in the nanocomposites with 1.5 wt% and 1.75 wt% MWCNTs.The Figure 6.35illustrates the gauge factor overtime for Type I andFigure 6.45for Type II. The thickness of the nanocomposite does not affect the gauge factor stability.

For a given amount of wt% MWCNT nanocomposite does not become more or less sensitive over time, but it does become more stable overtime. This stable material, exhibiting linear piezoresistive behaviour is a valid candidate in sensing applications. The use of this nanocomposite will be application based and can be incorporated during fabrication to provide structural support with sensing capabilities. This flexibility of manufacturing can allow the sensor to be incorporated into the airframe and wings of a plane, polymer tires, pressure mats, etc. The nanocomposite will excel in area pressure sensing applications with its potential use limited only by the design imagination.

7.4 Future Work

The following areas require additional future research:

(1) Processing technique for fabricating PDMS-MWCNT.

(2) Developing algorithms to relate the change in electrical properties to mechanical deformation.

(3) Develop a thin film piezoresistive area sensor which can tell the force and location of deformation.

The PDMS-MWCNT nanocomposite samples are stable but experience hysteresis. The hysteresis can be reduced by improvements in processing techniques, mainly in MWCNT dispersion and removal of trapped air bubbles.

The MWCNT can be dispersed more homogeneously which should decrease the conductivity variation between samples of same wt% MWCNT. Moreover, the nanotubes can be aligned and the effect of alignment direction to loading direction should be characterized. The removal of trapped air is also crucial, as an air cavity causes the nanocomposite to be mechanically compromised with the sample failing in few cycles of deformation.

The research on this material can also be progressed by developing model for simulating material, possibly using finite element methods. Moreover, having a numerical relation will push the nanocomposite towards being used as a smart piezoresistive sensor.

Finally, a piezoresistive patch/area sensor should be developed with the capability of determining amount and location of deformation. This area sensor can be made into a thin film, to be adapted into a “smart skin” and used in prosthetics to provide a feedback, creating a sense of touch. Another area of use could be providing machine health

monitoring, especially in hard to reach and constrained spaces.

References

1] K. Takei, W. Honda, S. Harada, T. Arie and S. Akita, "Toward Flexible and Wearable Human-Interactive Health-Monitoring Devices," *Advanced Healthcare Materials*, vol. 4, no. 4, pp. 487-500, 1 3 2015.

2] Y. Zang, F. Zhang, C.-a. Di and D. Zhu, "Advances of flexible pressure sensors toward artificial intelligence and health care applications," *Materials Horizons*, vol. 2, no. 2, pp. 140-156, 23 2 2015.

3] D. J. Lipomi, M. Vosgueritchian, B. C.-K. Tee, S. L. Hellstrom, J. A. Lee, C. H. Fox and Z. Bao, "Skin-like pressure and strain sensors based on transparent elastic films of carbon nanotubes," *Nature Nanotechnology*, vol. 6, no. 12, pp. 788-792, 23 10 2011.

4] K. Kim, J. Kim, B. G. Hyun, S. Ji, S.-Y. Kim, S. Kim, B. W. An and J.-U. Park, "Stretchable and transparent electrodes based on in-plane structures," *Nanoscale*, vol. 7, no. 35, pp. 14577-14594, 27 8 2015.

B. Zhang, B. Li and S. Jiang, "Poly(phenylmethylsiloxane) functionalized

5] multiwalled carbon nanotube/poly(dimethylsiloxane) nanocomposites with high piezoresistivity, low modulus and high conductivity," *Journal of Materials Science: Materials in Electronics*, 2017.

6] X. Liu, C. Tang, X. Du, S. Xiong, S. Xi, Y. Liu, X. Shen, Q. Zheng, Z. Wang, Y. Wu, A. Horner and J.-K. Kim, "A highly sensitive graphene woven fabric strain sensor for wearable wireless musical instruments Conceptual insights," *Mater. Horiz*, vol. 4, no. 4, pp. 477-486, 2017.

7] Z.-M. Dang, M.-J. Jiang, D. Xie, S.-H. Yao, L.-Q. Zhang and J. Bai, "Supersensitive linear piezoresistive property in carbon nanotubes⁄silicone rubber nanocomposites," *Journal of Applied Physics*, vol. 104, no. 2, p. 024114, 15 7 2008.

8] J. Hwang, J. Jang, K. Hong, K. N. Kim, J. H. Han, K. Shin and C. E. Park, "Poly(3-hexylthiophene) wrapped carbon nanotube/poly(dimethylsiloxane) composites for use in finger-sensing piezoresistive pressure sensors," *Carbon*, 2011.

9] Ajayakumar C Katageri and B G Sheeparamatti, "Carbon Nanotube based Piezoresistive Pressure Sensor for Wide Range Pressure Sensing Applications - A Review," *International Journal of Engineering Research and*, vol. V4, no. 08, 27 8 2015.

10] D. S. McLachlan, C. Chiteme, C. Park, K. E. Wise, S. E. Lowther, P. T. Lillehei, E. J. Siochi and J. S. Harrison, "AC and DC percolative conductivity of

single wall carbon nanotube polymer composites," *Journal of Polymer Science Part B: Polymer Physics,* vol. 43, no. 22, pp. 3273-3287, 15 11 2005.

11] D. E. Hanson, M. Hawley, R. Houlton, K. Chitanvis, P. Rae, E. B. Orler and D. A. Wrobleski, "Stress softening experiments in silica-filled polydimethylsiloxane provide insight into a mechanism for the Mullins effect," *Polymer,* vol. 46, no. 24, pp. 10989-10995, 21 11 2005.

12] C. X. Liu and J. W. Choi, "Strain-dependent resistance of PDMS and carbon nanotubes composite microstructures," in *IEEE Transactions on Nanotechnology*, 2010.

13] J. P. Heggers, N. Kossovsky, R. W. Parsons, M. C. Robson, R. P. Pelley and T. J. Raine, "Biocompatibility of silicone implants.," *Annals of plastic surgery,* vol. 11, no. 1, pp. 38-45, 7 1983.

14] H. Zhao and J. Bai, "Highly Sensitive Piezo-Resistive Graphite Nanoplatelet–Carbon Nanotube Hybrids/Polydimethylsilicone Composites with Improved Conductive Network Construction," *ACS Applied Materials & Interfaces,* vol. 7, no. 18, pp. 9652-9659, 13 5 2015.

15] J. Zhao, G. Wang, R. Yang, X. Lu, M. Cheng, C. He, G. Xie, J. Meng, D. Shi and G. Zhang, "Tunable Piezoresistivity of Nanographene Films for Strain Sensing," *ACS Nano,* vol. 9, no. 2, pp. 1622-1629, 24 2 2015.

S. Iijima and T. Ichihashi, "Single-shell carbon nanotubes of 1-nm diameter,"
16] *Nature,* vol. 363, no. 6430, pp. 603-605, 17 6 1993.

Thess, Lee, Nikolaev, Dai, Petit, Robert, Xu, Lee, Kim, Rinzler, Colbert,
17] Scuseria, Tomanek, Fischer and Smalley, "Crystalline Ropes of Metallic Carbon Nanotubes," *Science (New York, N.Y.),* vol. 273, no. 5274, pp. 483-7, 26 7 1996.

M.-F. Yu, O. Lourie, M. J. Dyer, K. Moloni, T. F. Kelly and R. S. Ruoff,
18] "Strength and breaking mechanism of multiwalled carbon nanotubes under tensile load," *Science (New York, N.Y.),* vol. 287, no. 5453, pp. 637-40, 28 1 2000.

L. Hu, D. S. Hecht and G. Grüner, "Carbon Nanotube Thin Films:
19] Fabrication, Properties, and Applications," *Chemical Reviews,* vol. 110, no. 10, pp. 5790-5844, 13 10 2010.

W. Obitayo and T. Liu, "A Review: Carbon Nanotube-Based Piezoresistive
20] Strain Sensors," *Journal of Sensors,* vol. 2012, pp. 1-15, 17 4 2012.

B. Mensah, H. G. Kim, J.-H. Lee, S. Arepalli and C. Nah, "Carbon nanotube-
21] reinforced elastomeric nanocomposites: a review," *International Journal of Smart and Nano Materials,* vol. 6, no. 4, pp. 211-238, 2 10 2015.

X. Liu, C. Tang, X. Du, S. Xiong, S. Xi, Y. Liu, X. Shen, Q. Zheng, Z. Wang,
22] Y. Wu, A. Horner and J.-K. Kim, "A highly sensitive graphene woven fabric strain sensor for wearable wireless musical instruments," *Materials Horizons,* vol. 4, no. 3,

pp. 477-486, 9 5 2017.

S. Jung, J. H. Kim, J. Kim, S. Choi, J. Lee, I. Park, T. Hyeon and D.-H. Kim,
23] "Reverse-Micelle-Induced Porous Pressure-Sensitive Rubber for Wearable Human-Machine Interfaces," *Advanced Materials,* vol. 26, no. 28, pp. 4825-4830, 1 7 2014.

E. Roh, B.-U. Hwang, D. Kim, B.-Y. Kim and N.-E. Lee, "Stretchable,
24] Transparent, Ultrasensitive, and Patchable Strain Sensor for Human–Machine Interfaces Comprising a Nanohybrid of Carbon Nanotubes and Conductive Elastomers," *ACS Nano,* vol. 9, no. 6, pp. 6252-6261, 23 6 2015.

C. S. Boland, U. Khan, C. Backes, A. O'Neill, J. McCauley, S. Duane, R.
25] Shanker, Y. Liu, I. Jurewicz, A. B. Dalton and J. N. Coleman, "Sensitive, High-Strain, High-Rate Bodily Motion Sensors Based on Graphene–Rubber Composites," *ACS Nano,* vol. 8, no. 9, pp. 8819-8830, 23 9 2014.

W. Xu and M. G. Allen, "Deformable strain sensors based on patterned
26] MWCNTs/polydimethylsiloxane composites," *Journal of Polymer Science Part B: Polymer Physics,* vol. 51, no. 20, pp. 1505-1512, 15 10 2013.

X. Song, S. Liu, Z. Gan, Q. Lv, H. Cao and H. Yan, "Controllable fabrication
27] of carbon nanotube-polymer hybrid thin film for strain sensing," *Microelectronic Engineering,* vol. 86, no. 11, pp. 2330-2333, 1 11 2009.

S. Luo and T. Liu, "Structure–property–processing relationships of single-

28] wall carbon nanotube thin film piezoresistive sensors," *Carbon,* vol. 59, pp. 315-324, 1 8 2013.

29] L. Gao, E. T. Thostenson, Z. Zhang and T.-W. Chou, "Coupled carbon nanotube network and acoustic emission monitoring for sensing of damage development in composites," *Carbon,* vol. 47, no. 5, pp. 1381-1388, 1 4 2009.

30] P. Fernberg, G. Nilsson and R. Joffe, "Piezoresistive Performance of Long-Fiber Composites with Carbon Nanotube Doped Matrix," *Journal of Intelligent Material Systems and Structures,* vol. 20, no. 9, pp. 1017-1023, 28 6 2009.

31] M. H. G. Wichmann, S. T. Buschhorn, J. Gehrmann and K. Schulte, "Piezoresistive response of epoxy composites with carbon nanoparticles under tensile load," *Physical Review B,* vol. 80, no. 24, p. 245437, 29 12 2009.

32] S. Gong and Z. H. Zhu, "Giant piezoresistivity in aligned carbon nanotube nanocomposite: account for nanotube structural distortion at crossed tunnel junctions," *Nanoscale,* vol. 7, no. 4, pp. 1339-1348, 5 1 2015.

33] S. Gong and Z. H. Zhu, "On the mechanism of piezoresistivity of carbon nanotube polymer composites," *Polymer,* vol. 55, no. 16, pp. 4136-4149, 5 8 2014.

34] Wen Pei Lim, *. a. Kui Yao and Y. Chen, "Alignment of Carbon Nanotubes by Acoustic Manipulation in a Fluidic Medium," 2007.

K. M. Seemann, J. Ebbecke and A. Wixforth, "Alignment of carbon

35] nanotubes on pre-structured silicon by surface acoustic waves," *Nanotechnology,* vol. 17, no. 17, pp. 4529-4532, 14 9 2006.

36] Y. Miao, Q. Q. Yang, R. Sammynaiken, W. J. Zhang, J. Maley and G. Schatte, "Influence of aligned carbon nanotube networks on piezoresistive response in carbon nanotube films under in-plane straining," *Applied Physics Letters,* vol. 102, no. 23, p. 233106, 10 6 2013.

37] A. Oliva-Avilés, F. Avilés and V. Sosa, "Electrical and piezoresistive properties of multi-walled carbon nanotube/polymer composite films aligned by an electric field," *Carbon,* vol. 49, no. 9, pp. 2989-2997, 1 8 2011.

38] Y.-F. Zhu, C. Ma, W. Zhang, R.-P. Zhang, N. Koratkar and J. Liang, "Alignment of multiwalled carbon nanotubes in bulk epoxy composites via electric field," *Journal of Applied Physics,* vol. 105, no. 5, p. 054319, 13 3 2009.

39] W. Obitayo and T. Liu, "Effect of orientation on the piezoresistivity of mechanically drawn single walled carbon nanotube (SWCNT) thin films," *Carbon,* vol. 85, pp. 372-382, 1 4 2015.

40] S.-H. Yao, J.-K. Yuan, T. Zhou, Z.-M. Dang and J. Bai, "Stretch-Modulated Carbon Nanotube Alignment in Ferroelectric Polymer Composites: Characterization of the Orientation State and Its Influence on the Dielectric Properties," *J. Phys. Chem. C,* vol. 115, pp. 20011-20017, 2011.

K. Parmar, M. Mahmoodi, C. Park and S. S. Park, "Effect of CNT alignment
41] on the strain sensing capability of carbon nanotube composites," *Smart Materials and Structures*, vol. 22, no. 7, p. 075006, 1 7 2013.

Junyong Lu, Miao Lu, A. Bermak and Yi-Kuen Lee, "Study of
42] piezoresistance effect of carbon nanotube-PDMS composite materials for nanosensors," in *2007 7th IEEE Conference on Nanotechnology (IEEE NANO)*, 2007.

Z. Zeng, M. Liu, H. Xu, W. Liu, Y. Liao, H. Jin, L. Zhou, Z. Zhang and Z.
43] Su, "A coatable, light-weight, fast-response nanocomposite sensor for the in situ acquisition of dynamic elastic disturbance: from structural vibration to ultrasonic waves," *Smart Materials and Structures*, vol. 25, no. 6, p. 065005, 1 6 2016.

J.-l. Yao, X. Yang, N. Shao, H. Luo, T. Zhang and W.-g. Jiang, "A Flexible
44] and Highly Sensitive Piezoresistive Pressure Sensor Based on Micropatterned Films Coated with Carbon Nanotubes," *Journal of Nanomaterials*, vol. 2016, pp. 1-5, 25 8 2016.

C.-F. Hu, W.-S. Su and W. Fang, "Development of patterned carbon
45] nanotubes on a 3D polymer substrate for the flexible tactile sensor application," *Journal of Micromechanics and Microengineering*, vol. 21, no. 11, p. 115012, 1 11

2011.

46] P. Dharap, Z. Li, S. Nagarajaiah and E. V. Barrera, "Nanotube film based on single-wall carbon nanotubes for strain sensing," *Nanotechnology,* vol. 15, no. 3, pp. 379-382, 1 3 2004.

47] J.-S. Kim and G.-W. Kim, "Hysteresis Compensation of Piezoresistive Carbon Nanotube/Polydimethylsiloxane Composite-Based Force Sensors.," *Sensors (Basel, Switzerland),* vol. 17, no. 2, 24 1 2017.

48] "NC7000™ - Nanocyl," [Online]. Available: http://www.nanocyl.com/product/nc7000/.

49] "Dow Corning- 184 Silicone Encapsulant | Paisley Products of Canada Inc.," [Online]. Available: https://www.paisleyproducts.com/en-us/dow-corning-184-silicone-encapsulant-avdc0184#.W3cCM8IpDX4.

50] ASTM, "D 638-02a Standard Test Method for Tensile Properties of Plastics," no. 02.

51] F. M. Smits, "Measurement of Sheet Resistivities with the Four-Point Probe," *Bell System Technical Journal,* vol. 37, no. 3, pp. 711-718, 5 1958.

52] Y. SINGH, "ELECTRICAL RESISTIVITY MEASUREMENTS: A REVIEW," *International Journal of Modern Physics: Conference Series,* vol. 22, pp. 745-756, 1 2013.

S. Gong, Z. Zhu and S. Meguid, "Carbon nanotube agglomeration effect on
53] piezoresistivity of polymer nanocomposites," *Polymer,* vol. 55, no. 21, pp. 5488-5499, 9 10 2014.